Title

Protein Translation Regulation in Cardiac Hypertrophy and Heart Failure

Author

Wang, Yifan

Publication Date

2023

Peer reviewed|Thesis/dissertation

UNIVERSITY OF CALIFORNIA

Los Angeles

Protein Translation Regulation in Cardiac Hypertrophy and Heart Failure

A dissertation submitted in partial satisfaction of the

requirements for the degree Doctor of Philosophy

in Molecular, Cellular & Integrative Physiology

by

Yifan Wang

2023

ABSTRACT OF THE DISSERTATION

Protein Translation Regulation in Cardiac Hypertrophy and Heart Failure

by

Yifan Wang

Doctor of Philosophy in Molecular, Cellular & Integrative Physiology

University of California, Los Angeles, 2023

Professor Yibin Wang, Chair

Cardiac hypertrophy is an adaptive process during hemodynamic stress induced by various pathophysiological conditions. During this process, individual myocyte grows bigger in size under complex and multi-layered regulations, which required a large amount of *de novo* protein synthesis. It has already been well-established back in the 1960s and 70s that protein synthesis is induced early on during induced hypertrophic stress, which is a dominating factor leading to hypertrophic myocytes and hearts. Over the years, scientists have extensively investigated different regulatory steps in cardiac hypertrophy, such as signaling pathways, transcription regulation, and metabolism. However, translation remained poorly studied. Moreover, recent discoveries on transcriptome/translatome mismatch brought these questions to our attention, as it is challenging the prevalent interpretation of the central dogma. Therefore, there's a dire need to achieve a deeper understanding of translation regulation in cardiac hypertrophy to fill the knowledge gap and coordinate the conflict and discrepancies between the knowns and the novel discoveries.

In this thesis, we discussed protein translation regulation in cardiac hypertrophy in many different aspects, including toolkits to study translation, translation efficiency, translation capacity, and the emerging field of spatial-temporal regulation of translation machinery. Aiming to obtain a comprehensive understanding of translation regulation in cardiac hypertrophy, we combined novel mouse and cell culture models with cutting-edge technologies including deep RNA sequencing and proteomics to investigate the translatome landscape and underlying molecular mechanisms. We identified striking remodeling of the translatome and nascent proteome during hypertrophic stress with an emphasis on ribosome biogenesis. We identified a long non-coding RNA (lncRNA) named Myocardial Infarction Associated Transcript (Miat) as a critical regulator of translation during cardiac hypertrophy. For molecular mechanisms, we demonstrated Miat interacts with a nucleolar protein nucleolin (NCL) to mediate ribosome biogenesis. We also discovered important regulatory roles of Miat in nucleolar (center of ribosome biogenesis) dynamics and transportation of translation machinery. Taken together, this thesis gave a holistic and comprehensive depiction of translation regulation in pathological cardia hypertrophy with a well-characterized lncRNA mediating multiple aspects of the translation process and translation machineries. Our study filled the knowledge gap in our understanding of cardiac hypertrophy and gave inspirations on protein synthesis regulation in heart, which could be generalized to many other non-cardiac contexts and lead to a paradigm shift. Our discoveries shed light on current clinical resolutions of cardiac hypertrophy and may potentially lead to the development of novel therapies.

The dissertation of Yifan Wang is approved.

Thomas M Vondriska

James Akira Wohlshlegel

Xia Yang

Yibin Wang, Committee Chair

University of California, Los Angeles

2023

DEDICATION

To my parents, Wenmin and Yong, for your unconditional love and support during the toughest times;

To my sweetheart Difei, for all your encouragement and company through this journey, especially when I am down and don't hold myself together;

To my cat Toto, for all the joy and laughter you brought to us.

I will never be able to complete this work without you standing by my side.

TABLE OF CONTENTS

LIST OF FIGURES

GLOSSARY

BUNCAT/FUNCAT (Bio-orthogonal/Fluorescent non-canonical amino acid tagging)

Dilated cardiomyopathy (DCM)

Data-dependent acquisition mass spectrometry (DDA-MS)

Data-independent acquisition mass spectrometry (DIA-MS)

Genome-wide association studies (GWAS)

Hybrid mouse diversity panel (HMDP)

Immunofluorescence staining (IF)

Isoproterenol (ISO)

Knockdown (KD)

Knockout (KO)

Long non-coding RNA (lncRNA)

Mammalian/mechanistic target of rapamycin (mTOR)

Mass spectrometry (MS)

Mouse embryonic fibroblast (MEF)

Myocardial infarction (MI)

Neonatal rat ventricular myocyte (NRVM)

O-propargyl-puromycin (OPP)

Phenylephrine (PE)

Pre-initiation complex (PIC)

Pulse stable isotope labeling by amino acids (pSILAC)

Ribosomal DNA (rDNA)

Ribosomal Protein (RP)

Ribosomal RNA (rRNA)

RNA Immunoprecipitation (RIP)

RNA polymerase I (RNPI)

Single molecule RNA in situ hybridization (smFISH)

Small nucleolar RNA (snoRNA)

Surface sending of translation (SUnSET)

Translation efficiency (TE)

Translating ribosome affinity purification (TRAP)

Transverse aortic constriction (TAC)

Upstream open reading frame (uORF)

ACKNOWLEDGEMENTS

This is my 8th year at UCLA and I am incredible grateful to start and enjoy my scientific endeavors at such an extraordinary institution. I have learned to not only become a better scientist, but also a better person with resilience, courage, kindness, and passions.

I am extremely lucky to have Dr. Yibin Wang as my PhD mentor. There was an old Chinese saying that goes “better to teach someone to fish than to give him a fish.” I joined in the lab as an undergraduate student in 2017 and was completely ignorant about how become a good scientist. You not only taught me everything about research, but also the way of thinking critically and asking the best questions. We were facing many challenging situations such as COVID and the lab relocation, and I was extremely struggling going through all the bumps. I cannot express how thankful I was to have you by my side and support me with your patience and kindness. I have learned so much from you over the years, and these lessons will be invaluable for the rest of my life.

I would like to thank all my other committee members, Dr. Tom Vondriska, Dr. James Wohlshlegel, and Dr. Xia Yang, who supported me in every way they can for my PhD thesis. I appreciate all your help and encouragement along the way, especially during the past year when Dr. Wang had to mentor me virtually. I will never achieve what I have achieved so far and enjoyed my time in research without your endless support.

This project cannot be in such a good shape without efforts and suggestions from many other people. I would like to first thank Iris Wang, who started this project and did a lot of

preliminary works. You taught me all the basics in scientific research, and I am incredibly grateful to have you as my very first mentor in science. I also want to thank Dr. Christoph Rau and Jihui Sha from the Wohlshlegel lab for helping with analyzing RNAseq and proteomics data. I would like to thank Dr. William Pu, Dr. Benjamin Prosser, and Dr. Izhak Kehat for your insightful comments and suggestions toward this project.

I would like to thank my wife Difei, who has been supporting me from my first day as a PhD student. I feel extremely lucky to have you as my lifelong companion. I really enjoyed and valued our time together and all the discussions about sciences.

I would like to thank everyone in the MCIP program, especially Dr. Mark Frye and Yesenia Rayos, who runs one of the best graduate programs in UCLA, and my MCIP cohort. You made my life as a graduate student beyond wonderful.

Last but not least, I would like to thank everyone in the Wang lab who have helped me in the past. Although most of us have moved on to new positions at different places, I still feel that we are all families and care about each other. We are a strong team doing cutting-edge sciences and daring to step into the unknown challenges. This project cannot be completed without supports from you.

BIOGRAPHICAL SKETCH

NAME: Wang, Yifan (Frank)

POSITION TITLE: Graduate Student Researcher

EDUCATION/TRAINING *(Begin with baccalaureate or other initial professional education, such as nursing, include postdoctoral training and residency training if applicable. Add/delete rows as necessary.)*

INSTITUTION AND LOCATION	DEGREE	TIME	FIELD OF STUDY
University of California, Los Angeles	BS	09/2015 - 06/2019	Biochemistry
University of California, Los Angeles	PhD	09/2019 - 06/2023 (Expected)	Molecular, Cellular & Integrative Physiology

Date of advancement to doctoral candidacy: October 1st, 2021

A. Positions and Honors

Positions in Research

2017/02 – 2019/06 **Undergraduate Student Research Assistant, UCLA**
2018/06 – 2018/08 **Summer Undergraduate Research Student, The Chinese University of Hong Kong (CUHK)**
2019/09 – Present **Graduate Student Researcher, UCLA**

Other Experience/Positions

2017/10 – Present **Activity Organizer, UCLA-Chinese-American Students and Scholars Seminar (UCLA-C3S)**
2020/09 – Present **Co-founder & Secretary, GAIN at UCLA**

Teaching and Mentorship

2021/03 – 2021/06 **Teaching Assistant,** Life Sciences Core Education, UCLA **Physiology and Human Biology**
2021/06 **–** 2021/08. **Undergraduate Student Mentor**, UCLA
2022/03 – 2022/06 **Teaching Assistant,** Life Sciences Core Education, UCLA Physiology and Human Biology

Honors and Awards

2016 **–** 2019 **Dean's Honors List** (7-times), UCLA
2019/06 **Departmental Honor**, Department of Chemistry and Biochemistry, UCLA
2022/06 **Poster Award**, Gordon Research Conference – Cardiac Regulatory Mechanisms

C. Contributions to Science

Publications

Research Article:

- **Yifan Wang**, He (Iris) Wang, Zhihua Wang, Christopher Rau, Jihui Sha, Shuxun Ren, Jonelle White, Steven G. Clarke, James Wohlschlegel, Yibin Wang. ***"Regulation of Ribosomal Reprogramming and Protein Synthesis by a Long Non-coding RNA Miat in Cardiac Hypertrophy"***. (Manuscript in Preparation)

Review Article:

- **Yifan Wang,** Yibin Wang. ***"Translation Regulation in Cardiac Hypertrophy and Heart Failure"***. (Manuscript in Preparation)

Editorial:

- **Yifan F. Wang,** Yibin Wang. ***"Location-Specific and Kinase-Independent GRK5 Function in Heart"***. JACC: Basic to Translational Science. 2022 Apr 25;7(4):381-383. doi: 10.1016/j.jacbts.2022.02.016. PMID: 35540094; PMCID: PMC9079850.

Abstract:

- Yibin Wang, He Wang, and **Frank Yifan Wang**. ***"Regulation of the Translatome in Cardiac Remodeling."*** *The FASEB Journal*36 (2022).
- He Wang, Zhihua Wang, **Yifan Wang**, Christoph D. Rau, Shuxun Ren, Yibin Wang. ***"Abstract 608: Long Non Coding RNA Miat Contributes to Cardiac Hypertrophy and Regulates Ribosomal Genes"*** Circulation Research 125.Suppl_1 (2019): A608-A608.

Selected Poster Presentations

2018/08 **Specific Inhibition of Histone Deacetylase HDAC8 Promotes Immunogenic Cell Death via Controlling HMGB1 Equilibrium**
Summer Undergraduate Research Program (SURP), CUHK

2018/10 **Matter of Translation: The Long Non-coding RNA MIAT Contributes to Cardiac Hypertrophy**
UCLA Cardiovascular Symposium

2021/09 **MIAT-NCL Mediated Translatome Reprogramming in Pathological Hypertrophy and Heart Failure**
40th Meeting ISHR-NAS

2022/06 **Protein Translation Regulation in Cardiac Hypertrophy and Remodeling**
Gordon Research Conference/Seminar – Cardiac Regulatory Mechanisms, 2022

Conference/Seminar Talks

2022/03 **Protein Translation Regulation in Cardiac Hypertrophy and Remodeling**
CVS AVP Research Seminar Series, National Heart Centre Singapore

2022/06 **Protein Translation Regulation in Cardiac Hypertrophy and Remodeling**
Gordon Research Seminar – Cardiac Regulatory Mechanisms, 2022

2023/01 **Protein Translation Regulation in Cardiac Hypertrophy and Remodeling**
UCLA MCIP Student Seminar

CHAPTER I. TRANSLATION REGULATION IN CARDIAC HYPERTROPHY

1.1 Introduction

1.1.1 Central dogma and layers of regulation from gene to phenotype

All gene expression must follow the rule of central dogma, which was first stated by Francis Crick in the late 1950s. The central dogma demonstrates a linear flow of genetic information from the starting material (genomic DNA) to the intermediate (RNA), and then to the final product (protein), with complicated and tight regulations at each step. Over the last few decades, we have achieved in-depth understandings about many different aspects of cardiac hypertrophy such as intracellular signaling pathways[1], epigenetics and chromatin remodeling[2, 3], transcription factors[1, 4], metabolic remodeling[5, 6], and potential therapeutics[7]. However, translation regulation remains poorly studied with many imperative questions to be solved.

1.1.2 Cardiac hypertrophy

Like many terminally differentiated cells, adult cardiomyocytes do not proliferate. Therefore, it is not surprising that the basal protein synthesis rate in adult heart is lower compared to other tissues[8, 9]. However, the heart still responds to growth stimuli during hypertrophy, in which individual cardiac myocyte grows bigger in size, leading to the enlargement of the whole heart. During hypertrophic response, a tremendous amount of dynamic regulation of gene expression is required to maintain proper cellular function and viability. It is well established early on that protein synthesis in heart increased drastically during early stage when hypertrophic stress was introduced in various animal models[10, 11], and the increased total protein abundance is dominated by increased protein synthesis rather than changes in protein degradation[12]. Later on, a study used

pulmonary artery constriction-induced pressure overload model and showed that both translation efficiency and capacity significantly increased rapidly in right ventricular hypertrophy[13].

1.1.3 Rationale of studying translation regulation in heart

Many recent studies that combined and compared transcriptomic and proteomic profiling revealed a striking and widespread uncoupling between protein and mRNA transcript abundance in various scenarios[14-16], including human DCM (dilated cardiomyopathy) patients[17]. This implies that translational control is essential in tuning gene expression, especially in many cardiovascular diseases such as cardiac hypertrophy where there's a significant and urgent demand of protein synthesis. There are many different steps at which translation activity can be fine-tuned and can be mainly categorized into translation efficiency, which refers to how fast mRNAs are being translated, and translation capacity, which refers to quantity and availability of ribosomes. In this chapter, we will discuss each category in detail and explain how they can work together and lead to the pathogenesis of cardiac hypertrophy.

1.2 Modern Toolkits to Study Protein Translation

1.2.1 Luminescence labeling-based methods

One of the most prevalent readouts to study protein translation is luminescence (**Figure 1-1**). Newly synthesized proteins can be easily labeled in bulk by puromycin, a well-established alternative to radioactive labeling. It is a naturally occurring translation inhibitor that was obtained from *Streptomyces alboniger*. Puromycin is an aminoacyl tRNA analog that can be incorporated into the elongating polypeptide chain, leading to premature termination and chain release. In this manner, all the actively synthesizing

proteins will be puromycylated, separating them apart from the existing proteins. These proteins can be detected by an anti-puromycin antibody, which is a method named surface sensing of translation (SUnSET)[18]. A derivative of puromycin called O-propargyl-puromycin (OPP) was also developed later, which can be labeled and visualized with desired fluorophores by an *in situ* copper(I)-catalyzed azide-alkyne cycloaddition, also known as CLICK chemistry[19].

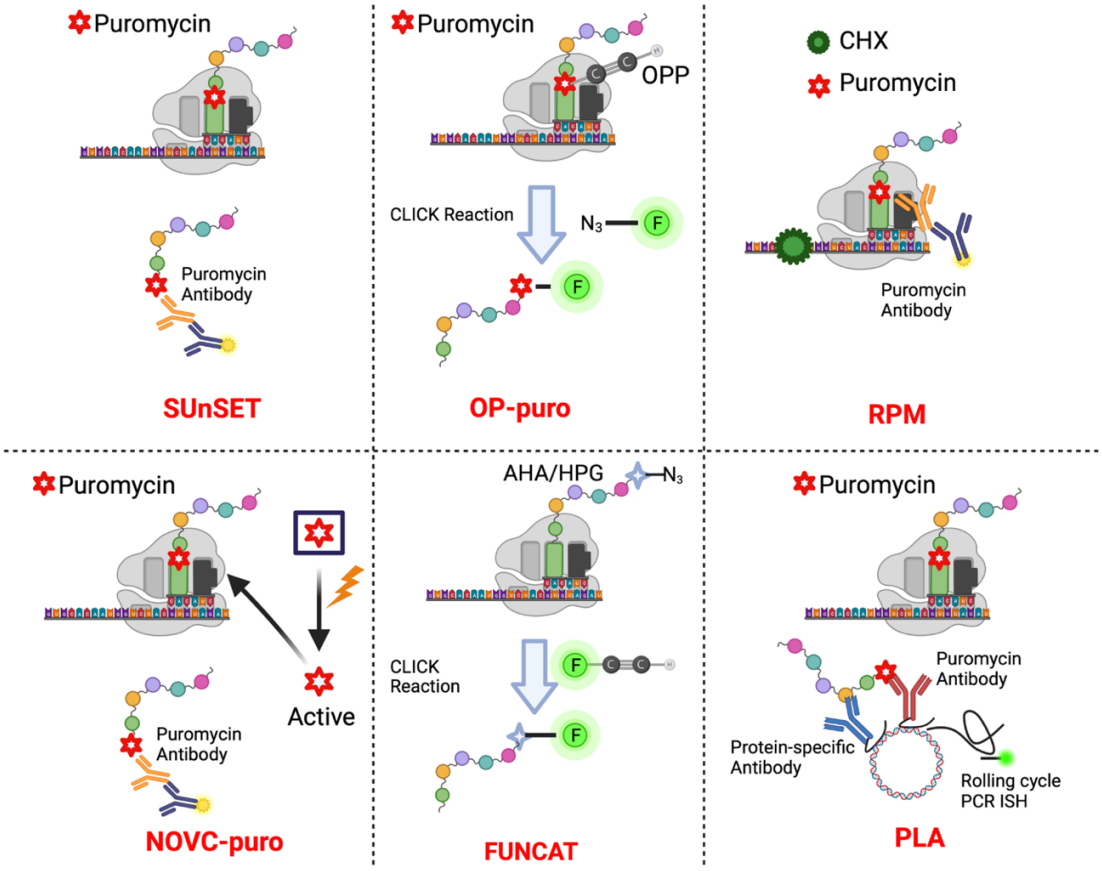

Figure 1-1. Summary of luminescence labeling-based methods to study translation regulation.

Location of active translation within cells is another important feature to consider. Subcellular localization of translation hotspot can be monitored by combining puromycin labeling and cycloheximide, which is a drug that blocks detachment peptide chains from ribosomes. Therefore, the ribo-puromycylation (RPM) traps newly synthesized proteins

at the site of active translation that can be visualized by immunofluorescence via anti-puromycin antibodies[20, 21]. Another puromycin-based method that can provide high spatial-temporal resolution on translation is photo-caged puromycin (NVOC-puromycin), which could be activated by UV light exposure[22].

However, these puromycin-based methods were challenged by a recent study which demonstrated that puromycylated peptides do not necessarily reflect the active translation sites in all situations, urging cautions on interpretations of spatial information provided by puromycin-based assay[23]. Nevertheless, it can still provide robust information on global, quantitative changes in translation.

To gain spatial-temporal information of translation, an alternative way of labeling and newly synthesized proteins in a puromycin-free manner is metabolic incorporation of amino acid analogs, namely azidohomoalanine (AHA) and homopropargylglycine (HPG). Both AHA and HPG are methionine analogs and can be incorporated into translating proteins. By performing CLICK reaction with either the azide on AHA or alkyne on HPG, a fluorophore could be conjugated to the newly synthesized proteins. This technology is named fluorescent non-canonical amino acid tagging, or FUNCAT[24]. These amino acid surrogates do not impede normal translation and do not cause significant cellular toxicities compared to puromycin. However, the efficiency of incorporating these non-canonical amino acids also depends on methionine contents in proteins, and methionine-free media should be used to maximize labeling. Moreover, a recent study comparing puromycin and AHA labeling observed striking discrepancies between these two methods during energy starvation. It questioned the accuracy of protein synthesis quantification with puromycin

labeling during glucose starvation and emphasizes the necessity of validation when puromycin incorporation is applied to new experimental settings[25].

To monitor translation of a specific protein species *in situ* rather than in bulk, proximity ligation assay (PLA)-based method can be used in combination with either puromycylation or FUNCAT. This technology works by detecting the spatial coincidence of two antibodies: one targeting FUNCAT or puromycylation, and one targeting the protein of interest. Both antibodies have proximity probes-oligonucleotides attached, which will become circularized when in the vicinity of each other[26]. A downstream, localized rolling cycle PCR could be performed to visualize this protein pair via *in situ* hybridization, marking the location of active translation[27].

1.2.2 Mass Spectrometry-based Methods

Although the methods mentioned above can look at translation activity in a global and quantitative manner, sometimes even at individual protein of interest, it is crucial to have the capability to look at specific protein species in a high-throughput and unbiased way. Mass spectrometry has been playing an important role in addressing this demand in combination with technologies that allowed effective isolation of the newly synthesized proteins from the total protein pool (**Figure 1-2, left**).

Pulse stable isotope labeling by amino acids (pSILAC) is a widely used method to monitor protein turnover. Protein samples from cells cultured with essential amino acids containing either heavy or medium-heavy isotopes can be mixed and examined by mass spectrometry to examine protein translation during a defined period of time. Mass spectrometry could distinguish differentially labeled samples and therefore compare translation activity in “heavy” or “medium-heavy” conditions without interference from the

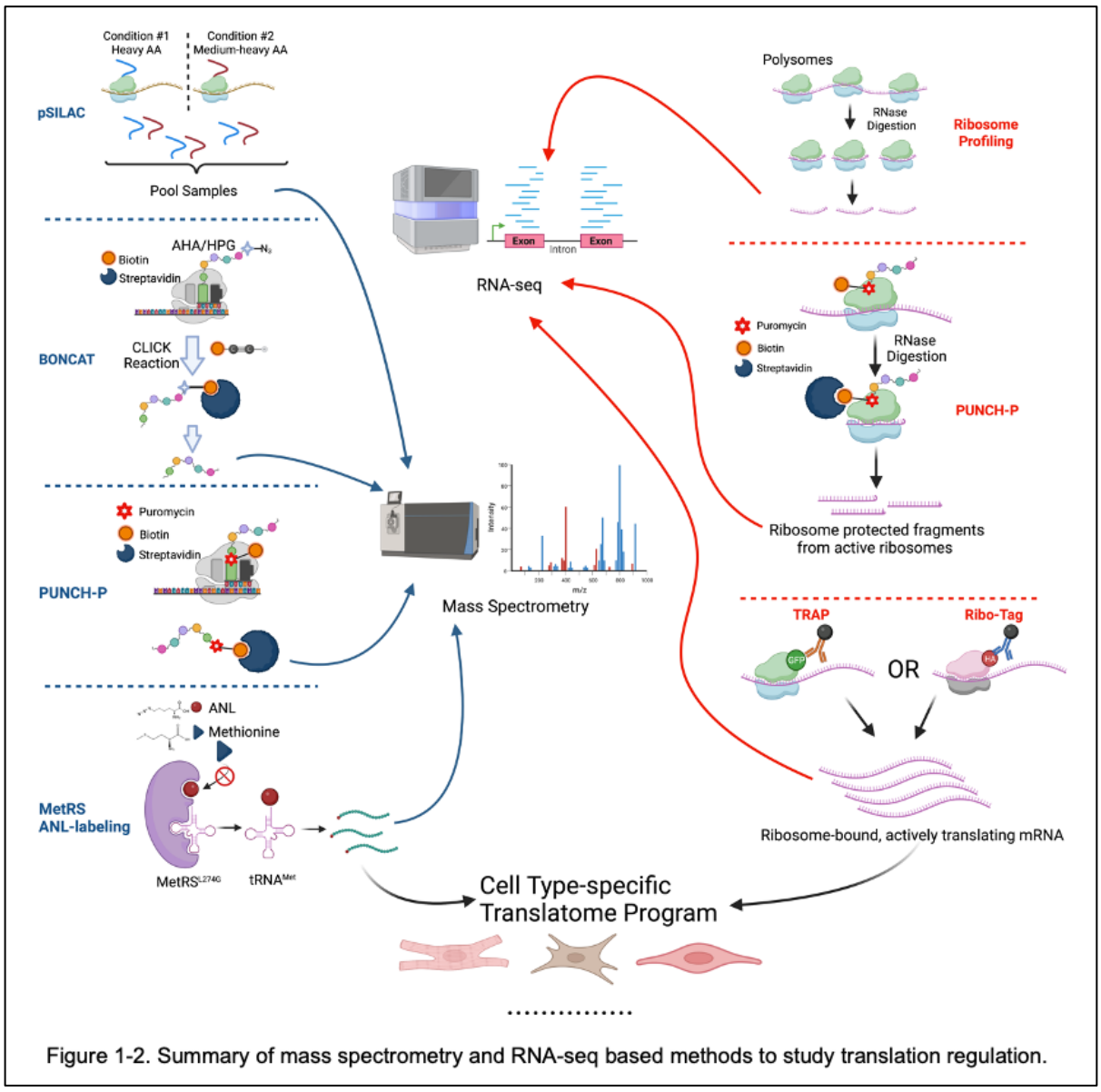

Figure 1-2. Summary of mass spectrometry and RNA-seq based methods to study translation regulation.

preexisting proteins[28]. For example, a recent study thoroughly examined mitochondrial translation program by combining pSILAC with mitochondria isolation[29].

Alternatively, newly synthesized proteins can be distinguished using bio-orthogonal non-canonical amino acid tagging, or BONCAT, which is very similar to FUNCAT discussed above that works by metabolic labeling. This method also uses CLICK chemistry to label newly synthesized proteins with biotin-alkyne that can be purified and enriched with

streptavidin/neutravidin beads, instead of a fluorophore conjugation[30, 31]. This purified newly synthesized protein pool can be analyzed deeper with mass spectrometry without background and noise from pre-existing proteins.

Another technique that can resolve this issue without using metabolic labeling is puromycin-associated nascent chain proteomics (PUNCH-P), which uses a biotinylated puromycin derivative that can be catalytically incorporated into the nascent peptide chain. Streptavidin affinity purification could then be used to isolate translating ribosomes together with nascent peptides, which can be analyzed using LC-MS/MS[32].

1.2.3 RNA sequencing-based methods

Besides mass spectrometry, RNA sequencing is another powerful too and common readout to study translation regulation (**Figure 1-2, right**). Ribosome profiling, or Ribo-seq, is one of the most common methods used in studying translation dynamics in a systematic way. Generally, mRNA fragments that are protected by ribosomes can be purified and analyzed by deep sequencing. These quantified footprints can reflect translation efficiency of specific mRNAs to their corresponding proteins[33]. This technology is not to be confused with polysome profiling, which separates polysomes from monosomes by sedimentation in a sucrose gradient. Higher number of ribosomes associated with a mRNA indicates a higher degree of translation, which is reflected by the optical density of the fractions[34].

Although Ribo-seq can help us to examine protein translation quantitatively at high prevision, it is still unable to distinguish RNA fragments coming from active ribosomes and inactive ribosomes. A few years ago, the RiboLace technology was developed to circumvent this situation by pulling down active ribosomes in an antibody-free and tag-

free way using a biotinylated puromycin analog called 3P[35]. With this construct, the puromycylated, active ribosomes will be immobilized with the bound transcript and can be purified by streptavidin. Ribo-seq could be performed subsequently to capture the dynamics of active ribosome on specific transcripts.

1.2.4 Determining Cell-type Specific Translation Program

Thanks to the rapid development and growing accessibility of single cell transcriptomics[36] and single cell proteomics[37], it is now highly appreciated that different cell types may have drastically different gene expression patterns within a single type of tissue. Therefore, monitoring translation program *in vivo* in a cell type-specific manner is critical in many conditions to fully dissect the underlying molecular mechanism. However, it is necessary to isolate the cell type of interest from tissues before performing polysome profiling, which introduces a lot more complications such as large amount of tissue input required and potential contamination from other cell types. To circumvent this issue, translating ribosome affinity purification (TRAP)[38] and RiboTag[39] have been developed. Both methods rely on expressing a tagged ribosomal protein driven by a cell type-specific promoter. Rpl10a-GFP and RPl22-HA were expressed in TRAP and RiboTag models, respectively. Ribosome-bound mRNA could be purified by immunoprecipitation using corresponding antibodies and examined by RNA sequencing. Using this method, translation efficiency could be monitored by comparing translatome and transcriptome data. These methods were utilized and effectively revealed dynamics in translationally regulated gene expression during cardiac hypertrophy in cardiac myocyte and endothelial cells[40, 41]. Cardiac regulatory networks in early cardiac

remodeling were also established with identification of novel hub genes based on the translatome profiles[42].

Like translatome, nascent proteome could also be monitored in a cell type-specific manner *in vivo*. The non-canonical amino acid azidonorleucine, or ANL in short, could be incorporated into the synthesizing polypeptides only when a mutant methionyl-tRNA synthetase (MetRS) is present. ANL-containing, newly synthesized proteins can be biotinylated with CLICK chemistry, allowing for downstream immunoblotting, imaging, or mass spectrometry analysis. The transgenic mouse line carrying this Cre-recombinase induced MetRS mutant can be crossed with any desired Cre lines to achieve cell type-specific proteomic analysis on newly synthesized proteins[43].

In summary, nowadays we have many great tools to study translation by looking at both translating mRNA and/or newly synthesized proteins with various readouts. This is only made possible by recent the advancement of genomics and proteomics analysis. Many of these techniques have been widely applied in cardiovascular research to understand the alteration of translation programs in pathological hypertrophy and heart failure, some of which will be discussed in the rest of this review article.

1.3 Translation Efficiency

1.3.1 General Overview

Translation efficiency generally refers to how fast mRNA could be translated into proteins. Translation efficiency has many layers of regulation. When ribosome encounters mRNAs that are ready to be translated, it generally followed three steps: translation initiation, elongation, and termination. Some features of the mRNA itself can also be important in translation efficiency, including its own sequence such as 5'TOP sequence and uORFs,

and modifications such as m6A methylation. It is also controlled by signaling pathways in response to any stimulations, namely mTOR signaling (**Figure 1-3, Ref [44]**).

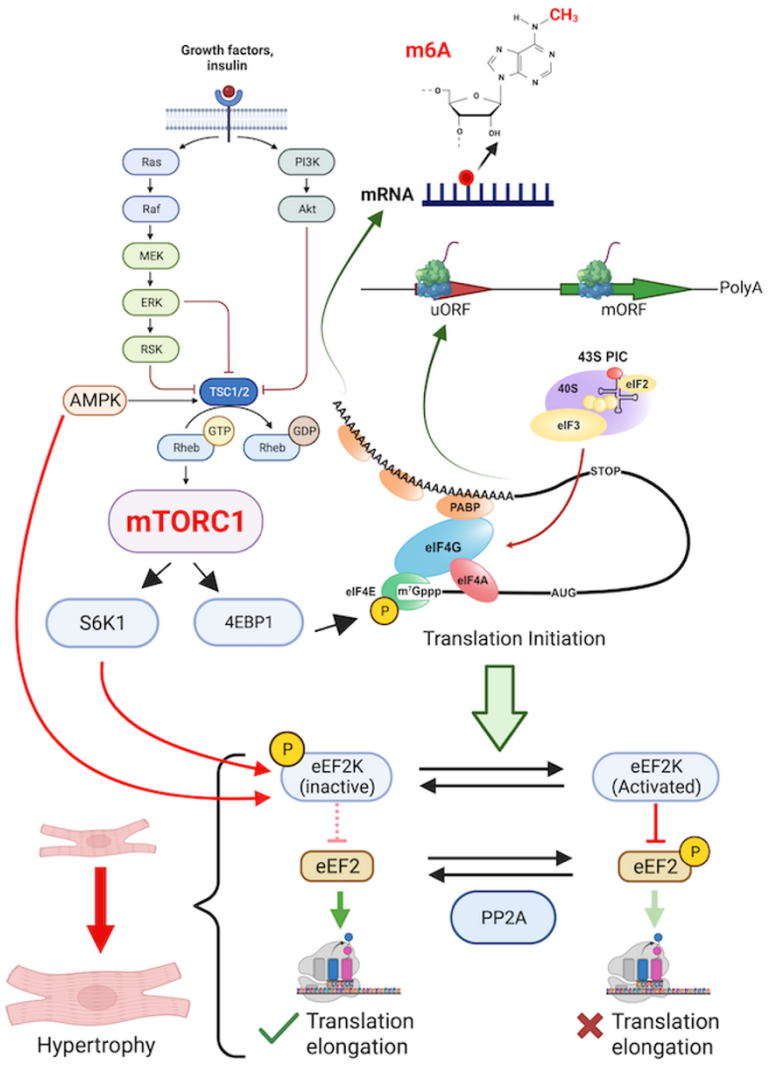

Figure 1-3. Overview of translation efficiency regulation in cardiac hypertrophy. Modified from Ref [44].

1.3.2 Translatome Profile Shifts during Hypertrophy

Recent advancement of genomics and proteomics technologies allowed us to move beyond RNA sequencing (RNA-seq) to ribosome and polysome profiling to look at gene expression regulation, particularly in a cell type-specific manner. A study done by Doroudgar et al. crossed the RiboTag mouse with αMHC-Cre mouse to achieve cardiac myocyte-specific pulldown of ribosome-bound translating mRNA in acute (3h), intermediate (2 days), and chronic (2 weeks) pressure overload induced by TAC[40]. These samples were then subjected to Ribo-seq to examine the ribosome-protected RNA fragments, which were then compared with the transcriptome by bulk RNA-seq. Dynamic translatome reprogramming was observed overtime, which is

drastically different from the changes in transcriptome profile. This was consistent with and supported the idea of transcriptome-translatome mismatches. GO analysis of differentially expressed genes after TAC revealed that translation of metabolic and heart development genes is among the top DEGs, which is different from ECM and angiogenesis genes found in the RNA-seq dataset. Ten gene clusters were identified by comparing data in both omics, including genes that are translationally up or down regulated and those who are involved in immediate early response to the hypertrophic stress. Interestingly, this study identified regulatory upstream open reading frames (uORFs) as translational repressors during the development of cardiac hypertrophy.

1.3.3 uORF as translation regulators

uORFs are defined as the open reading frames in the 5'UTR region of an mRNA. uORFs usually can repress translation efficiency of mRNAs and are therefore considered as cis-regulatory elements of translation[45]. In heart, uORFs were found to regulate translation efficiency independently from translation rates[17]. In the study done by Doroudgar et al., by examining uORFs identified in Ribo-seq, they found that transcripts with conserved uORFs tend to be less translated in TAC-induced hypertrophic stress[40]. Particularly, the translation profile of two known regulators of metabolism, Fnip1 and Flcn, were found to be repressed by uORFs without changes in their mRNA expression level.

1.3.4 Translation Initiation

Translation initiation is the most tightly regulated and rate-limiting step of protein synthesis. The canonical pathway of eukaryotic translation builds upon the model of ribosome scanning of mRNA transcript for the AUG start codon, which is very well established[46]. Generally, the eIF2-GTP-Met-tRNA$^{Met}_{i}$ ternary complex will bind to the 40S small

ribosomal subunit, forming the 43S preinitiation complex (PIC). The m^7G cap of mRNA transcript recruits eIF4F complex via its interaction with eIF4E, leading to the unwinding of the mRNA cap-proximal region in an APT-dependent manner by eIF4A (RNA helicase) together with eIF4B. Poly(A) binding protein C1 (PABPC1) links the poly(A) tail and eIF4G, bending the mRNA into a circularized structure and forms the 48S complex [47]. The PIC can now scan the 5'UTR region until it hit the initiation codon AUG. The 60S large ribosomal subunit then joins the 48S complex, forming the 80S ribosome when the eIF5-mediated hydrolysis of eIF2-bound GTP and P_i release occurs concomitantly. Finally, the hydrolysis of eIF5B-bound GTP occurs, leading to the release of eIF5B and eIF1A from the complex. The 80S ribosome can now move to the elongation step.

Since eIF4E specifically binds to the m^7G cap and mediates the binding between eIF4F complex and RNA[48-50], eIF4E is considered as one of the critical players in regulating cap-dependent translation. Properly regulated eIF4E expression and activity is important for normal cell growth and cellular functions. It is known that eIF4E expression is upregulated during hypertrophic growth of cardiac myocytes, which is in concomitant with increased protein synthesis[51]. However, elevated eIF4E expression alone is not the whole story, as there are additional layers of regulations of this critical initiation factor. eIF4E itself can be phosphorylated by the mitogen-activated protein kinase (MAPK)-interacting serine/threonine kinase 1 and 2 (Mnk1/2), which are both the substrates of Erk1/2 and p38 MAPKs[52, 53]. Although such phosphorylation has been shown to be not required for increased protein synthesis during cell growth in many tissues [52, 54, 55], studies have discovered that eIF4E phosphorylation by Mnk can preferentially promote translation of certain RNA species containing both a cap and 5'-terminal RNA

duplex (hairpin) *in vitro*, implying a potential selectivity associated with such phosphorylation[56]. Indeed, a previous study induced acute pressure overload mice using transverse aortic constriction (TAC) and screened for candidate mRNAs whose translation are selectively regulated because of their complicated 5'-UTR structure[57]. In response to LV pressure overload, 6 mRNAs were identified to have higher translation activity marked by their mobilization into polysomes without significant changes in mRNA abundance.

Another important new player discovered that regulates translation initiation in heart is PABPC1. PABPC1, as discussed above, binds to eIF4G and poly(A) tail and brings mRNA into a circularized shape. It is known to be important in translation initiation[58], termination[59], and mRNA stability[60, 61], but its specific role in translation regulation in the heart during hypertrophic growth was not unclear. A recent study by Chorghade et al. characterized PABPC1 as a direct regulator of cardiac hypertrophy[62]. In human and mice, PABPC1 protein expression was high before birth but dropped significantly after birth without changes at mRNA level. Its protein expression was found to be positively correlated with the length of its poly(A) tail, which is restored during hypertrophic stress. Re-expressed PABPC1 protein stimulated by hypertrophic stress regulates protein synthesis by interacting with eIF4G1, demonstrating a novel role of PABPC1 in translation regulation in hypertrophic hearts.

1.3.5 Translation Elongation

Translation elongation refers to the process when ribosome moves along the mRNA and add amino acids to the elongating polypeptide chain. Although this is not considered as the rate-limiting step of translation, it still requires close cooperation of aminoacyl tRNA,

aminoacyl-tRNA synthase, and multiple elongation factors to maintain appropriate protein synthesis. For example, the eukaryotic elongation factor 2 (eEF2) is important in the synthesis of polypeptide chain. Its activity can be inhibited by eEF2 kinase (eEF2k), leading to downregulation of protein synthesis[63]. In addition, eEF2k itself can also be phosphorylated by S6K1[64] in an mTOR-depend manner and AMP-activated protein kinase (AMPK) in an mTOR-independent manner[65]. On the other hand, eEF2 phosphorylation can be reversed and activated by protein phosphatase 2A (PP2A) during Angiotensin II administration, leading to increase protein synthesis in cardiomyocytes and cardiac hypertrophy[66, 67]. Recent study has shown that the tight coordination of expression and phosphorylation of eEF2 and eEF2k may be essential in hypertrophied cardiomyocytes, and eEF2k-eEF2 signaling could act as a potential regulator of cardiac hypertrophy[68].

1.3.6 mTOR Signaling

Another critical factor regulating translation in the heart is the mechanistic (or mammalian) target of rapamycin (mTOR). mTOR is the master regulator of protein synthesis, autophagy, and metabolism[69-71] by promoting anabolic processes and inhibiting catabolic processes. In cardiomyocytes, it is well appreciated that mTOR is crucial in maintaining cell integrity, growth, metabolism, and homeostasis across different developmental stages[72]. It consists of two multiprotein complexes called mTOR complex 1 (mTORC1) and 2 (mTORC2). Although mTORC2 is tightly connected to mTORC1 and is essential in maintaining cell viability, growth, and cardiac function [73-75], there is no direct evidence showing its association with protein synthesis regulation. Therefore, this review will focus mainly on mTORC1, as it is considered the main regulator

of cardiac hypertrophy via protein synthesis. In general, mTORC1 can be activated by various hypertrophic stimuli such as β-adrenergic stimulation, pressure overload, angiotensin II and IGF-1. Its activation is considered a double-edged sword. During pressure overload, mTORC1 is necessary for the compensatory response to maintain proper cardiac function. Previous studies have found that disrupting mTORC1 in mice will significantly impair adaptive hypertrophy and myocyte survival, eventually leading to heart failure[76, 77]. However, it could also lead to pathological cardiac hypertrophy if not properly regulated. Many studies have proved that inhibiting mTORC1 can ameliorates load-induced cardiac hypertrophy in mice[78, 79]. mTORC1 regulates proteins synthesis by mainly via ribosomal S6 kinase (S6K1) and eIF4E-binding protein-1 (4E-BP1).

S6K1 is considered the “positive” regulator for protein synthesis. S6K1 gene variants in human were reported to cause hypertrophic cardiomyopathy (HCM) by hyper-phosphorylating Rps6 and ERK1/2 signaling cascade[80]. mTORC1 can activate S6K1 by phosphorylating it at Thr389. Such phosphorylation will activate the kinase activity of S6K1, which can then phosphorylate its substrate eIF4B that can be recruited to the eIF3 translation initiation complex[81]. It can also inhibit programmed cell death 4 (PDCD4), which is a protein that can inhibit eIF4B incorporation into the translation initiation complex[82]. Another substrate of S6K1 is ribosomal protein S6. Previous studies have pointed out that it may facilitate the transcription of ribosomal genes [83] and the translation of mRNAs containing 5’-terminal oligopyrimidine (5’-TOP) sequences, which mainly includes ribosomal genes and translation elongation factors[84]. This is, however, challenged by other studies later on by a study showed that the preferential induction of TOP mRNA translation is fully dependent on PI3K signaling and is independent of S6K1

and Rps6 phosphorylation[85]. Furthermore, disrupting all serine residues of S6 that can be phosphorylated does not incur any defects in translation[86]. Therefore, the function of S6K1-mediated phosphorylation remains highly controversial, and more studies are required for a better understanding of this process. Recently, a new study identified G protein-coupled receptor 39 (GPR39) as an upstream player that can promote cardiac hypertrophy via regulating the AMPK-mTOR-S6K1 signaling pathway. GPR39 can repress AMPK activation, leading to higher mTOR and S6K1 activity and protein synthesis[87].

On the other hand, 4E-BP1 is known as the translation repressor. It can bind to and sequester eIF4E to prevent the formation of eIF4F complex, which is critical for translation initiation. When mTORC1 is activated by upstream stimuli, 4E-BP1 will be phosphorylated at multiple residues, leading to the loss of its binding ability with eIF4E and the induction of active protein synthesis[88-90]. Inhibiting 4E-BP1 in cardiomyocytes leads to increased protein synthesis, proving that mTORC1 is necessary for protein synthesis[76, 91].

1.3.7 m6A RNA Methylation

N6-adenosine methylation (m6A) of RNA transcripts, the most prevalent epigenetic modification of RNA[92], has been an emerging hot area of research in epi-transcriptomic regulation. In the past decade, more and more studies have demonstrated that m6A modification is also closely linked to the development of various cardiovascular diseases. Global m6A RNA methylation landscape was found to be altered in many cardiovascular disorders, including hypoxia[93, 94], cardiac hypertrophy, and heart failure[95-99], leading to aberrant hyper- or hypomethylation of certain mRNA species and consequently, disease progression. Although many studies agree that proper m6A methylation is critical

for maintaining normal cardiac function, different mechanisms of its functionality have been proposed. One study by Mathiyalagan el al. links m6A methylation of cardiac mRNAs to their stability in heart failure[98]. This study observed a transcriptome-wide hypermethylation post-MI due to the downregulation of demethylase FTO, which leads to decreased stability of mRNAs of selective cardiac pathways such as cardiac hypertrophy, muscle contraction, filament sliding, and sarcomere organization. This is consistent with a previous study showing that m6A can be selectively recognized in mammalian cells by the “reader” protein YTHDF2, which can bring bound mRNA to mRNA decay sites[100]. More recent studies indeed have observed an increased YTHDF2 (but not YTHDF1 or YTHDF3) expression in human heart failure samples[96, 101]. Mechanistically, YTHDF2 can bind to and regulate the stability of Myh7[101] and Eef2 mRNA[102], which are both important in cardiac growth and remodeling. On the other hand, however, an exciting study from Berulava et al. demonstrated that altered m6A methylation in heart failure promotes the corresponding mRNA translation without affecting mRNA stability[95]. Using Methylated RNA Immunoprecipitation and Next-Generation Sequencing (MeRIP-seq) and polysome profiling, they found that m6A methylation level of mRNA transcripts is positively correlated with their corresponding polysome binding level in both mouse and human heart failure without changes in total mRNA abundance. This is consistent with a previous finding that 5’UTR m6A can promote cap-independent translation by interacting with eIF3[103]. The discrepancies between these two mechanisms proposed may arise from the different animal and disease models used. More research needs to be done to address if these mechanisms are in parallel to each other.

1.4 Translation Capacity

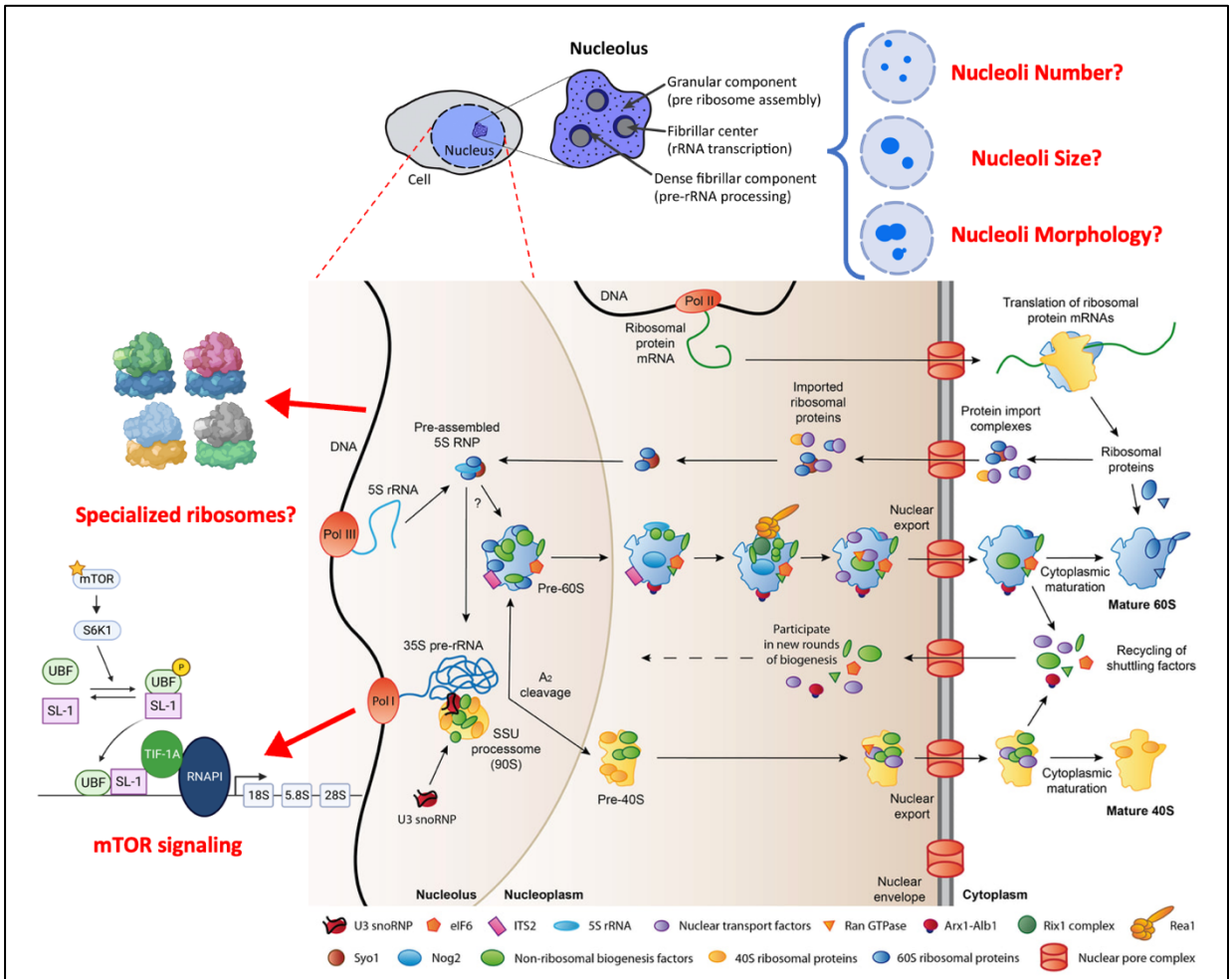

Figure 1-4. Overview of translation capacity regulation in cardiac hypertrophy. Modified from Ref [104] and Ref [118].

1.4.1 General Overview

Translation capacity mainly refers to the synthesis of translation machinery – the ribosome. Ribosome biogenesis is a tightly regulated and extremely complicated process that requires cooperation and coordination among many different steps[104]. The abundance of mature, available ribosomes in cells are determinant to the translation capacity at the very moment. Generally, ribosomal DNA (rDNA) was transcribed into ribosomal RNA (rRNA) first by RNA polymerase I (RNAPI) in the nucleolus and spliced into 18S, 5.8S, and 28S. One exception is 5S, which is transcribed by RNA polymerase

III instead. Simultaneously, ribosomal proteins (RP) translated in the cytoplasm are transported back into the nucleolus. RP and rRNA are assembled in the nucleolus with help of many assembly factors and small nucleolar RNA (snoRNA). Shuttling factors transport pre-60S and pre-40S ribosome subunits out into the cytoplasm to be assembled into the mature, translating 80S ribosome (**Figure 1-4**).

1.4.2 Ribosome Biogenesis

Eukaryotic ribosome consists of 4 ribosomal RNAs (rRNAs) and approximately 80 ribosomal proteins (RP). Its biogenesis and assembly take place in the nucleolus and require the close coordination of rRNAs, ribosomal proteins, small nucleolar RNAs (snoRNAs), as well as many assembly factors and biogenesis factors.

The ribosomal DNA (rDNA) transcription is the very first step of ribosomal biogenesis and is tightly regulated. Increased rRNA synthesis was observed in cultured neonatal cardiac myocytes during hypertrophic growth[105]. The upstream binding factor (UBF), a member of the high mobility group (HMG) box protein family, is known as a trans-activator of RNAPI that facilitates rDNA transcription. Increased UBF expression was observed in hypertrophic growth in the heart via increased rDNA transcription and thus ribosome biogenesis[106-108]. Overexpression of UBF was found to be sufficient to increase rRNA transcription in neonatal cardiomyocytes[109]. Disrupting UBF expression using antisense RNA abolished increased protein synthesis and hypertrophic growth in cultured cardiomyocytes[106].

SL-1 is a protein complex that consists of TATA-binding protein (TBP) and 3 TBP-binding factors (TAFs) that is specifically required for rDNA transcription. It stabilizes UBF's binding at rRNA promoter region and recruits RNAPI, directing the formation of RNAPI

pre-initiation complex formation[110]. The phosphorylation status of UBF determines its binding with SL-1. UBF/SL-1 binding is promoted when UBF is hyper-phosphorylated and vice versa in the condition of hypo-phosphorylation, showing its important role in growth-induced rRNA transcription[111-113]. In the heart, UBF phosphorylation was found to be associated with endothelin-1-induced cardiac hypertrophy in cultured neonatal cardiomyocytes[114]. Mechanistically, UBF can regulate the number of active ribosomal RNA genes in mammals by controlling the formation of active rDNA chromatin[115].

UBF phosphorylation was shown to be regulated by S6K1, which is a well-characterized downstream target of mTOR. S6K1 activity was known to be essential in regulating ribosome biogenesis, especially via regulation of rDNA transcription[116]. Previous study observed rapid de-phosphorylation of UBF and its dissociation from SL-1 during rapamycin treatment *in vitro*, which could be rescued by re-expression of recombinant phosphorylated UBF but not hypo-phosphorylated UBF, reiterating the importance of mTOR-mediated S6K1 activation in ribosomal biogenesis[117].

1.4.3 Nucleolus Dynamics

Nucleolus is the center of ribosome biogenesis. It consists of three different parts: the dense fibrillar component (DFC, pre-rRNA processing), the fibrillar center (FC, rRNA transcription), and the granular component (GC, pre ribosome assembly)[118]. Nucleolus usually works as a stress sensor, and its morphology and organization are highly dynamic during cellular growth[119]. Two main parameters of nucleolus dynamics are size and number. Early study has found that in myocardial nuclei, nucleolar number tends to be slightly higher in larger hearts[120]. On the other hand, the size of nucleolus is positively correlated with rRNA synthesis[118]. In cancer, nucleolus becomes hypertrophic during

growth stimulation, leading to higher rRNA transcription and ribosomal assembly[121]. Enlarged nucleoli are also observed in human hearts during hypertrophy, which indicates increased rRNA synthesis [122, 123]. Nucleolar organization and morphology were significantly altered in patients with ischemic (ICM) or dilated cardiomyopathy (DCM) as well, implying changes in ribosome biogenesis. Both nucleus and nucleolus sizes increased in hear failure[124]. However, the molecular mechanism and underlying player regulating the dynamics of nucleolus remains poorly understood for the last decade. A recent study demonstrated that nucleosome assembly protein 1 like 5 (Nap1l5) can regulate cardiomyocyte hypertrophy by promoting nucleolar hypertrophy, ribosome assembly, and subsequent protein synthesis. Mechanistically, interactome analysis of Nap1l5 implies its potential binding with several ribosome assembly and transport factors, but more studies need to be done to fully characterize and validate the molecular mechanism[125].

1.4.4 Ribosome Heterogeneity

In 1958, Francis Crick proposed the “One gene-one ribosome-one protein” hypothesis of translation, providing a model in which each ribosome carries the genetic information for each protein[126]. Although we now know that this is untrue, this bold statement really echoed with the heterogeneity in ribosomes that people started to observe and appreciate in the last decade. After his hypothesis was discredited, ribosomes have been widely considered as honest and conserved machineries that are all identical and can produce proteins strictly based on mRNA templates among in all cell types. This idea has been prevalent until 1980s and 1990s when differentially expressed ribosomal proteins and/or rRNAs was observed in multiple model organisms[127-129]. A recent study by Shi et al.

made a ground-breaking discovery by showing direct evidence of ribosome heterogeneity. Taking advantage of selected reaction monitoring (SRM)-based proteomics, they did absolute quantification of selected RPs in mouse embryonic stem cells. The stoichiometry reveals a shockingly heterogenous population of RPs in actively translating ribosomes. Particularly, RPS25 or RPL10A- containing ribosomes were found to preferentially translate a distinct subset of mRNAs, demonstrating the functional impact of different ribosomal compositions[130].

To date, there are a few studies looking at ribosome specialization in skeletal muscles. Unfortunately, ribosome heterogeneity was very poorly studied in heart, let alone in the setting of cardiac hypertrophy. Although only a minimal number of variations were found for 80-90% of RP genes across different tissues in human, there were indeed a few that showed robust tissue specificity, including Rpl3-like (Rpl3l)[131]. Rpl3l was discovered as a paralog to Rpl3 with around 74% sequence identity. Interesting, unlike ubiquitous expression of Rpl3, Rpl3l is exclusively expressed in skeletal muscle and cardiac muscle[132]. Rpl3l expression decreased upon hypertrophic stimuli in skeletal muscles. It was characterized as a negative regulator of muscle growth and was found to impair myotube growth[133]. Knocking down Rpl3l was found to be protective in mice with muscular dystrophy[134]. The mechanism, however, remains unclear.

In the past few years, mutations in Rpl3l has found to be associated with many cardiac complications, such as dilated cardiomyopathy (DCM) [135-137], ventricular tachycardia[138], and atrial fibrillation[139]. Knocking out Rpl3l showed no obvious phenotypes except increased heart weight when they were aged, mainly because the loss of Rpl3l were compensated by increased Rpl3 expression[140]. Consistent with this

dynamic interplay observed between Rpl3l and Rpl3, a very recent study using Ribo-seq and ribosome pulldown followed by Nanopore sequencing (Nano-TRAP) showed that rpl3l depletion can lead to increased production of Rpl3-containing ribosomes[141]. Although Rpl3l was found not to change translation efficiency or preference, depleting it can lead to altered ribosome-mitochondria interactions and mitochondrial activity in cardiomyocytes. This working model of Rpl3l-mediated spatial-temporal regulation of ribosome subcellular localization is very intriguing and puzzling. Future studies will be needed to fully characterize its role in cardiomyocytes with potential molecular mechanism linked to translation regulation.

1.5 Spatial Dynamics of Translation

1.5.1 General Overview

Sarcomere is the basic cardiac contractile unit in cardiomyocytes. It is a complex consists of many different proteins that are arranged with distinct localization and stoichiometry to function properly. During hypertrophy where there is an increase in heart weight and size, new sarcomeric proteins need to be added with proper spatial distribution in a timely manner to support cardiomyocyte growth. Indeed, subcellular localization of mRNA transcripts have been observed in various organisms and cell types, ranging from S. cerevisiae to mammalian neurons[142]. In neurons where some cellular compartments, such as axons and dendrites, are far away from the nucleus, it is well-established that local protein synthesis is critical to maintain normal cell function and plasticity[143]. In cardiomyocytes, subcellular localization of sarcomere mRNA has been observed in a few pioneering studies as well[144, 145], but the development of technologies nowadays

allows a closer examination of the dynamics of local translation with a much higher resolution at the subcellular level.

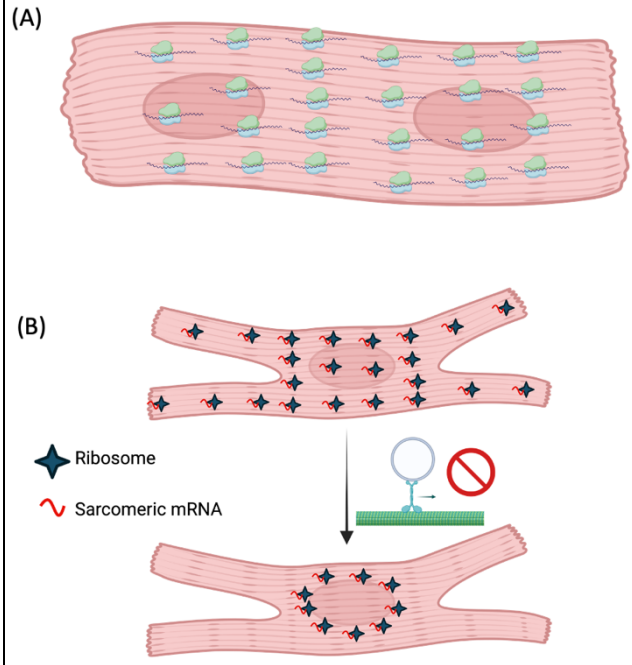

Figure 1-5. Overview of spatial-temporal regulation of translation in heart. **(A)** Ribosome and sarcomeric mRNAs co-localize at Z-band in cardiomyocytes. **(B)** Transportation of translation machinery and mRNAs is dependent on microtubules.

1.5.2 Spatial specific protein translation in cardiomyocytes

Previous study from Lewis et al. studied the mechanisms of sarcomere maintenance in cardiomyocytes. Using single molecule mRNA fluorescence in situ hybridization (smFISH), they observed that sarcomeric mRNA, ribosomes, and E3 ubiquitin ligase all localize to protein translation hotspots marked by O-propargyl-puromycin (OPP) incorporation on sarcomeres[146], supporting such local translation model in cardiomyocytes. They also demonstrated that such transport is cytoskeletal-dependent. However, this study only focused on sarcomere maintenances and did not address this issue under any stressed conditions, especially cardiac hypertrophy in which cardiomyocytes are actively growing. When it comes to cardiomyocyte cytoskeleton, microtubule proliferation has been observed in concert with hypertrophy, which leads to contractile dysfunction[147-151]. Indeed, inhibiting microtubule proliferation can rescue cardiac function and block pressure overload-induced cardiac hypertrophy[152-154]. However, the detailed molecular mechanism was still not clear. A recent study done by Emily et al. built upon these

previous discoveries and coupled the proliferating cardiomyocyte microtubules with mRNA and ribosome transport in cardiac hypertrophy[155], implicating their potential role in translation regulation. They discovered that microtubules are necessary for proper sarcomeric mRNA, ribosome, and protein synthesis localization in cardiomyocytes both *in vitro* and *in vivo*, which is concomitant with hypertrophy. These cargos are transported by Kinesin-1 and accumulates in the pattern of z-discs and at the intercalated discs (ICD). Cells exposed to colchicine still showed increased protein synthesis, but the mis-localized proteins are subject to degradation. This study demonstrated that translation location, in addition to the global increase of protein synthesis, is critical for cardiac hypertrophy. Another study published in the same year also supported this microtubule-dependent transportation mechanism, in which the researchers examined the distribution of sarcolemmal (SL) and sarcoplasmic reticulum (SR) proteins synthesis hotspots in cardiomyocytes[156]. The canonical secretary protein trafficking (SPT) mechanism claims that membrane protein synthesis should take place in the perinuclear area. However, this paper observed pan-cytosolic distribution of SL and SR mRNAs together with ribosomes via mRNA-rRNA proximity-ligated in situ hybridization (MR-PLISH), with hotspots near sarcomeres. Interestingly, such transportation was also found to be dependent on microtubules.

Although there have been many major breakthroughs in understanding the transportation dynamics of translation machinery and substrates (mRNA), there are still many remaining questions pertaining to this model. For example, ribosomes and mRNAs are delivered to their destinations with high spatial precision. The molecular mechanism that determines the destination of these cargos remains unknown. Additionally, it is unclear if dynein also

involved in such transportation. Is it important in positioning the translation machinery and substrates as well? Future studies may answer these questions and potentially establish a new paradigm in spatial regulation of translation.

1.6 Perspectives

Cardiac hypertrophy refers to the abnormal thickening of the cardiac muscle and the enlargement of the whole heart contributed largely by the growth of individual cardiomyocyte in size. It was beneficial in the early stage as it compensates the loss of cardiac function triggered by various reasons. However, without medical intervention, pathological hypertrophy can quickly develop into the decompensated stage and eventually lead to heart failure. Its molecular feature has been extensively studied in the last few decades with achievements in some therapeutics, such as angiotensin-aldosterone system (RAAS) blockers, β-blockers, and calcium channel blockers[7]. Translation regulation in cardiac hypertrophy, however, remains poorly understood. Many recent studies both within and without cardiomyocytes and cardiovascular diseases have revealed previously unrecognized transcriptome-translatome mismatches, indicating a specific layer of protein synthesis regulation and a dire need to understand functional impacts and mechanisms of translatome changes independent from transcriptome. Thanks to the rapid development of technology with different readouts, we can now closely examine translation regulation with significantly higher resolution and many different aspects.

Both translation efficiency and capacity are dynamically regulated in cardiac hypertrophy. Translation efficiency is tightly controlled signaling pathways, translation initiation, elongation, and termination. The m6A medication of mRNAs has recently been

characterized to be associated with translation efficiency particularly in heart failures. This mRNA modification has a lot of variations between tissue types and disease models, especially regarding its molecular mechanisms and specific molecules as underlying players. Future studies need to be done to fully address this highly controversial molecular process.

On the other hand, translation capacity refers to the availability and biogenesis of the translation machinery itself. Ribosome biogenesis is consistently upregulated in hypertrophic response, eluding that increased protein synthesis is predominantly dependent on the *de novo* ribosome biogenesis during stress conditions. Ribosome biogenesis can be reflected by the integrity and dynamics of nucleolus. Size, number, and morphology changes in nucleolus are some key features that can be, and already have been developed as potent biomarkers for ribosome biogenesis. At the same time, ribosome heterogeneity became more and more appreciated, and it may be crucial in differentially and dynamically regulated translation upon hypertrophic stress. We are currently extremely ignorant in this area, and future studies need to address some imperative questions, such as specialized ribosomes in different tissues, cell types, disease conditions, and their potential functional impacts in cellular and organ level.

The spatial-temporal regulation of translation is a novel yet rapidly emerging field of research, especially in the context of cardiac hypertrophy and cardiomyocyte growth. Technologies such as RNAscope and smFISH allowed us to directly visualize such dynamic process. It is well appreciated nowadays that in cardiac myocytes, proper cellular localization of mRNA and ribosomes are necessary for maintaining cellular structure and

function, especially during growth stress. This is a new paradigm to be established in translation regulation.

1.7 Thesis Goal

Cardiac hypertrophy is the summation and consequence of a series of molecular events. Translation regulation in cardiac hypertrophy is particularly understudied. Recent progress on discovering the mismatch between translatome and transcriptome reiterated the importance and dire need of understanding translation regulation during hypertrophic stress. In this thesis, we aim to examine changes in translation landscape during pathological cardiac hypertrophy and how translation can be regulated upon hypertrophic stress from many different aspects, including translation efficiency, translation capacity, and spatial-temporal regulation of translation machinery. We aim to uncover the molecular player mediating the translatome profile and investigate the molecular mechanism. The regulatory molecule and its mechanism of action identified may shed light on potential therapeutic targets to treat patients with cardiac hypertrophy and heart failure.

CHAPTER II. ESTABLISHING PROTEIN SYNTHESIS PROFILE DURING HYPERTROPHIC STRESS

2.1 Introduction

Although it is established that global protein synthesis significantly increases during cardiac hypertrophy to support growth of the myocardium, translation is an extremely dynamic process with multiple layers of regulations, rather than a simple, unidirectional increase throughout. Our current knowledge on the striking mismatch between transcriptome and translatome really brings translation regulation into our visions. With limited resources available, cells need to prioritize the translation of some proteins and tune down that of the other species. It is crucial for us to understand translation dynamics in two dimensions: proteins species, and time. In this chapter, we examined the global translation profile after PE-induced hypertrophic stress and showed significant translatome reprogramming both in vitro and in vivo upon hypertrophic stress. We also monitored ribosome compositions using proteomics analysis which helped identified significant shifts in stoichiometries of ribosomal proteins. This strongly supported the ribosomal heterogeneity theory, especially in heart where very few related studies have been done before.

2.2 Materials and Methods

2.2.1 Animals

All experimental procedures involving animals in this study were reviewed and approved by the Institutional Animal Care and Use Committees (IACUCs) of University of California at Los Angeles (UCLA) and conformed to the Guide for the Care and Use of laboratory Animals, published by the US National Institutes of Health. Phenylephrine was

administered using tail vein injection. TRAP mice generated by William Pu's lab[41] were mated with Mlc2a-Cre mice to achieve cardiomyocyte-specific ribosome labeling. Animals were euthanized and sacrificed using cervical dislocation before dissections. All mice were housed in a room maintained at 23±1°C and 55±5% humidity with a 12-h light-dark cycle and given ad libitum access to food and water.

2.2.2 Cell cultures

Neonatal rat ventricular myocytes (NRVMs) were prepared and cultured in Dulbecco's modified Eagle's medium (DMEM) supplemented with Corning® ITS + Premix Universal Culture Supplement (Corning) at 1:100 dilution, 100U/mL penicillin and 100μg/mL streptomycin for 24 hours before any treatment. To inhibit mTOR, cells were pre-treated with 20nM rapamycin for 3 hours. To inhibit ribosome biogenesis, cells were treated with 1μM BMH-21 for 1 hours. Phenylephrine (PE) at 100μM were administered to induce hypertrophic stress.

2.2.3 Surface Sensing of Translation (SUnSET)

SUnSET assay was performed as previously described to label newly synthesized proteins in NRVMs[18]. Cells were incubated with 1μg/mL puromycin for 20 minutes before two PBS washes followed by 20 minutes chase in normal culture media.

2.2.4 Western blotting

Cells were washed twice in ice-cold PBS and harvested in protein lysis buffer (50mM HEPES pH 7.4, 150mM NaCl, 1% Triton X-100, 1mM EDTA, 1mM EGTA, 1mM glycerophosphate, 2.5mM sodium pyrophosphate, 1mM sodium orthovanadate, 20mM NaF, 1mM PMSF, 1mM DTT, 1x cOmplete protease inhibitor (Roche)) using a cell scraper. Protein concentration was measured using Pierce BCA Protein Assay Kit (Thermo Fisher

Scientific) before mixing with NuPAGE LDS Sample Buffer (Thermo Fisher Scientific) and 1% Beta-Mercaptoethanol. Protein samples were separated using NuPAGE 4-12% Bis-Tris Protein Gels (Invitrogen) before transferred to PVDF membranes for blotting. Total protein was measure using Oriole Fluorescent Gel Strain (Bio-Rad).

2.2.5 Newly synthesized protein labeling

Newly synthesized proteins were labeled and analyzed as described before with modifications[157]. Cells were incubated labeled with Azidohomoalanine (Click Chemistry Tools) at 1mM for 1 hour before rinsed twice with ice-cold PBS. Cells were then harvested using a cell scraper and resuspended in lysis buffer (1x cOmplete protease inhibitor (Roche) in PBS). Samples were then sonicated using Fisherbrand Model 705 Sonic Dismembrator (Fisher Scientific) for 10 seconds on ice followed by 1 minute incubation on ice. This sonication cycle was repeated four times. Samples were centrifuged at 21,000g for 10 minutes at 4°C. Supernatant was saved, and the pellets were resuspend using in 0.5% (wt/vol) SDS in PBS and boiled for 10 minutes at 100°C. They were then combined with the supernatant saved in the previous step. Protein concentrations were measured using Pierce BCA Protein Assay Kit (Thermo Fisher Scientific). The same amount of protein was used for each sample and aliquoted into 10 different fractions for Click chemistry reaction. For each reaction, assemble the reaction mix in order (100μm TBTA (Sigma), 1mM Copper Sulfate (Sigma), 100μm Biotin-PEG4-alkyne (Sigma), and 1mM TCEP (Sigma)) and added to the aliquoted protein samples. Each reaction volume was brought up to 400μl using PBS. Samples were vortexed and incubated at room temperature for 60 minutes, with anther vortex at 30 minutes. After Click chemistry reaction, aliquoted reactions from the same sample were combined and proceed to TCA

precipitation. TCA (Sigma) were added to reaction mixture at 1:4 (vol/vol) ratio and incubated overnight at 4°C. Samples were then centrifuged at 3,000g for 30 minutes at 4°C. The pellets were resuspended and washed with ice-cold acetone before centrifuged at 17,000g for 10 minutes at 4°C. The pellets were dried at room temperature for at least 30 minutes before proceeding to streptavidin enrichment. Pellets were resuspended and dissolved in PBS/BSA (PBS, pH7.4 containing 0.01% (w/v) BSA). Sonication may be used if pellet is hard to dissolve. Dynabeads MyOne Stretavidin T1 beads (Invitrogen) were used to enrich biotinylated proteins following manufacture's protocol. After the last washing step, beads were resuspended in the elution buffer (8M urea, 100mM Tris [pH8.5]) before proceeding to on-bead digestion.

2.2.6 Digestion and Desalting

Samples were mixed with same volume of digestion buffer (8M Urea, 0.1M Tris-HCl pH 8.5), then each sample was reduced and alkylated via sequential 20-minute incubations with 5 mM TCEP and 10 mM iodoacetamide at room temperature in the dark while being mixed at 1200 rpm in an Eppendorf thermomixer. 6 µl of carboxylate-modified magnetic beads (CMMB and also widely known as SP31) was added to each sample. Ethanol was added to a concentration of 50% to induce protein binding to CMMB. CMMB were washed 3 times with 80% ethanol and then resuspended with 50µl 50mM TEAB.

The protein was digested overnight with 0.1 µg LysC (Promega) and 0.8 µg trypsin (Pierce) at 37 °C. Following digestion, 1ml of 100% acetonitrile was added to each to sample to increase the final acetonitrile concentration to over 95% to induce peptide binding to CMMB. CMMB were then washed 3 times with 100% acetonitrile and the peptide was

eluted with 50 µl of 2% DMSO. Eluted peptide samples were dried by vacuum centrifugation and reconstituted in 5% formic acid before analysis by LC-MS/MS.

2.2.7 TRAP ribosome pulldown

Phenylephrine (PE) was administered to mice via tail vein injection at 50µg/kg body weight. Heart was harvested after desired time of PE injection. Left ventricles were separated, washed twice with ice-cold PBS, and homogenized in lysis buffer (20mM HEPES KOH [pH 7.4], 5mM $MgCl_2$, 150mM KCl, 0.5mM Dithiothreitol, 1x cOmplete protease inhibitor (Roche), 100µg/ml Cycloheximide, 40 U/ml Rnasin (Fisher Scientific)) on ice using glass homogenizer, 20 strokes. Samples were centrifuged at 2,000g for 10 minutes at 4°C. 10% NP-40 (Thermo Fisher Scientific) was added to the collected supernatant and mixed thoroughly before centrifuged at 20,000g for 10 minutes at 4°C. Protein concentration was determined using Pierce BCA Protein Assay Kit (Thermo Fisher Scientific) and the same amount of proteins were used for the following immunoprecipitation for each sample. Dynabeads Protein G magnetic beads (Fisher Scientific) was washed with Low Salt Buffer (20mM HEPES KOH [pH 7.4], 5mM $MgCl_2$, 150mM KCl, 1% NP-40, 0.5mM Dithiothreitol, 100µg/ml Cycloheximide) three times both before and after incubating with Anti-GFP antibody (19C8 and 19F7, Heintz Lab) for 1 hour at room temperature.

Tissue lysate from left ventricles was incubated with antibody-bound beads for 1-hour incubation at room temperature. Beads were washed 4 times with High Salt Buffer (20mM HEPES KOH [pH 7.4], 5mM $MgCl_2$, 350mM KCl, 1% NP-40, 0.5mM Dithiothreitol, 100µg/ml Cycloheximide). For RNA-seq analysis, RNA was eluted and purified using RNeasy Kit (Qiagen) following the manufacture's protocol. For mass spectrometry, beads

were washed once with Pre-urea Wash Buffer (50mM Tris [pH8.5], 1mM EGTA, 75mM KCl) instead. Proteins were eluted by adding 100μl Urea Elution Buffer (8M Urea, 20mM Tris [pH7.5], and 100mM NaCl) and incubating for 5 minutes at room temperature with frequent agitation (900rpm). Repeat twice and combine the supernatant from all three rounds of elution.

2.2.8 TRAP RNA-seq

Libraries for RNA-Seq were prepared with Nugen Universal plus mRNA-Seq Kit (part number: 0508) to generate strand-specific RNA-seq libraries. The workflow consists of poly(A) RNA selection, RNA fragmentation and double-stranded cDNA generation using a mixture of random and oligo(dT) priming, followed by end repair to generate blunt ends, adaptor ligation, strand selection, and PCR amplification to produce the final library. Different index adaptors were used for multiplexing samples in one sequencing lane. Sequencing was performed on Illumina Hiseq 3000 for SE 1x65 bp run. Data quality check was done on Illumina SAV. Demultiplexing was performed with Illumina Bcl2fastq2 v 2.19.1.403 program.

Samples were sent for 2x50bp paired end sequencing on a Hiseq3000 instrument (Illumina). Resulting reads were demultiplexed and quality measured by fastQC followed by adaptor and low quality read trimming by seqtk (https://github.com/lh3/seqtk). Reads were aligned to the mm10 genome using Salmon 1.3[158]. Outliers were detected and removed through PCA using the ggbiplot R package (https://github.com/vqv/ggbiplot). Translation efficiencies were calculated for each sample by dividing the transcript abundance in the TRAP data vs the abundance in the INPUT datasets and differential abundances detected by benjamini-hochberg corrected

T-tests (q<0.05). Differential expression between input and MIAT KO mice were ascertained through DESEQ2[159].

2.2.9 LS-MS Acquisition

Peptide samples were separated on a 75μM ID, 25cm C18 column packed with 1.9 μM C18 particles (Dr. Maisch GmbH HPLC) using a 140-minute gradient of increasing acetonitrile concentration and injected into a Thermo Orbitrap-Fusion Lumos Tribrid mass spectrometer. MS/MS spectra were acquired using Data Dependent Acquisition (DDA) or Data Independent Acquisition (DIA) mode[160].

2.2.10 Statistical analysis

Comparisons in multiple groups were analyzed by one-way ANOVA with Dunnett's multiple comparison test. Data are presented as mean ± SEM or SD for biological

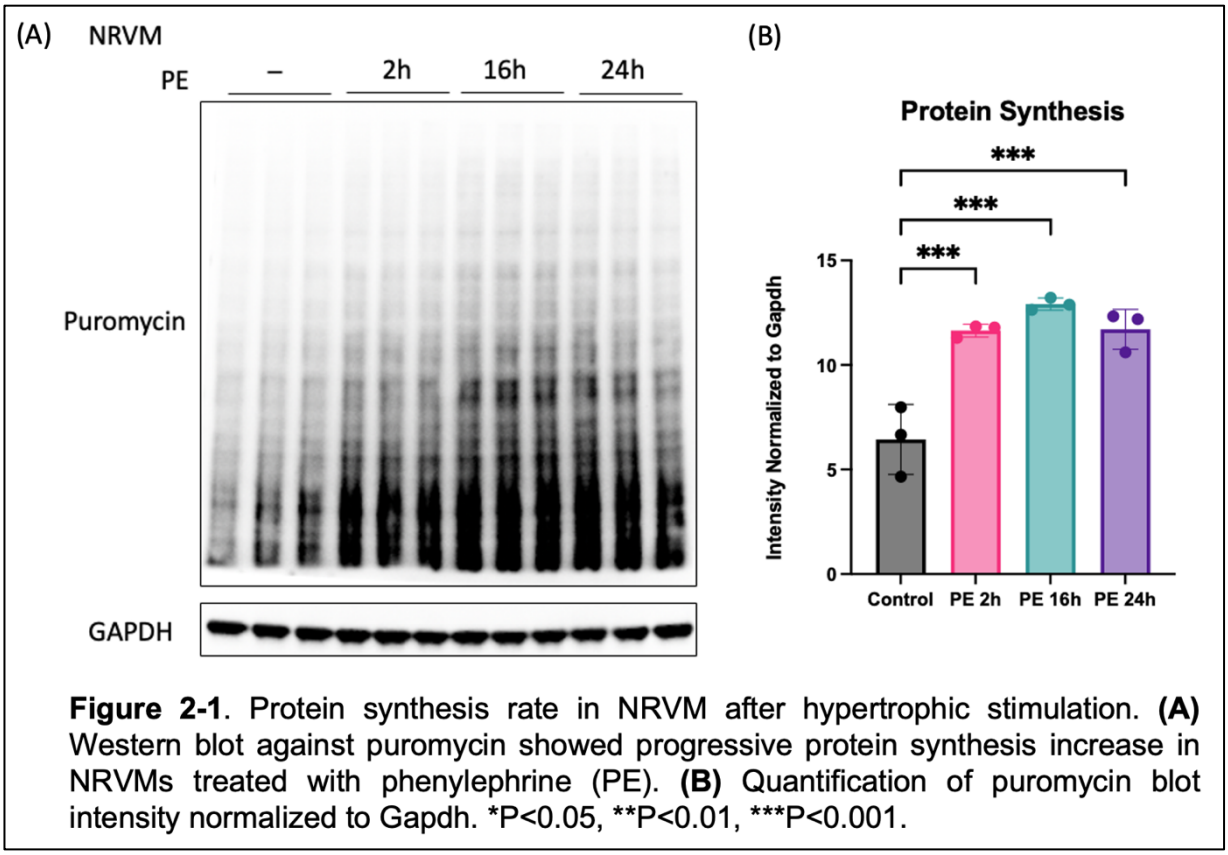

Figure 2-1. Protein synthesis rate in NRVM after hypertrophic stimulation. **(A)** Western blot against puromycin showed progressive protein synthesis increase in NRVMs treated with phenylephrine (PE). **(B)** Quantification of puromycin blot intensity normalized to Gapdh. *P<0.05, **P<0.01, ***P<0.001.

duplicates. The sample size was calculated by holding the probability of a type I error at $\alpha = 0.05$.

2.3 Results

2.3.1 Global Protein Synthesis Profile during Hypertrophic Stress

To monitor changes in global protein synthesis during hypertrophy, we used phenylephrine (PE), an α-adrenergic receptor agonist to induce hypertrophic stress in

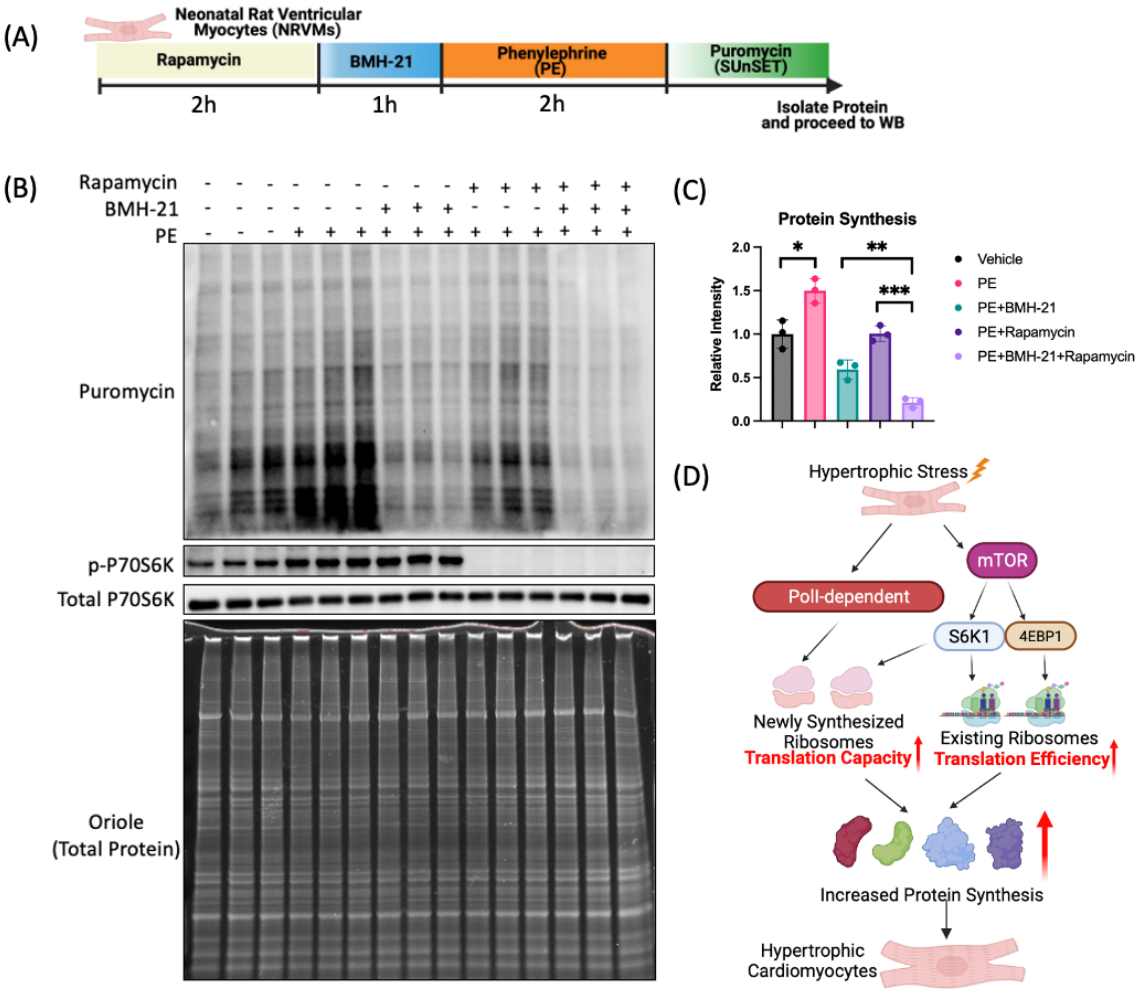

Figure 2-2. mTOR signaling-independent *de novo* ribosome biogenesis is necessary in PE-induced protein synthesis. **(A)** Schematic diagram of experimental design. **(B)** Western blot showing protein synthesis in NRVMs with different treatment. Oriole staining was used as loading control. P-P70S6K marks mTOR activation and inhibition. **(C)** Quantification of B. **(D)** Schematic diagram showing mTOR-mediated and mTOR-independent translation regulation. *P<0.05, **P<0.01, ***P<0.001.

cultured neonatal rat ventricular myocytes (NRVM). All newly synthesized proteins were labeled by puromycin incorporation using SUnSET assay and visualized by western blot using anti-puromycin antibody. We checked protein synthesis rate at different time points after PE treatment at 2 hours, 16 hours, and 24 hours. A progressive increase of protein synthesis was observed after PE was administered and peaked at 16 hours. Interestingly, protein synthesis increased significantly as early as 2 hours after PE treatment, demonstrating a very rapid cellular response in tuning up global translation **(Figure 2-1)**.

2.3.2 *De Novo* Ribosome Biogenesis is Necessary to Induce Protein Synthesis in Acute Hypertrophic Stress

mTOR is one of the most important regulators of cellular growth and protein synthesis. It mainly regulates protein synthesis via S6K1 and 4E-BP1. S6K1, when activated, can phosphorylate eIF4B and promote translation initiation. It can also regulate rRNA transcription via UBF. 4E-BP1, on the other hand, is considered as the negative regulator of translation. It can bind to and sequester eIF4E, preventing the formation of eIF4F complex to inhibit translation initiation. To see if the increased protein synthesis at 2h post PE treatment is dependent on mTOR activation, we pre-treated NRVM with rapamycin before PE-stimulated hypertrophic stress. We also used BMH-21, an RNA polymerase I (RNAPI) inhibitor, to block ribosome biogenesis via specifically inhibiting translation of rRNA without affecting other RNA species (**Figure 2-2A**). As expected, mTOR inhibition blunted increased protein synthesis after PE stimulation. Interestingly, inhibiting *de novo* ribosome biogenesis could also effectively blunt PE-induced protein synthesis at such an early time point, implying that newly synthesized ribosomes are necessary for stress-induced protein synthesis at early stage. Existing ribosomes alone could not maintain the

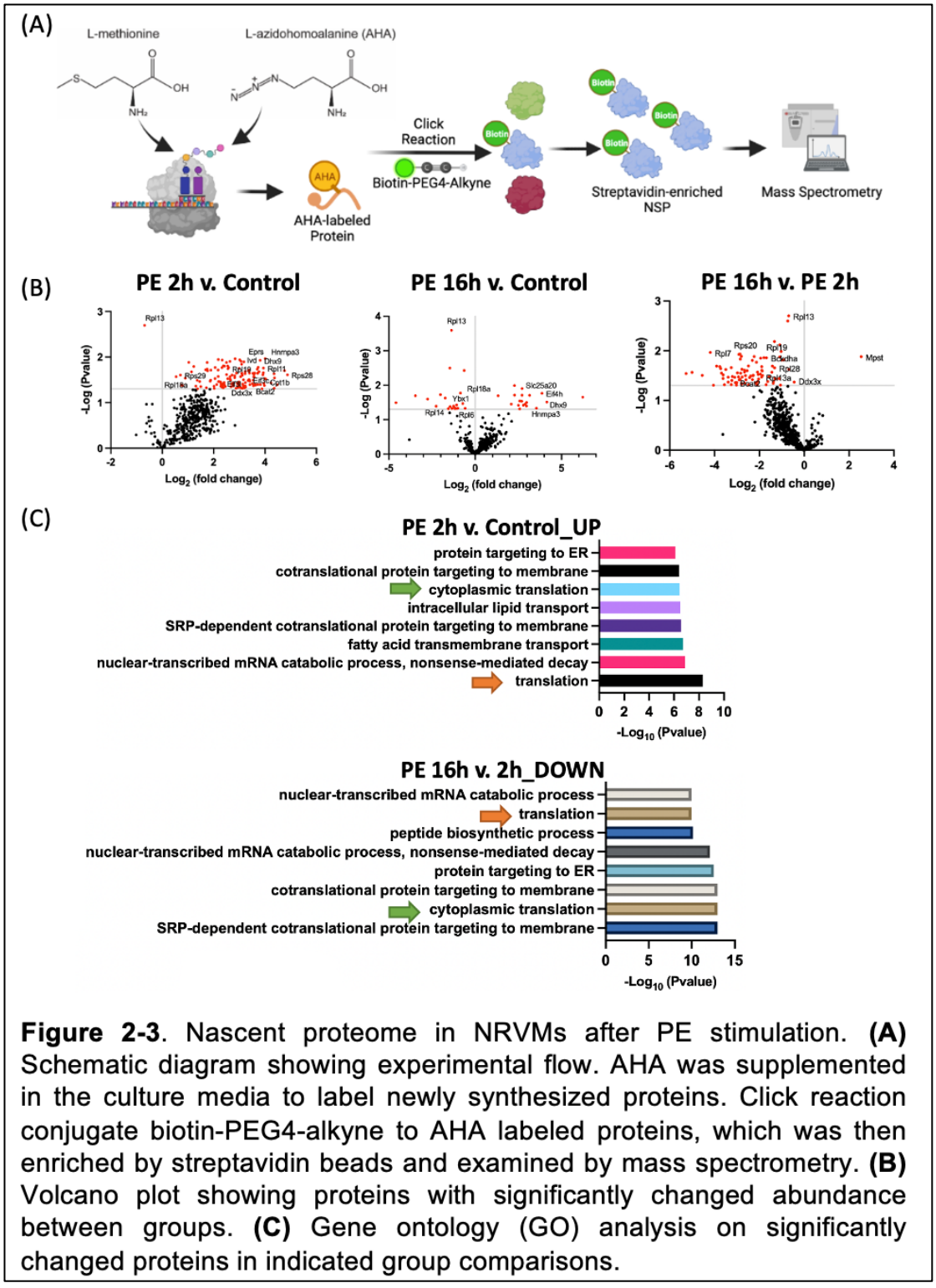

Figure 2-3. Nascent proteome in NRVMs after PE stimulation. **(A)** Schematic diagram showing experimental flow. AHA was supplemented in the culture media to label newly synthesized proteins. Click reaction conjugate biotin-PEG4-alkyne to AHA labeled proteins, which was then enriched by streptavidin beads and examined by mass spectrometry. **(B)** Volcano plot showing proteins with significantly changed abundance between groups. **(C)** Gene ontology (GO) analysis on significantly changed proteins in indicated group comparisons.

increased demand of protein synthesis in the context. Moreover, we found a further decrease of protein synthesis when mTOR signaling and ribosome biogenesis were

inhibited simultaneously (**Figure 2-2B and C**). Taken together, these data suggested that early increase of protein synthesis induced by PE stimulation is attributed to newly synthesized ribosomes but not so much to the existing ones, and this process is not entirely dependent on mTOR activation. Our data established a new paradigm that the existing ribosomes are mostly occupied at baseline, and the acute demand of protein synthesis during stress condition relies on the *de novo* ribosome biogenesis (**Figure 2-2D**).

2.3.3 Ribosomal Protein Translation is Prioritized Upon Acute Hypertrophic Stress

To examine the nascent proteome during these dynamic changes, we used non-canonical amino acids to metabolically label newly synthesized proteins. Azidohomoalanine (AHA) is a methionine analog and can be readily incorporated into the synthesizing peptide chain. NRVM was incubated with Azidohomoalanine (AHA)-containing media before harvesting. Click reaction was performed to conjugate Biotin-alkyne onto AHA labeled proteins. Streptavidin beads were used to purify this nascent protein pool, which was then examined by mass spectrometry (**Figure 2-3A**). We found a significant shift of nascent proteome after 2h of PE treatment compared to the vehicle treated group. Generally, translation of most proteins increased 2 hours after PE administration. Surprisingly, such shift was mostly reversed after 16h of PE treatment. Only a few proteins had their abundance altered compared to the control group (**Figure2-3B**). GO analysis showed that many translation and metabolism related genes were upregulated after 2 hours of PE treatment. On the other hand, many of the same terms are downregulated at 16 hours of PE treatment (**Figure 2-3C**). Indeed, these significantly changed gene groups include many ribosomal proteins and translation initiation factors.

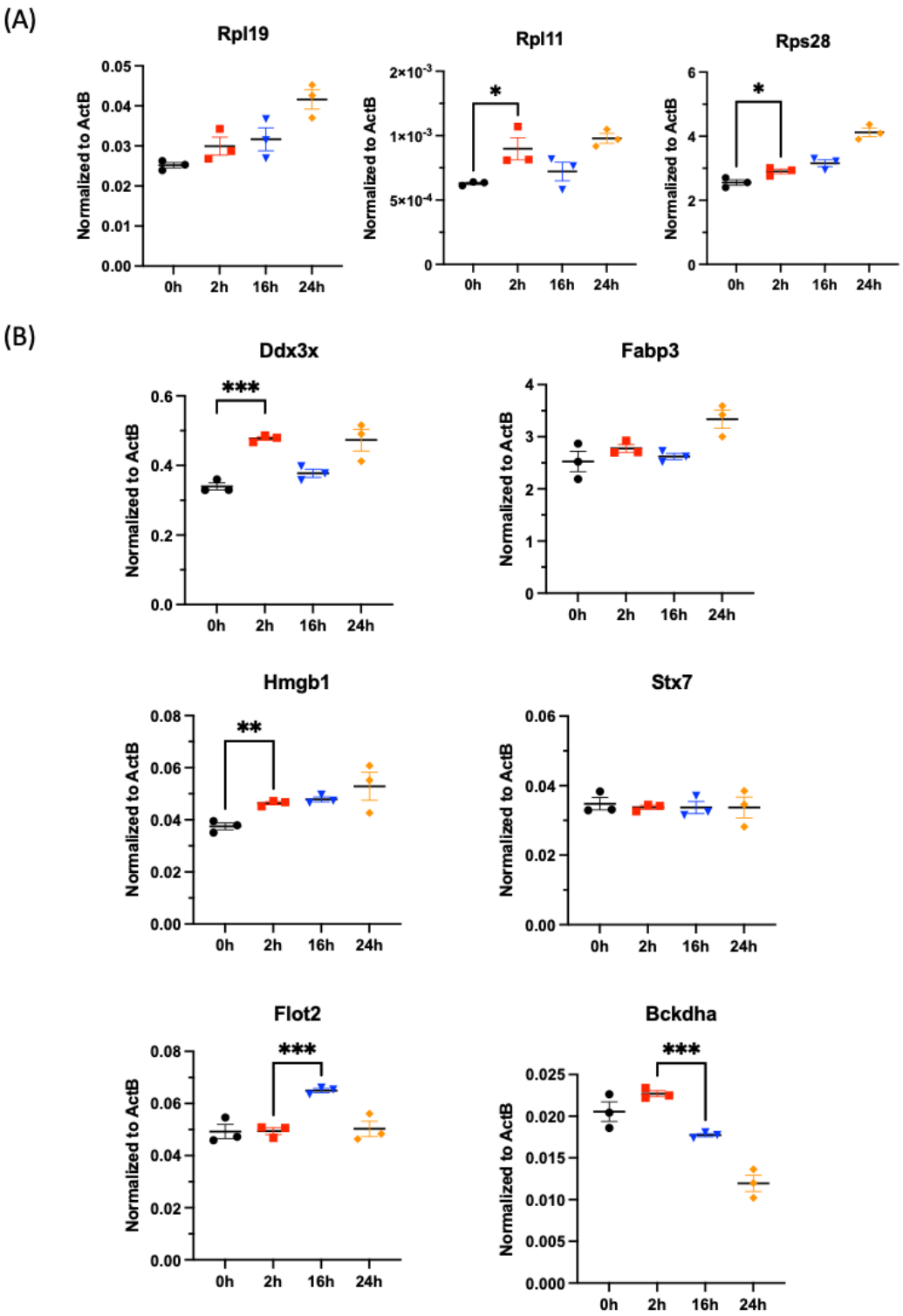

Figure 2-4. Representative gene expression at transcription level at different time points after PE treatment. qPCR results of **(A)** representative ribosomal proteins that were upregulated 2 hours after PE and **(B)** other proteins that were upregulated 2 hours after PE. *P<0.05, **P<0.01, ***P<0.001.

This demonstrated a surge of translation at early stage for translation machinery-related

and translation efficiency-related genes.

We picked out some genes with high translation activity at 2h post treatment and baseline-level translation activity at 16h post treatment and looked at their expression at transcription level. Interestingly, we found obvious disagreements of the abundance of their mRNA and newly synthesized proteins, showing translation regulations independent from transcriptome (**Figure 2-4**).

2.3.4 Cardiomyocyte-Specific Translatome Landscape

Although the above results gave us a close observation of global translation profile during hypertrophic stress, there are many different cell types involved in heart growth, with cardiomyocyte being the most abundance cell type in the heart. To closely examine translatome profile in a cell type-specific manner, we used translating ribosome affinity purification (TRAP) to pulldown ribosomes specifically in cardiomyocytes. The TRAP mice developed by William Pu's lab have a transgenic expression of GFP fused to Rpl10a driven by Cre. We crossed the TRAP mice with Mlc2a-Cre mice to isolate ribosomes and ribosome-bound, translating mRNAs selectively in cardiomyocytes (**Figure 2-5A**). These mice were injected with either saline or PE for 1.5 hours via tail vein injections before heart tissue was collected. TRAP was performed using GFP antibodies to pull down translating mRNAs. Total mRNA was extracted in parallel from the same tissue. Both fractions were QCed and sent for RNA sequencing (**Figure 2-5B**). Among all groups, gene ontology (GO) analysis on the most differentially regulated genes showed that translation and metabolism genes are the top hits. Most genes included in this GO term are ribosomal proteins. For these genes, we calculated translation efficiency (TE) by dividing the mRNA abundance pulled down by TRAP over the total mRNA abundance.

We looked at all genes identified within this GO term. The heatmap showed that the translation efficiency of these genes is differentially altered after PE injection. Some

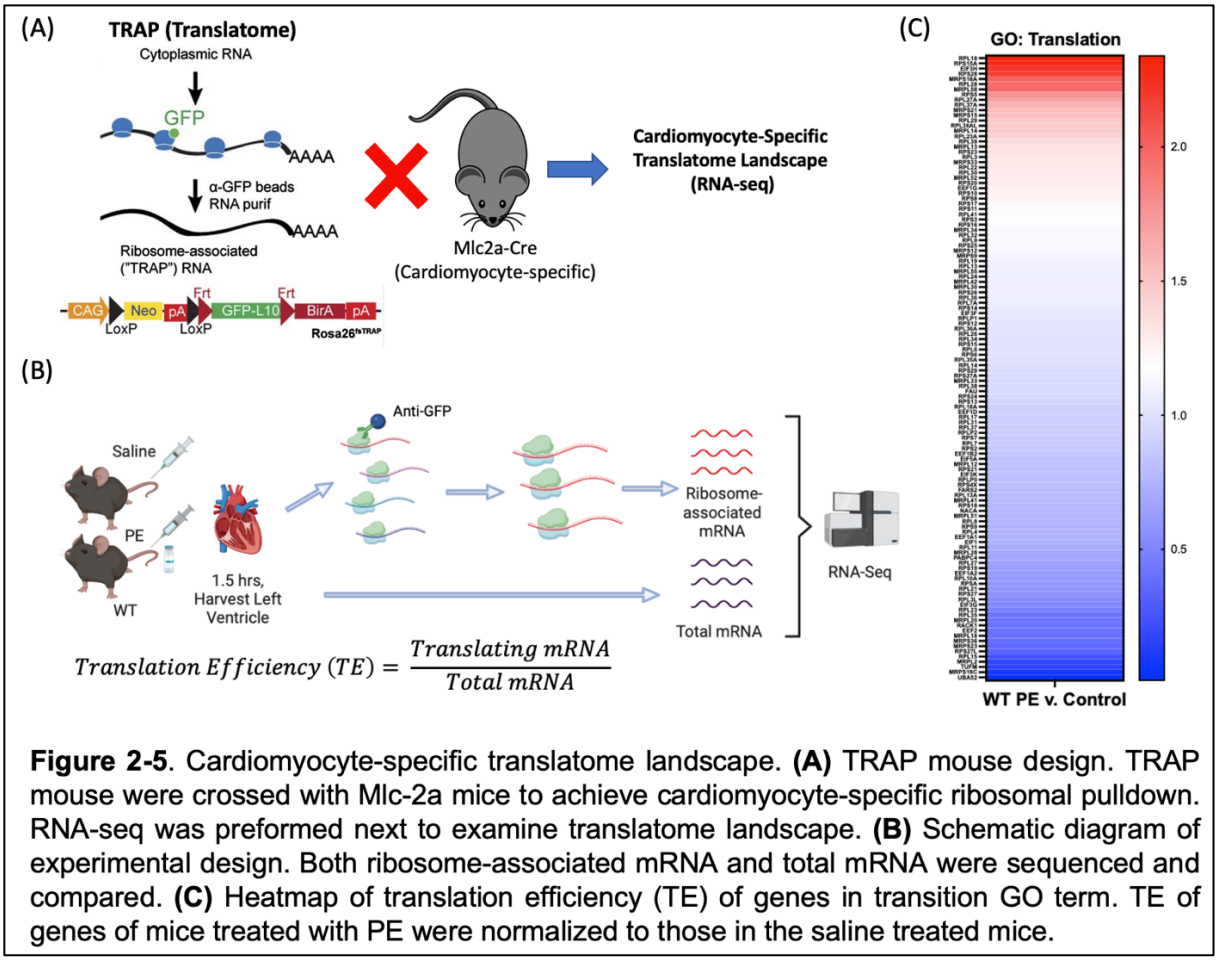

Figure 2-5. Cardiomyocyte-specific translatome landscape. **(A)** TRAP mouse design. TRAP mouse were crossed with Mlc-2a mice to achieve cardiomyocyte-specific ribosomal pulldown. RNA-seq was preformed next to examine translatome landscape. **(B)** Schematic diagram of experimental design. Both ribosome-associated mRNA and total mRNA were sequenced and compared. **(C)** Heatmap of translation efficiency (TE) of genes in transition GO term. TE of genes of mice treated with PE were normalized to those in the saline treated mice.

genes have significantly increased TE after PE stimulation, while the translation of some others is repressed (**Figure 2-5D**). Taken together, these data suggested that translation efficiency of ribosome was differentially regulated during early hypertrophic stress.

2.3.5 Ribosomal Protein Composition is Altered During Hypertrophy *in vivo*

For a long time, people have treated ribosome as a conserved, honest translation machinery that produces proteins based on mRNA availability. For the last decade or two, scientist started to appreciate the ribosome heterogeneity theory, which believes that there are specialized ribosomes existed in different cell types and cellular conditions.

These specialized ribosomes may preferentially translate a certain species of mRNA and may have different functional outcomes. Indeed, evidence has been shown in many

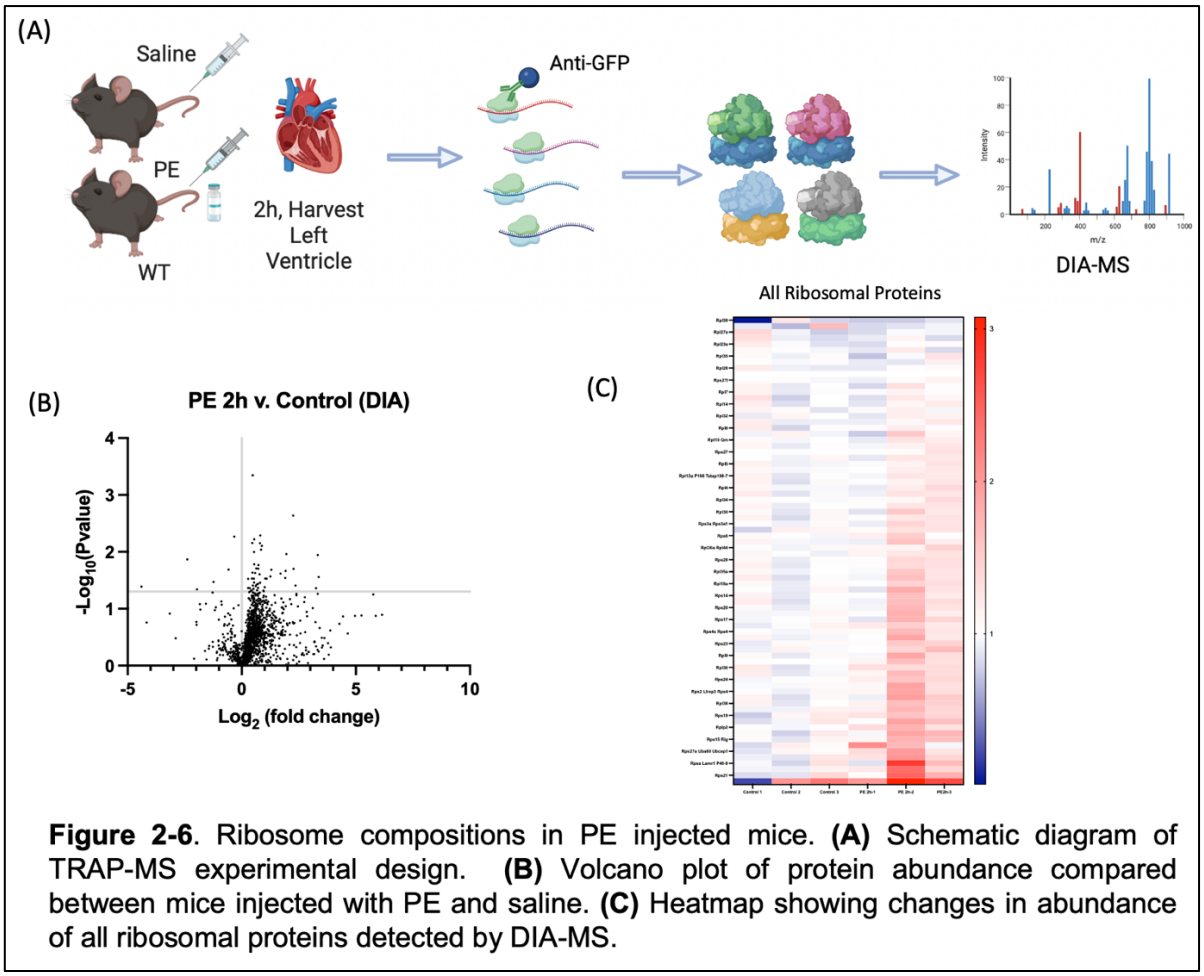

Figure 2-6. Ribosome compositions in PE injected mice. **(A)** Schematic diagram of TRAP-MS experimental design. **(B)** Volcano plot of protein abundance compared between mice injected with PE and saline. **(C)** Heatmap showing changes in abundance of all ribosomal proteins detected by DIA-MS.

different cells and tissues, but not many studies has been focusing on this interesting new direction in the cardiovascular system.

Since we observed changes in TE of many ribosomal proteins, we wanted to ask if this change can be observed at the level of ribosome composition as well. To address this question, we again used the mouse with cardiomyocyte-specific TRAP expression to pull down translating ribosomes, from which ribosomal proteins were examined by data-independent acquisition mass spectrometry (DIA-MS) (**Figure 2-6A**). Different from data-dependent acquisition mass spectrometry (DDA-MS), DIA-MS sends multiple precursors

from MS1 within a defined range of m/z instead of single precursor to MS2 for further fragmentation. This method allows for better quantification and could pick up signals that tend to be overlooked in DDA-MS by some highly abundant precursors. Similarly, we used tail vein injection of PE to induce acute hypertrophic stress before harvesting heart tissue. We found many ribosome-associated genes are changed during acute stress response. Among all the genes that passed the threshold, only found a few ribosomal proteins that are significantly changed, showing a highly specific regulation on stoichiometry. When looking at all ribosomal proteins by their raw abundance, we saw changes of their abundance in both directions, suggesting a highly specified rather than a universal regulation for different ribosomal protein incorporations (**Figure 2-6B and C**).

2.4 Discussion

In this chapter, we closely examined the translation profile using different methods and readouts, including immunoblot and RNA-seq. We witnessed a progressive increase of *de novo* protein synthesis after PE-stimulated hypertrophic stress. We found that inhibiting ribosome biogenesis could dampen a robust induction of protein synthesis in an acute response to hypertrophic stimulation independent from mTOR signaling. From this observation, we have established the fact that all ribosomes are occupied at baseline, and *de novo* ribosome biogenesis is the driving force behind increase protein synthesis in response to growth stimulation in an mTOR-independent manner. This is also supported by the TRAP-seq data showing changes in TE of ribosome proteins after growth stimulation *in vivo*.

In addition, we showed specialized ribosomal protein translation during hypertrophic stress by both RNA-seq and proteomics analysis. The stoichiometry of ribosomal proteins

was discussed in a previous study using polysome profiling, and our data supported this observation from various angles. Future studies may investigate individual ribosomal proteins that are highly altered at translation level to study their potential functional impact on hypertrophy.

Acknowledgements

We would like to thank Dr. William Pu from Boston Children's Hospital for providing the TRAP mice and technical support on the corresponding assays. We thank Jing Gao for isolating NRVMs. We would like to thank Jihui Sha from the Wohlshlegel lab at UCLA for providing support on all the proteomics analysis and protocol optimization. We thank the Technology Center for Genomics & Bioinformatics (TCGB) at UCLA for their support on library construction and RNA sequencing. Lastly, we thank Dr. Christoph D. Rau at University of North Carolina at Chapel Hill for his help on RNA-seq analysis. Animal breeding was supported by Haiying Pu. Schematic diagrams were generated with Biorender.com.

CHAPTER III. lncRNA MIAT-MEDIATED PROTEIN SYNTHESIS IN PATHOLOGICAL HYPERTROPHY

3.1 Introduction

As we have established the dynamics of translatome, we wanted to identify the molecular player that is regulating this drastic shift in translation. In this chapter, we identified a long non-coding RNA (lncRNA) Miat that is tightly associated with cardiac hypertrophy and heart failure. We found that Miat is necessary in the development of pathological cardiac hypertrophy. Functionally, Miat promotes protein synthesis increase during hypertrophic growth of the myocardium. Knocking out Miat can protect cardiac function in both TAC and MI hearts.

3.2 Identification of lncRNA Miat in Heart

A GWAS study comparing healthy and myocardial patients in Japanese population in 2006. In this study, six SNPs that fall into the locus of a long non-coding RNA (lncRNA) was found to be highly associated with the onset of myocardial infarction. This lncRNA was later named Myocardial Infarction Associated Transcript (Miat). Over the years, Miat has been studied extensively in cancers and was characterized as potential diagnostic and prognostic biomarkers for many cancer types[161], demonstrating its strong clinical relevance. On the other hand, Miat has also been shown to be important in various cardiovascular complications, such as atherosclerosis[162], myocardial infarction[163-165], atrial fibriliation[166], atrial fibrosis[167] and diabetic cardiomyopathy[168]. However, its role in cardiac hypertrophy has not been extensively studied. A few studies characterized Miat as miRNA sponges[169] and regulator of m6A RNA methylation in cardiac hypertrophy[170]. However, these mechanisms do not fully explain the robust

effect of Miat in pathological cardiac hypertrophy that we and others observed, and none of these studies linked Miat to protein translation regulation.

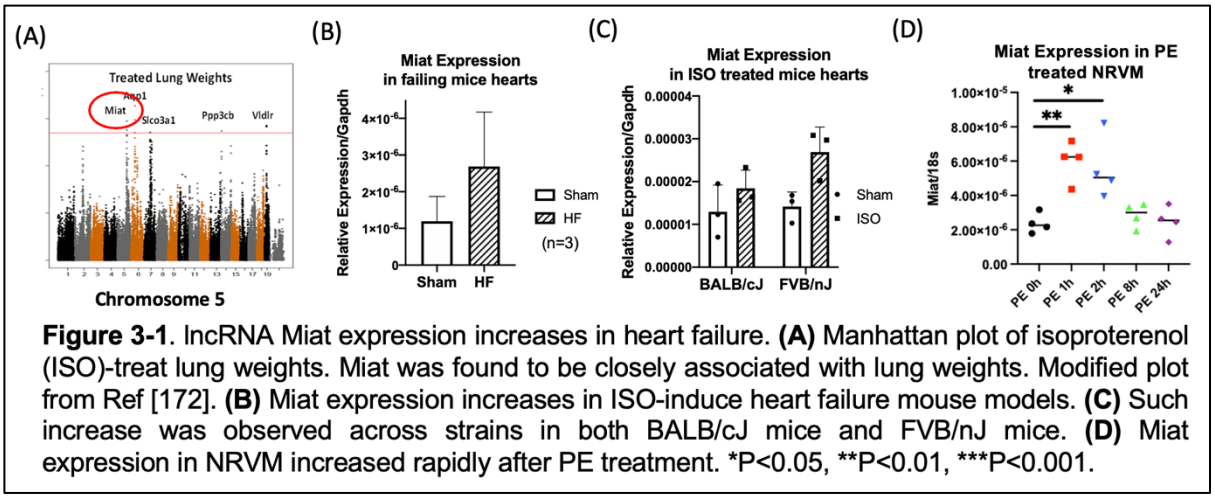

Figure 3-1. lncRNA Miat expression increases in heart failure. **(A)** Manhattan plot of isoproterenol (ISO)-treat lung weights. Miat was found to be closely associated with lung weights. Modified plot from Ref [172]. **(B)** Miat expression increases in ISO-induce heart failure mouse models. **(C)** Such increase was observed across strains in both BALB/cJ mice and FVB/nJ mice. **(D)** Miat expression in NRVM increased rapidly after PE treatment. *P<0.05, **P<0.01, ***P<0.001.

By generating around 100 well-characterized inbred mouse strains, the hybrid mouse diversity panel (HMDP) was developed earlier to mimic the heterogeneity in human population and to study both genetic and environmental factors associated with many different traits[171]. A previous GWAS study done in our lab with these mice on chronic treatment of the β-adrenergic receptor agonist isoproterenol (ISO) identified Miat as one of the top gene is that highly associated with ISO-treated lung weight, which is one commonly seen complication seen in end-stage heart failure patients (**Figure 3-1A**)[172].

3.3 Materials and Methods

3.3.1 Animals

All experimental procedures involving animals in this study were reviewed and approved by the Institutional Animal Care and Use Committees (IACUCs) of University of California at Los Angeles (UCLA) and conformed to the Guide for the Care and Use of laboratory Animals, published by the US National Institutes of Health. Animals were euthanized and sacrificed using cervical dislocation before dissections. All mice were housed in a room

maintained at 23±1°C and 55±5% humidity with a 12-h light-dark cycle and given ad libitum access to food and water. Both male and female C57BL/6 (WT) and Miat KO mice at 10-12 weeks were used in this study. TRAP mice were mated with Mlc2a-Cre mice to achieve cardiomyocyte-specific ribosome labeling. These mice were then crossed with $Miat^{fl/fl}$ mice to introduce Miat KO background.

For surgeries, after anesthesia (Ketamine/Xylazine 80mg/kg / 5 mg/kg, IP), the mouse is fixed in a supine position with tape, the neck is slightly extended. The tongue is retracted and held with forceps. A 20-G catheter is inserted through the larynx into the trachea with care taken not to puncture the trachea or other structures in the pharyngeal region (endotracheal incubated). The catheter is then attached to the mouse ventilation. The ventilation is performed with a tidal volume of 200μl, respiratory rate of 120/min, 95% oxygen. Body temperature was maintained as close as possible to 37.0°C throughout the experiment by using a self-regulating heating pad (FST, cat# 21061-90)

3.3.2 Transverse Aortic Constriction (TAC)

Cardiac hypertrophy was induced in mice by transverse aortic constriction (TAC). The incision area of the chest is disinfected with 2% iodine. The chest cavity is open by an incision of the left second intercostal space. Aortic arch is dissected from the surrounding tissue. The pericardial sac is opened 6-0 suture is passed underneath the transverse aortic and ligated against a 27-G needle, then the latter is removed to provide a lumen. The lungs are overinflated. The chest cavity, muscle and skin are closed layer by layer. The mice were observed until recovery by using a 37.0°C heating cage.

3.3.3 Myocardial Infarction (MI)

Myocardial infarction was induced in mice by ligation of the left anterior artery, the incision of the chest is disinfected with 2% iodine. The chest cavity is opened by an incision of the left second intercostal space. An 8-0 nylon suture was passed with a tapered needle under the left anterior descending coronary artery 2-3 mm from the tip of the left auricle. Coronary artery was occluded. Successful performance of coronary occlusion was verified by visual inspection (i.e., by noting the development of a pale color). The lungs are overinflated, then the chest cavity, muscle and skin are closed layer by layer. The mice were removed from the ventilator, kept warm with a recovery cage which was followed 24 hours.

3.3.4 Echocardiography

In vivo cardiac function was assessed by transthoracic echocardiography [Acuson P300, 18-MHz transducer (Siemens Healthcare Diagnostics) and VisualSonics 2100 (Fujifilm Visualsonics)] in anesthetized mice for both TAC and MI study. From a left ventricle short-axis view, an M-mode echocardiogram was acquired to measure end-systolic and diastolic parameters in left ventricle. Ejection fraction and fractional shorterning were calculated using Vevo Imaging System 2100 (Fujifilm Visualsonics).

3.3.5 Cell Cultures

Neonatal rat ventricular myocytes (NRVMs) were prepared and cultured in Dulbecco's modified Eagle's medium (DMEM) supplemented with Corning® ITS + Premix Universal Culture Supplement (Corning) at 1:100 dilution, 100U/mL penicillin and 100μg/mL streptomycin for 24 hours before any treatment. PE at 100μM were administered to induce hypertrophic stress. Immortalized mouse embryonic fibroblasts (MEF) from

C57BL/6 and Miat KO mice were generated as described before. MEFs were cultured in DMEM supplemented with 10%FBS, 2mM L-glutamine, 100U/ml penicillin and 100μg/ml streptomycin. Serum starvation was used to induce cell growth in MEFs. Cells were starved in the low serum starvation medium (0.5%FBS, 2mM L-glutamine, 100U/ml penicillin and 100μg/ml streptomycin) for 30 hours. Cells were then washed twice with PBS and cultured in the normal media (10%FBS) for 4 hours before puromycin incorporation. For knocking down Miat expression *in vitro,* siRNA target Miat (Thermo Fisher Scientific) was transfected into NRVMs using Lipofectamine RNAiMAX Transfection Reagents (Thermo Fisher Scientific) following manufacture's protocol. Negative control siRNA (siNeg) transfected NRVMs were used as control. All cells were transfected with siRNA for at least 48 hours before any downstream treatment or analysis.

3.3.6 Surface Sensing of Translation (SUnSET)

SUnSET assay was performed as previously described to label newly synthesized proteins both *in vitro* and *in vivo*[18]. Cells were incubated with 1μg/mL puromycin for 20 minutes before two PBS washes followed by 20 minutes chase in normal culture media. For *in vivo* labeling, puromycin was delivered using intraperitoneal injection at 40μmol/kg body weight. Heart was collected 30 minutes after injections.

3.3.7 Real-time polymerase chain reaction (Real-time PCR)

RNA was isolated from either cultured cells or heart tissue using TRIzol reagent (Thermo Fisher Scientific). 1μg RNA was used in first-strand complementary DNA synthesis using the iScript Reverse Transcription Supermix (Bio-Rad) following manufacture's instruction. Real-time PCR was conducted using IQ SYBR Green Supermix (Bio-Rad) with CFX-96 Real-time PCR Detection System (Bio-Rad).

3.3.8 Histological studies

After mice were sacrificed, hearts were dissected out and washed in ice-cold PBS twice before fixed with 10% neutral buffered formalin (Sigma-Aldrich). Heart was dehydrated by incubating with 10%, 20% and 30% sucrose solution overnight in PBS consecutively before embedded using Tissue-Teck O.C.T Compound (Sakura Finetek) and stored at -80°C. Frozen sections were prepared using cryotome. Cardiomyocyte cross-sectional area was measured using Fiji (ImageJ) based on wheat germ agglutinin staining (WGA) with cTnI immunostaining as a myocyte marker.

3.3.9 TRAP ribosome pulldown

Phenylephrine (PE) was administered to mice via tail vein injection at 50μg/kg body weight. Heart was harvested after desired time of PE injection. Left ventricles were separated, washed twice with ice-cold PBS, and homogenized in lysis buffer (20mM HEPES KOH [pH 7.4], 5mM $MgCl_2$, 150mM KCl, 0.5mM Dithiothreitol, 1x cOmplete protease inhibitor (Roche), 100μg/ml Cycloheximide, 40 U/ml Rnasin (Fisher Scientific)) on ice using glass homogenizer, 20 strokes. Samples were centrifuged at 2,000g for 10 minutes at 4°C. 10% NP-40 (Thermo Fisher Scientific) was added to the collected supernatant and mixed thoroughly before centrifuged at 20,000g for 10 minutes at 4°C. Protein concentration was determined using Pierce BCA Protein Assay Kit (Thermo Fisher Scientific) and the same amount of proteins were used for the following immunoprecipitation for each sample. Dynabeads Protein G magnetic beads (Fisher Scientific) was washed with Low Salt Buffer (20mM HEPES KOH [pH 7.4], 5mM $MgCl_2$, 150mM KCl, 1% NP-40, 0.5mM Dithiothreitol, 100μg/ml Cycloheximide) three times both

before and after incubating with Anti-GFP antibody (19C8 and 19F7, Heintz Lab) for 1 hour at room temperature.

Tissue lysate from left ventricles was incubated with antibody-bound beads for 1-hour incubation at room temperature. Beads were washed 4 times with High Salt Buffer (20mM HEPES KOH [pH 7.4], 5mM $MgCl_2$, 350mM KCl, 1% NP-40, 0.5mM Dithiothreitol, 100μg/ml Cycloheximide). For RNA-seq analysis, RNA was eluted and purified using RNeasy Kit (Qiagen) following the manufacture's protocol. For mass spectrometry, beads were washed once with Pre-urea Wash Buffer (50mM Tris [pH8.5], 1mM EGTA, 75mM KCl) instead. Proteins were eluted by adding 100μl Urea Elution Buffer (8M Urea, 20mM Tris [pH7.5], and 100mM NaCl) and incubating for 5 minutes at room temperature with frequent agitation (900rpm). Repeat twice and combine the supernatant from all three rounds of elution.

3.3.10 TRAP RNA-seq

Libraries for RNA-Seq were prepared with Nugen Universal plus mRNA-Seq Kit (part number: 0508) to generate strand-specific RNA-seq libraries. The workflow consists of poly(A) RNA selection, RNA fragmentation and double-stranded cDNA generation using a mixture of random and oligo(dT) priming, followed by end repair to generate blunt ends, adaptor ligation, strand selection, and PCR amplification to produce the final library. Different index adaptors were used for multiplexing samples in one sequencing lane. Sequencing was performed on Illumina Hiseq 3000 for SE 1x65 bp run. Data quality check was done on Illumina SAV. Demultiplexing was performed with Illumina Bcl2fastq2 v 2.19.1.403 program. Samples were sent for 2x50bp paired end sequencing on a Hiseq3000 instrument (Illumina). Resulting reads were demultiplexed and quality

measured by fastQC followed by adaptor and low quality read trimming by seqtk (https://github.com/lh3/seqtk). Reads were aligned to the mm10 genome using Salmon 1.3[158]. Outliers were detected and removed through PCA using the ggbiplot R package (https://github.com/vqv/ggbiplot). Translation efficiencies were calculated for each sample by dividing the transcript abundance in the TRAP data vs the abundance in the INPUT datasets and differential abundances detected by benjamini-hochberg corrected T-tests ($q<0.05$). Differential expression between input and MIAT KO mice were ascertained through DESEQ2[159].

3.3.11 Statistical analysis

Comparisons in multiple groups were analyzed by one-way ANOVA with Dunnett's multiple comparison test. Data are presented as mean ± SEM or SD for biological duplicates. The sample size was calculated by holding the probability of a type I error at $\alpha = 0.05$.

3.4 Results

3.4.1 Miat expression is induced during hypertrophic stress

We have observed increased Miat expression in failed mouse hearts induced by ISO across different strains, showing the universal nature of Miat as an important player in heart failure (**Figure 3-1B and C**). Upon acute hypertrophic stimulation by PE in NRVM, we observed a robust increase of Miat expression as early as 1 hour after PE was administered. Its expression peaked around 1-2 hours post PE treatment and quickly fell back to the baseline, implying its role as stress responder, especially during acute stress **(Figure 3-1D)**.

3.4.2 Miat is necessary in hypertrophic growth of the heart

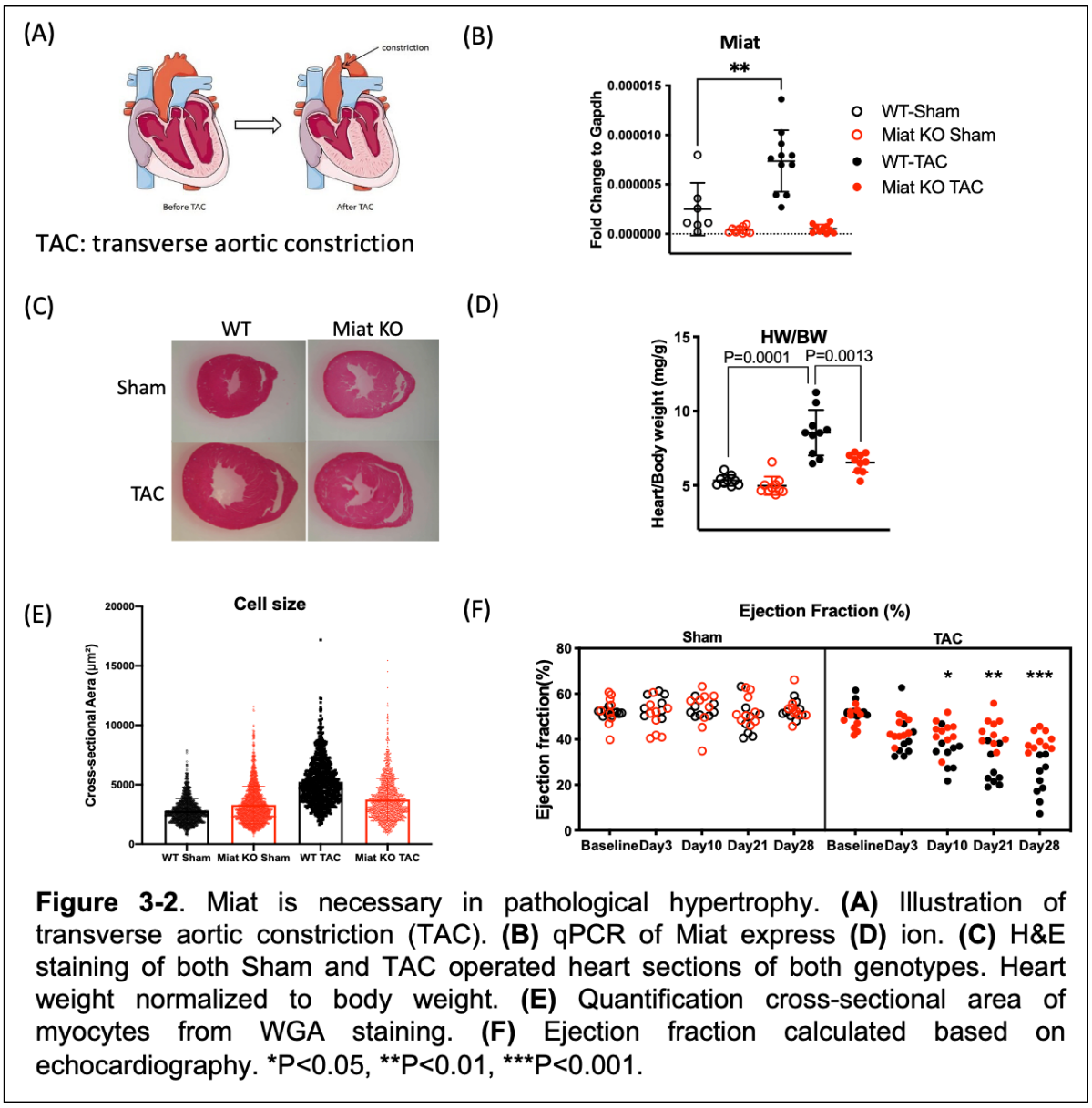

Figure 3-2. Miat is necessary in pathological hypertrophy. **(A)** Illustration of transverse aortic constriction (TAC). **(B)** qPCR of Miat express **(D)** ion. **(C)** H&E staining of both Sham and TAC operated heart sections of both genotypes. Heart weight normalized to body weight. **(E)** Quantification cross-sectional area of myocytes from WGA staining. **(F)** Ejection fraction calculated based on echocardiography. *P<0.05, **P<0.01, ***P<0.001.

To examine whether Miat is important in cardiac hypertrophy and heart failure, we generated Miat KO mice in the C57BL/6 background. Both WT and Miat KO mice were subjected to transverse aortic constriction (TAC) surgery to induce pressure overload (**Figure 3-2A**). Cardiac function was assessed by echocardiography weekly until 4 weeks after TAC, before heart tissue was collected. Miat expression significantly increased after TAC (**Figure 3-2B**). Heart weight and size increased significantly in WT mice after TAC,

which was effectively blunted by Miat KO (**Figure 3-2C and D**). We also quantified individual myocyte size using wheat germ agglutinin (WGA) staining. Myocyte size significantly increases after TAC in WT hearts but not as much in Miat KO hearts (**Figure 3-2E**). These data suggests that Miat KO is protective to pathological hypertrophy. Cardiac function in WT mice decreased after TAC shown by ejection fraction (EF). In

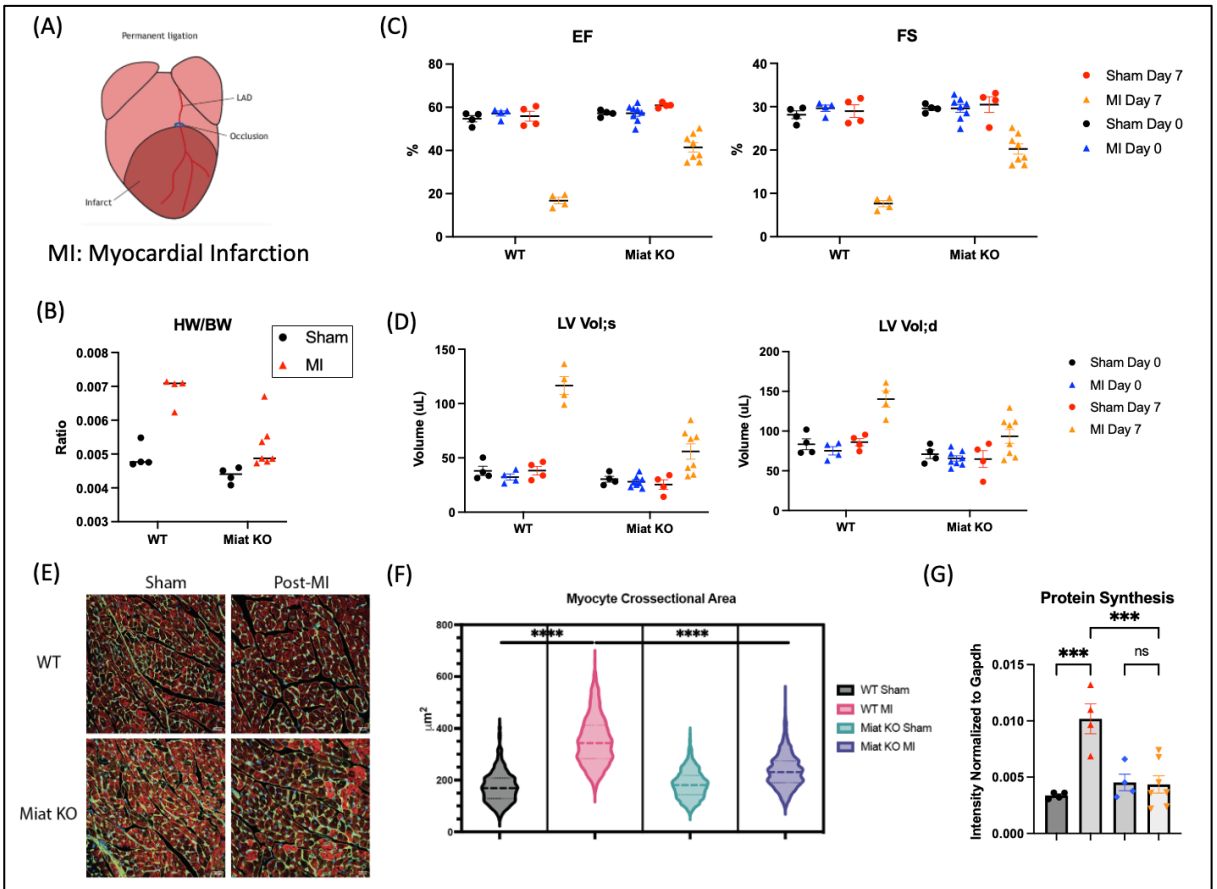

Figure 3-3. Myocardial Infarction study in WT and Miat KO mice. **(A)** Illustration of myocardial infarction procedure. **(B)** Heart weight normalized to body weight. **(C)** Ejection fraction and fractional shortening showing cardiac functions. **(D)** Left ventricular end-systolic and end-diastolic volume showing chamber dilation and remodeling. **(E)** Representative WGA staining (Green) of remote, non-infarcted myocardium. Red: cTnI. **(F)** Quantification of myocyte size based on WGA staining in E. **(G)** Protein synthesis in non-infarcted myocardium was monitored by puromycin labeling. *P<0.05, **P<0.01, ***P<0.001.

comparison, Miat KO mice had significantly better cardiac function (**Figure 3-2F**),

showing a potent protective effect of Miat KO. We also did a one-week-long myocardial infarction (MI) study in both WT and Miat KO mice (**Figure 3-3A**). The remote, non-infarcted myocardium underwent adaptive growth to compensate for the partial loss of cardiac contraction and output for the infarcted zone. Therefore, we wanted to check if Miat KO can blunt such compensatory growth. Heart weight significantly increased in WT one week after MI, which is blocked by knocking out Miat (**Figure 3-3B**). Consistent with

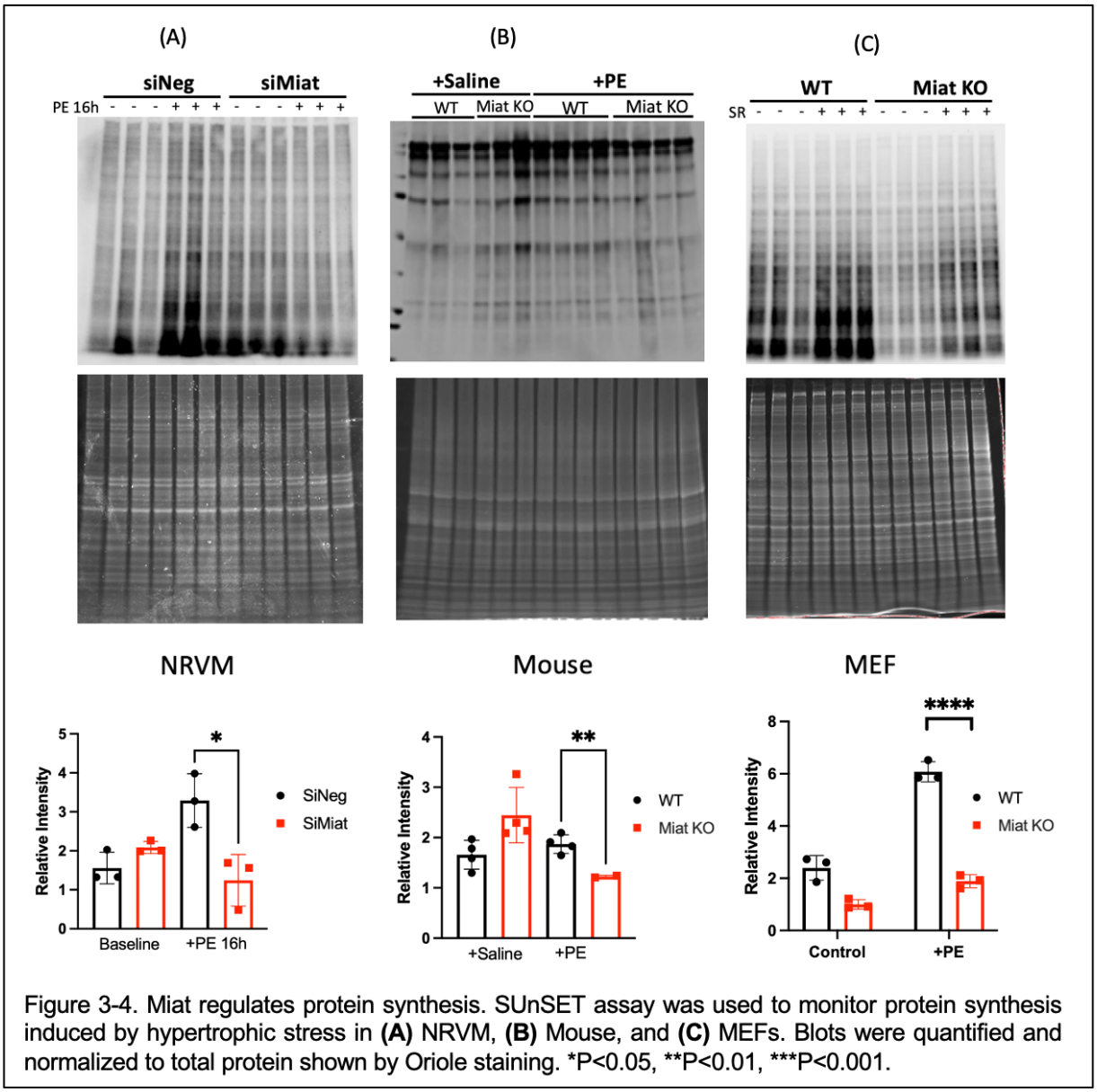

Figure 3-4. Miat regulates protein synthesis. SUnSET assay was used to monitor protein synthesis induced by hypertrophic stress in **(A)** NRVM, **(B)** Mouse, and **(C)** MEFs. Blots were quantified and normalized to total protein shown by Oriole staining. *P<0.05, **P<0.01, ***P<0.001.

other previous study in MI models, Miat KO showed a very robust protective effect in cardiac function and remodeling (**Figure 3-3C and D**). WGA staining showed increased cardiomyocyte size in remote area in WT mice post-MI but not in Miat KO mice (**Figure 3-3E and F**). Taken together, these data suggested that Miat is necessary in hypertrophic growth of the heart.

3.4.3 Miat regulates protein synthesis

To check if Miat has any impact on protein synthesis, we used siRNA to knock down Miat in NRVMs and performed SUnSET assay. Upon PE treatment, increased protein synthesis was observed in cells transfected with negative control siRNA. However, such increase was significantly blunted by Miat knockdown (**Figure 3-4A**). In addition, we observed increased protein synthesis in vivo upon PE injection in WT mouse heart, which was also repressed in the Miat KO hearts (**Figure 3-4B**). In mouse MI hearts, protein synthesis rate marked by puromycin incorporation in the remote, non-infarcted myocardium also increased compared to the sham-operated hearts (**Figure 3-4D**).

To check if Miat's regulatory role in protein synthesis is exclusive to cardiomyocyte, we isolated and generated immortalized mouse embryonic fibroblasts (MEF) from both WT and Miat KO mice. We used the serum starvation-refeed regimen to induce growth stimulation in MEF cells. Similarly, WT MEF cells responded to growth stimulation by increased protein synthesis, which is potently repressed in Miat KO condition (**Figure 3-3G**). Taken together, these data suggested that Miat is important in regulating protein synthesis in hypertrophic hearts, and similar functional impact can be observed in other cell types under growth stimulation.

3.4.4 Miat is essential in maintaining translatome landscape

In chapter 2, we observed a robust shift in translatome landscape in WT mouse upon acute PE stimulation. Since we know Miat can regulate protein synthesis during cardiac hypertrophy, we wonder if Miat is important in such shift in translatome landscape at all. We crossed the cardiomyocyte-specific TRAP expressing mice with Miat$^{fl/fl}$ mice to closely

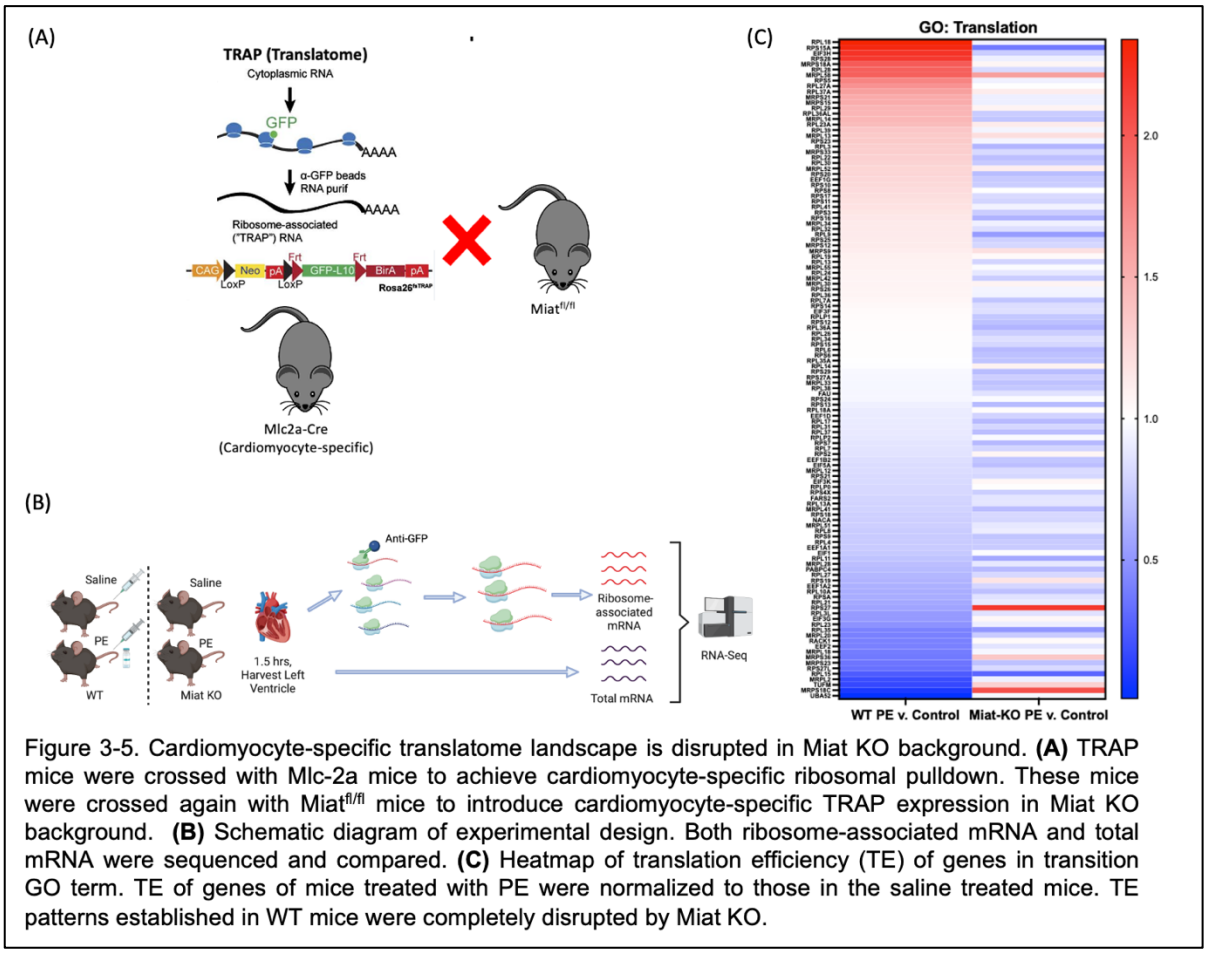

Figure 3-5. Cardiomyocyte-specific translatome landscape is disrupted in Miat KO background. **(A)** TRAP mice were crossed with Mlc-2a mice to achieve cardiomyocyte-specific ribosomal pulldown. These mice were crossed again with Miat$^{fl/fl}$ mice to introduce cardiomyocyte-specific TRAP expression in Miat KO background. **(B)** Schematic diagram of experimental design. Both ribosome-associated mRNA and total mRNA were sequenced and compared. **(C)** Heatmap of translation efficiency (TE) of genes in transition GO term. TE of genes of mice treated with PE were normalized to those in the saline treated mice. TE patterns established in WT mice were completely disrupted by Miat KO.

examine translatome profile in the absence of Miat expression (**Figure 3-5A**). These mice were subjected to the same treat described in 2.3.4, and TRAP-seq was done to monitor translation efficiency (**Figure 3-5B**). Strikingly, we found that the trends of TE change of ribosomal genes found in WT mice after PE stimulation were completely disrupted when Miat is absent, suggesting that Miat is critical in maintaining translatome landscape during hypertrophic stress (**Figure 3-5C**).

3.5 Discussion

In this chapter, we demonstrated that Miat is necessary in pathological cardiac hypertrophy, and knocking out Miat is protective to both the hypertrophic phenotype and cardiac function. By using puromycin incorporation, we found that Miat is necessary in stress-induced protein synthesis. We also found that the reprogramming of translatome landscape in response to PE-induce hypertrophic stress is completely disrupted in the Miat KO hearts. Particularly, Miat is important in maintaining the translation efficiency of ribosomal proteins and many other translation-related genes. Taken together, these data demonstrated the important role of Miat in translation regulation during pathological hypertrophy.

Acknowledgements

We thank Vincent (Shuxin) Ren for performing all surgical procedures. We thank Jing Gao for isolating NRVMs and He Wang for generating the immortalized mouse embryonic fibroblasts (MEFs) from both genetic backgrounds. Animal Breeding was supported by Haiying Pu. Schematic diagrams were generated with Biorender.com.

CHAPTER IV. MOLECULAR MECHANISM OF MIAT-MEDIATED PATHOLOGICAL HYPERTROPHY

4.1 Introduction

In the previous chapters, we have the established the dynamics of protein synthesis profile and translatome landscape during early response to hypertrophic stress. Since Miat could mediate cardiac hypertrophy via translation regulation, we would like to further explore the molecular mechanisms. In this chapter, we discovered nucleolin (NCL) as Miat binding partner, and their binding is necessary for proper rRNA processing and ribosome biogenesis. On the other hand, we found that Miat is necessary in maintaining nucleoli dynamics during hypertrophy-induced nucleoli stress. We also identified Miat's potential functional impact in regulating spatial-temporal distribution of ribosome and target mRNAs.

4.2 Materials and Methods

4.2.1 Animals

All experimental procedures involving animals in this study were reviewed and approved by the Institutional Animal Care and Use Committees (IACUCs) of University of California at Los Angeles (UCLA) and conformed to the Guide for the Care and Use of laboratory Animals, published by the US National Institutes of Health. Phenylephrine was administered using tail vein injection. Animals were euthanized and sacrificed using cervical dislocation before dissections. All mice were housed in a room maintained at 23±1°C and 55±5% humidity with a 12-h light-dark cycle and given ad libitum access to food and water.

4.2.2 Cell Culture and cloning

Neonatal rat ventricular myocytes (NRVMs) were prepared and cultured in Dulbecco's modified Eagle's medium (DMEM) supplemented with Corning® ITS + Premix Universal Culture Supplement (Corning) at 1:100 dilution, 100U/mL penicillin and 100μg/mL streptomycin for 24 hours before any treatment. PE at 100μM were administered to induce hypertrophic stress. Immortalized mouse embryonic fibroblasts (MEF) from C57BL/6 and Miat *KO* mice were generated as described before. MEFs were cultured in DMEM supplemented with 10%FBS, 2mM L-glutamine, 100U/ml penicillin and 100μg/ml streptomycin. Miat fragments (Miat1 and Miat2) were cloned from mouse cDNA with KOD Hot Start DNA Polymerase (Novagen) and inteserted into pcDNA5-CMV vector with s1m tag on the 5'end for transient overexpression. Plasmids are transfected into MEF cells using Lipofectamine 3000 Transfection Reagent (Thermo Fisher Scientific) following manufacture's protocol. For knocking down Miat expression *in vitro,* siRNA target Miat (Thermo Fisher Scientific) was transfected into NRVMs using Lipofectamine RNAiMAX Transfection Reagents (Thermo Fisher Scientific) following manufacture's protocol. Negative control siRNA (siNeg) transfected NRVMs were used as control. All cells were transfected for at least 48 hours before any downstream treatments.

4.2.3 RNA Immunoprecipitation (RIP)

MEFs were treated as desired. Cells were washed twice with ice-cold PBS before harvested using cell scraper. RIP was done using Magna RIP RNA-Binding Protein Immunoprecipitation Kit (EMD Millipore) and NCL antibody (Abcam, ab22758) following manufacture's instructions. For each RIP reaction, $5x10^6$ cells were used. 5% of the total lysate was saved as input.

4.2.4 Immunofluorescence Staining (IF)

Cells were washed with ice-cold PBS twice and fixed in 4%PFA/PBS at room temperature for 20 minutes. Cells were then rinsed in PBS 3 times and permeabilized using 0.1% Triton-X/PBS at room temperature for 15 minutes. Cells were rinsed in PBS 3 times and blocked in 10% BSA/PBS for 1 hour. After blocking, cells were incubated with the primary antibody diluted in 10% BSA/PBS at desired concentration overnight at 4°C before washed in PBS four times, 5 minutes each. Cells were then incubated with secondary antibody diluted in 10% BSA/PBS at desired concentration for 90 minutes at room temperature. Cells were washed twice in PBS for 5 minutes each before nuclear staining with DAPI at 1μg/ml (Thermo Fisher Scientific). Slides were mounted using ProLong Gold Antifade Mountant (Thermo Fisher Scientific) before imaging using Nikon A1R HD25 Confocal Microscope System. Nucleoli was marked using fluorescent signal from NCL and/or FBL. Nucleoli and nuclei sizes were measured using Fiji (ImageJ).

4.2.5 RNAscope

RNAscope Multiplex Fluorescent v2 Kit (ACD Bio) was used with modifications. All reagents used were from the kit unless otherwise noted. All incubation steps were performed in the humidity control tray at 40°C in the hybridization oven unless otherwise noted. Cryosections of heart was kept at room temperature for 10 minutes before washed twice in PBS, 5 minutes each. Tissue section was incubated with hydrogen peroxide for 10 minutes at room temperature. Protease treatment, probe incubation and signal amplification were performed following manufacturer's instruction. Opal 520, 570, and 690 Fluorophore were used (Akoya Biosciences). Slides were imaged using Nikon A1R HD25 Confocal Microscope System and/or Zeiss LSM 880 Confocal Laser Scanning Microscope.

4.2.6 Northern blotting

RNA was extracted using TRIzol reagent (Thermo Fisher Scientific) per the manufacturer's protocol. Aliquot(s) of 3-4 μg of RNA were made and re-precipitated with 1/10th the volume of 3M NaOAc, 2-3 volumes of 100% ethanol (cold), and 2 μL pellet paint. Samples were incubated for at least 20 min at -20 º C, then spin at 4º C for 25 min at 14000 rpm. Pellets were washed twice with 1 mL 75% ethanol and spun down at 4º C for 5 min at 14000 rpm. 1% agarose was mixed formaldehyde. Gel was poured and lightly covered with saran wrap to minimize formaldehyde evaporation before sitting for ~1 hr. Running buffer (17 mL of 50X Tri/Tri buffer bring to 850 mL with ddH2O) was added right before samples were added, again to minimize loss of formaldehyde from gel. Ethanol wash was removed in its entirety from RNA pellets, which were dried the pellets for around 10 mins. RNA pellets were resuspended in 7.5 μL of formamide in a bench-top shaker for ~5 min. When completely resuspended, 7.5 μL of loading buffer was added (14 volumes of loading dye to 1 volume of 37% formaldehyde). Flick to mix and do a quick spin to bring sample to the bottom of the tube. Samples were Incubated at 65 º C for 10 mins to denature the RNA. Samples were loaded on to the gel and run at 140V for 5 mins, and then at 110V for 2-3 hours (until the yellow dye in TriTrack buffer is at the bottom of the gel). Once the gel was done running, it was taken out to a clean container and rinsed 3x with ddH2O. The gel was incubated in 0.05M NaOH for 15 mins with gentle shaking to hydrolyze the large pre-rRNA intermediates, allowing for more effective transfer of the large RNAs to the nylon membrane. Total incubation time should not exceed 15 mins. The gel was rinsed again 3 times with ddH2O. The gel was then incubated with ~200 mL of 10X SSC for 5 min with gentle shaking. Nylon membranes (Hybond XL) were used for

transfer overnight. When done transfer, membrane was crosslinked and incubated with 0.025% (w/v) methylene blue staining solution. Bands for 18S and 28S were imaged. Pre hyb was carried out for 3 hours at 37ºC. 15 to 30 μL of radioactive probe(s) was added to 500 μL of the prehyb solution that was kept in a locking tube. Samples were denatured by heating at 95ºC for 3 mins before mixed with the denatured probe solution. Hybridization was carried out overnight at 42º C. The membrane was washed three times at 42º C for 20 min each before imaging.

4.2.7 Statistical Analysis

Comparisons in multiple groups were analyzed by one-way ANOVA with Dunnett's multiple comparison test. Data are presented as mean ± SEM or SD for biological duplicates. The sample size was calculated by holding the probability of a type I error at $\alpha = 0.05$.

4.3 Results

4.3.1 Miat expresses exclusively in the nucleus

To understand the detailed molecular mechanism, we first asked where Miat expresses in cells. RNAscope was used to check the subcellular localization of Miat. Probe targeting 47S pre-rRNA was co-stained as a nucleolus marker. Miat was found to express exclusively in the nucleus in both brain tissue and non-myocytes in infarcted myocardium (**Figure 4-1A**). Unfortunately, RNAscope did not successfully capture Miat in cardiac myocytes due to its low expression in such cell type. However, subcellular fractionation followed by RT-qPCR showed that Miat expression can only be found in nuclear fractions but not cytosolic fractions in both mouse hearts and NRVMs. Moreover, Miat does not seem to translocate under growth stimulation either *in vitro* or *in vivo* (**Figure 4-1B**).

Overall, these results confirmed that Miat expresses exclusively in the nucleus. This

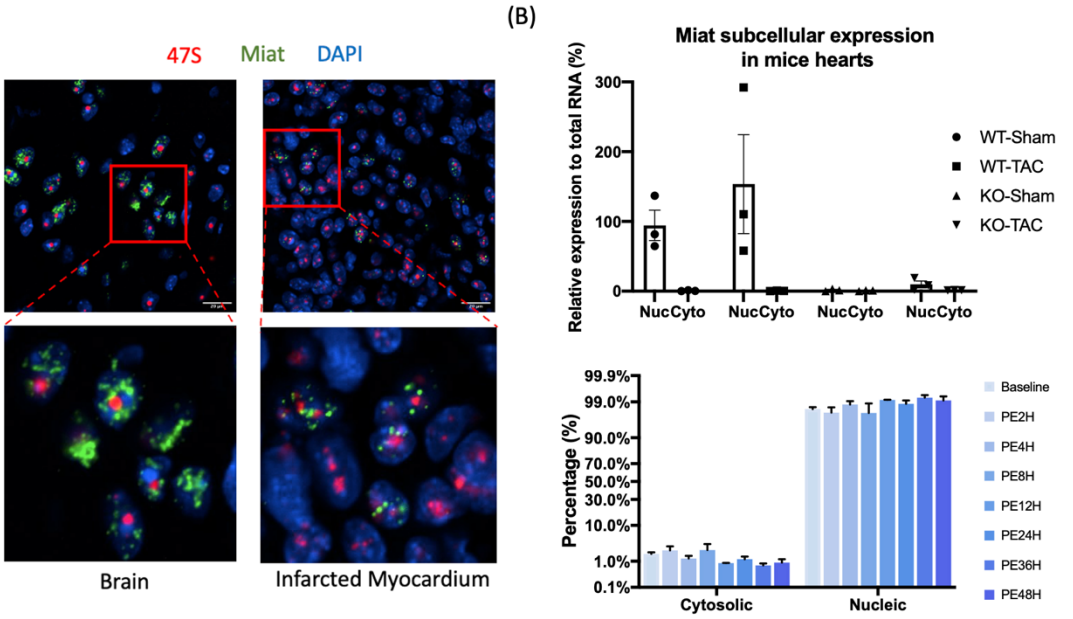

Figure 4-1. Miat expresses exclusively in the nucleus. **(A)** RNAscope showed exclusive nuclear expression of Miat in brain and infarcted myocardium. 47S was stained as nucleolar marker. **(B)** Miat subcellular expression in mouse heart and NRVMs. Miat does not translocate upon hypertrophic stress both *in vitro* and *in vivo*.

pointed us to focus on nuclear cellular processes rather than those happening in the cytoplasm.

4.3.2 Miat interacts with nucleolin (NCL) to regulate ribosome biogenesis

We used online bioinformatics tools RBPPred [173] and PRISeq [174] to look for potential Miat binding partners based on their sequences (**Figure 4-2A**). Among all the candidates, Nucleolin (NCL) was the most promising target and had a very high binding potential with lncRNA Miat based on their RNA and amino acid sequence (**Figure 4-2B and C**). NCL is a nucleolar protein that is well-characterized as an important player in ribosome biogenesis. It is a very versatile protein that has RNA, DNA, and protein-binding ability[175]. It can interact with rRNA and affect RNA polymerase I (RNAPI)-mediated rRNA transcription by regulating heterochromatin (H3K9me2) and euchromatin marks

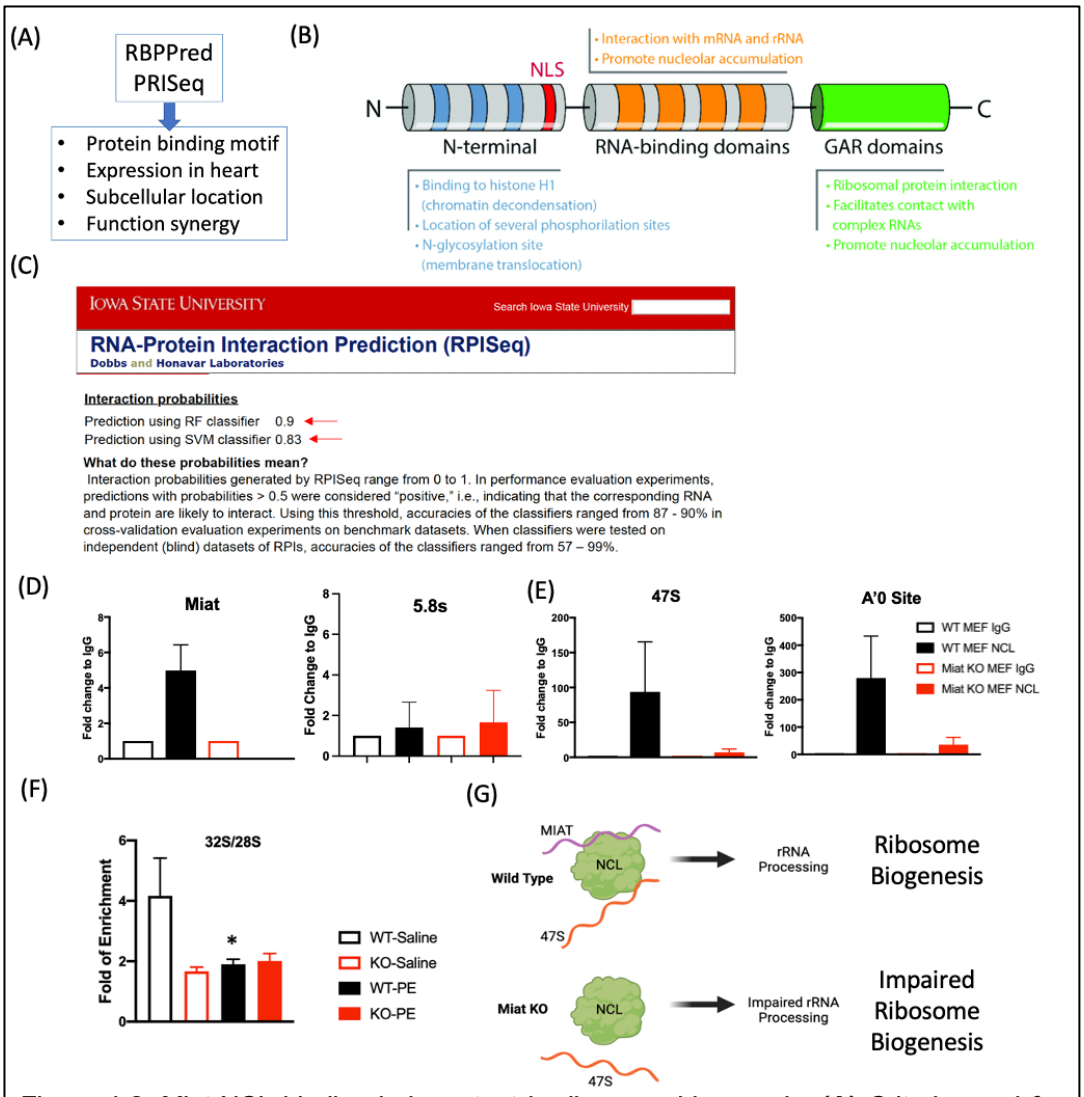

Figure 4-2. Miat-NCL binding is important in ribosome biogenesis. **(A)** Criteria used for Miat-binding partner prediction. RBPPred [173] and PRIseq [174] were used to screen Miat-interacting protein candidates. **(B)** Gene structure of nucleolin. Obtained from Ref[175]. **(C)** Snapshot of interaction probability predicted by RPIseq. **(D)** RIP-qPCR showed that Miat can be pulled down with anti-NCL antibody. 5.8s was used as negative control, as it is known not to interact with Miat. **(E)** RIP-qPCR showed that Miat-NCL binding is necessary for NCL interaction with 47S pre-rRNA. **(F)** Quantification of Northern blot of RNAs from PE injected mouse heart. **(G)** Schematic diagram of the current working model.

(H4K12Ac and H3K4me3) (Reviewed in Ref [176]). Besides, it is also heavily involved in rRNA processing, maturation, and ribosome assembly[177]. Earlier study characterized NCL as a regulator of cardiomyocyte growth and plasticity[178]. Therefore, we hypothesized that NCL could be a Miat-interacting protein, and their interaction regulates

protein synthesis via ribosome biogenesis. To validate NCL-Miat binding, we performed RNA immunoprecipitation (RIP) using antibodies targeting NCL protein. We successfully pulled down Miat using NCL antibody compared to the IgG control (**Figure 4-2D)**. It is well established that NCL can bind to 47S pre-rRNA and is essential in rRNA processing. To examine if Miat binding has any functional significance, we did RT-qPCR to check 47S abundance after RIP. In WT MEF, both 47S and A'0 processing sites are significantly enriched compared to the IgG group. However, this interaction was completely disrupted in Miat KO cells (**Figure 4-2E**). To examine if Miat KO have any functional impact on ribosome biogenesis, we performed northern blot in PE-injected mouse heart in both

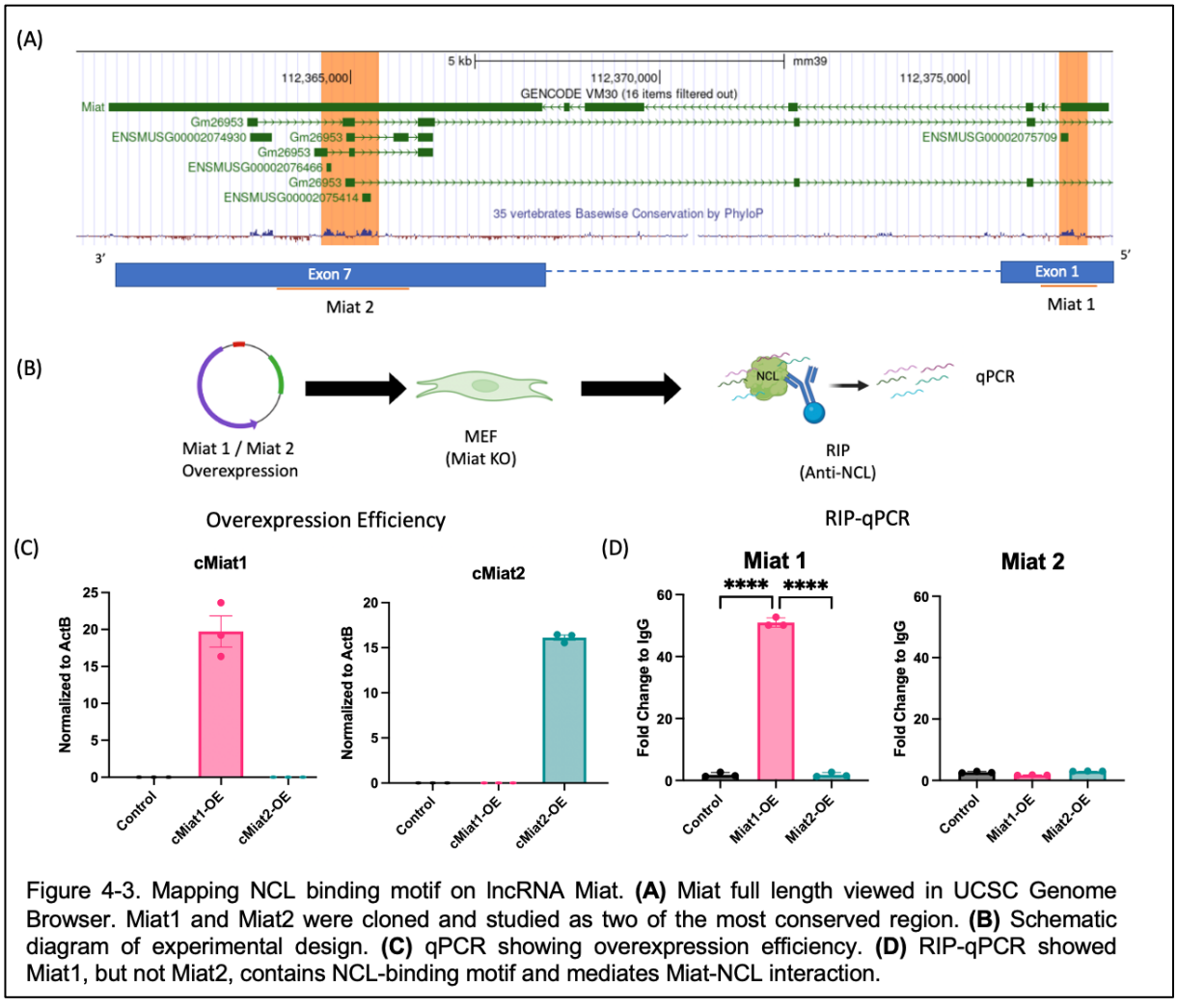

Figure 4-3. Mapping NCL binding motif on lncRNA Miat. **(A)** Miat full length viewed in UCSC Genome Browser. Miat1 and Miat2 were cloned and studied as two of the most conserved region. **(B)** Schematic diagram of experimental design. **(C)** qPCR showing overexpression efficiency. **(D)** RIP-qPCR showed Miat1, but not Miat2, contains NCL-binding motif and mediates Miat-NCL interaction.

genetic backgrounds and quantified the ratio between 32S and 28S rRNA. We observed major defects of RNA processing in Miat KO hearts, as the 32S/28S ratio basically remained the same after PE-induce hypertrophic stress (**Figure 4-2F**). These results suggested that Miat-NCL binding is necessary for NCL-mediated rRNA processing. It also served as an important piece of evidence for Miat's regulation on protein synthesis via ribosome biogenesis (**Figure 4-2G**).

Unlike many well-characterized lncRNAs, Miat is highly conserved across different species. To map out NCL binding motif on Miat, we chose the two most conserved regions in Miat (named Miat1 and Miat2) and cloned them from mouse cDNA (**Figure 4-3A**). These fragments were inserted into pcDNA5-CMV plasmids, which are then transfected and expressed in Miat KO MEFs to minimize background (**Figure 4-3B**). qPCR was performed to validate transfection efficiency (**Figure 4-3C**). We then performed RIP-qPCR in cells expressing these fragments using anti-NCL antibody. Our result showed that anti-NCL antibody could be used to pulldown Miat1 but not Miat2 fragment, suggesting that Miat1 contains the NCL-binding motif, and NCL specifically binds to Miat via Miat1 fragment (**Figure 4-3D**).

To see if overexpressing Miat1 have any functional impact on growth-induced protein synthesis, we overexpressed Miat1 in MEFs with both WT and Miat KO background and used serum starvation-refeed regimen to induce protein synthesis. SUnSET assay was performed to monitor protein synthesis. Surprisingly, Miat1 overexpression does not increase protein synthesis further in both genetic backgrounds (**Figure 4-4A)**. RIP data showed that overexpressing Miat1 disrupted NCL-47S binding (**Figure 4-4B**). These data

suggested that Miat1 overexpression showed a dominant negative effect, and Miat1 overexpression alone cannot achieve functional rescue, at least in protein synthesis.

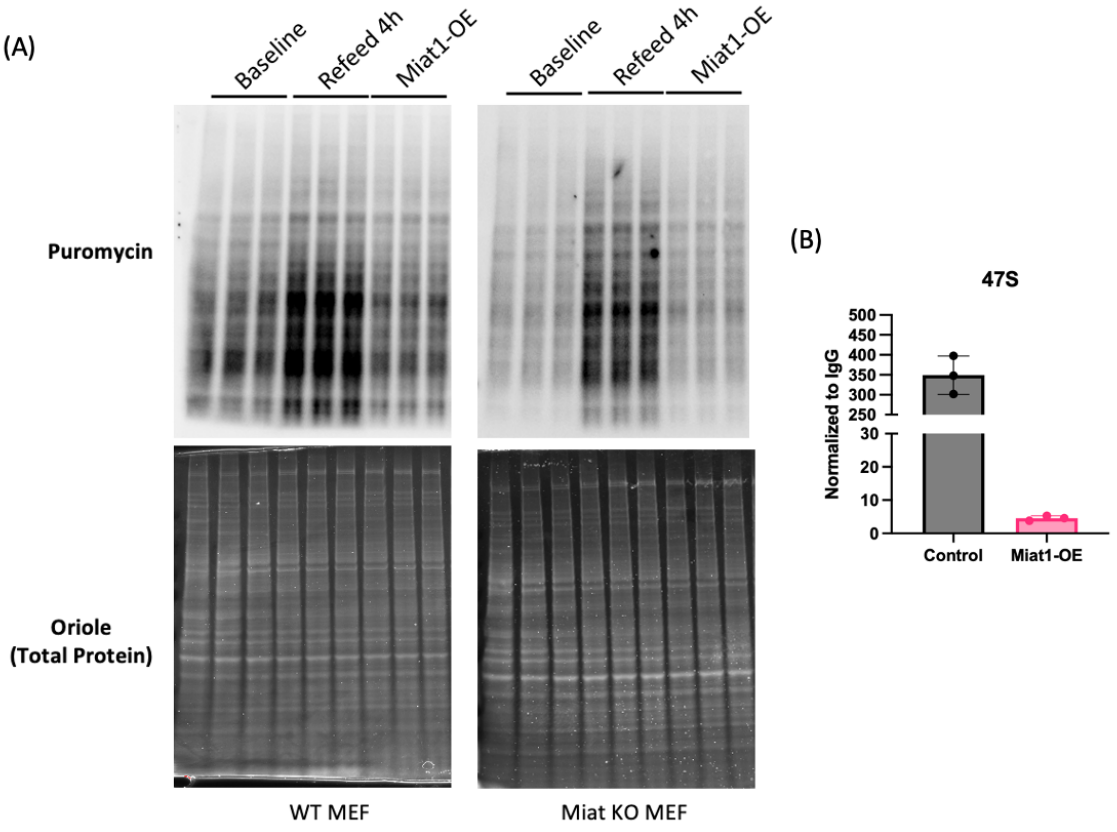

Figure 4-4. Functional impact of overexpressing Miat1 fragment. Plasmids containing Miat1 fragment were transfected into MEFs, in which SUnSET assay was used to monitor protein synthesis after growth stimulation by serum starvation-refeed regimen. **(A)** Western blot showed no rescue effect of Miat1 in both genetic backgrounds. **(B)** RIP-qPCR showed that Miat1 overexpression had a dominant negative effect reflected by disrupted NCL-47S interaction.

4.3.3 Miat is necessary in maintaining proper nucleolar dynamics

Nucleolus is a multilayered biomolecular condensate that is formed by liquid-liquid phase separation (LLPS). It is the center of ribosome biogenesis, including rRNA transcription, pre-rRNA processing, and pre ribosome assembly. The number of nucleolar organizer regions (NORs) generally determines how many nucleoli can possibly form within one nucleus. It is widely acknowledged that the morphology, size, and number of nucleoli can

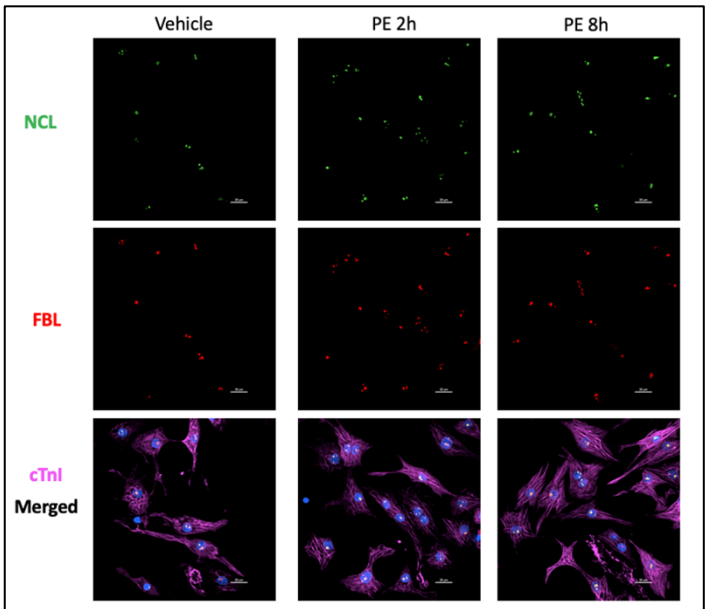

Figure 4-5. Immunofluorescence staining of siNeg transfected NRVMs treated with PE. NRVMs were transfected with negative control siRNA for 48hours before PE was added. Red: FBL, Green: NCL, Magenta: cTnI, Blue: DAPI.

change upon stress. Nucleoli numbers tend to vary a lot among different cell types. It is generally accepted that cells in a faster growing status tend to have increased nucleolar size and number. Therefore, nucleolus is a highly dynamic structure that is worth investigating during stressed conditions.

Since we have established Miat-NCL interaction mediated ribosome biogenesis, we hypothesized that Miat is important in maintaining proper nucleoloar dynamics during hypertrophic stress. To test this hypothesis, we knocked down Miat in NRVM using siRNA. We treated NRVM with PE and stained nucleolin (NCL) and fibrillarin (FBL) as nucleoli marker, and cardiac troponin I (cTnI) as cardiomyocyte marker (**Figure 4-5 and Figure 4-6**). As baseline, most nuclei have 1 to 2 nucleoli in both genetic backgrounds. During PE-stimulated hypertrophic stress, we observed a significant increase in

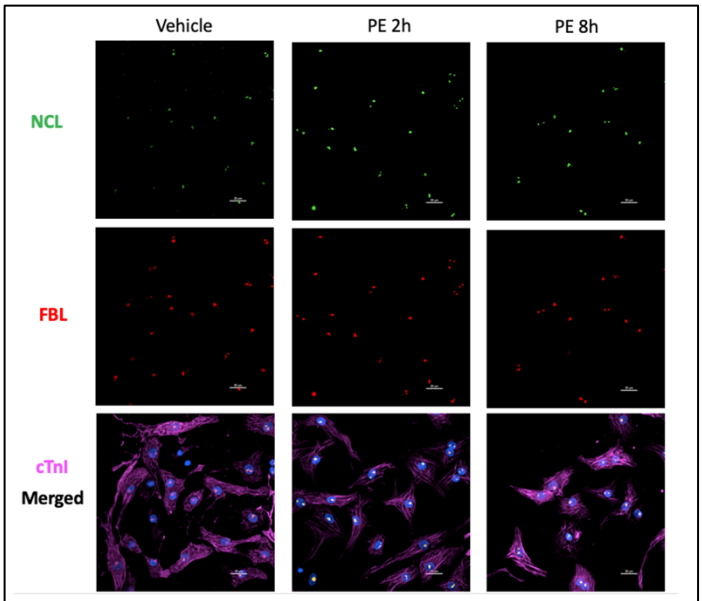

Figure 4-6. Immunofluorescence staining of siMiat transfected NRVMs treated with PE. NRVMs were transfected with siRNA targeting lncRNA Miat for 48hours before PE was added. Red: FBL, Green: NCL, Magenta: cTnI, Blue: DAPI.

NVRM populations with more nucleoli in siNeg treated cells. However, such increase was blunted by Miat knockdown (**Figure 4-7A**). Interestingly, we did not see further increase of nucleoli number from 2 hours to 8 hours post PE treatment in the siNeg treated cells, suggesting that the initial reprogramming of nucleoli was completed within the first 2 hours of stress stimulation. This is consistent with our previous observation of the nascent proteome surge at this early time point.

Besides nucleoli number, their sizes are also an important parameter of nucleolar dynamics, especially for evaluating cell growth. Bigger nucleoli are usually associated with faster ribosome biogenesis and cellular growth. Previous studies have found a positive correlation between nucleoli size and myocardial weight in both healthy and pathological patient samples. A recent study identified Nucleosome Assembly Protein 1 Like 5 (NAP1L5) as an important player in translation regulation via promoting nucleolar hypertrophy. To date, however, no studies have looked at nucleoli size in cardiac myocytes during acute stress. Therefore, we wanted to ask if Miat is important in mediating changes in nucleolar size. Surprisingly, we did not observe any change of nucleoli size either at 2 or 8 hours of PE treatment in NRVMs. However, we saw a significant decrease in nucleoli size when knocking down Miat only at 8 hours after PE treatment. This is showing that Miat knockdown disrupted cellular ability to cope with nucleolar stress induced by PE so that the nucleolar size eventually shrank down (**Figure 4-7B**).

Lastly, we also looked at nucleoli morphology. We noticed many “merged” nucleoli, and the occurrence increased to almost 20% when cells were treated with PE in siNeg groups. However, Miat knockdown disrupted this increasing “merged nucleoli” feature, which only

occurred in less than 5% of the cells we quantified throughout the PE treatment (**Figure 4-7C**). We think this is a feature indicating new nucleoli formation, which is consistent with our previous observation of lower nucleoli number after Miat knockdown.

Taken together, we have demonstrated the functional impact of Miat on nucleolar dynamics, including number, size, and morphology. These striking observations showed that Miat is necessary in maintaining proper nucleolar dynamics and subsequent ribosome biogenesis during acute hypertrophic stress.

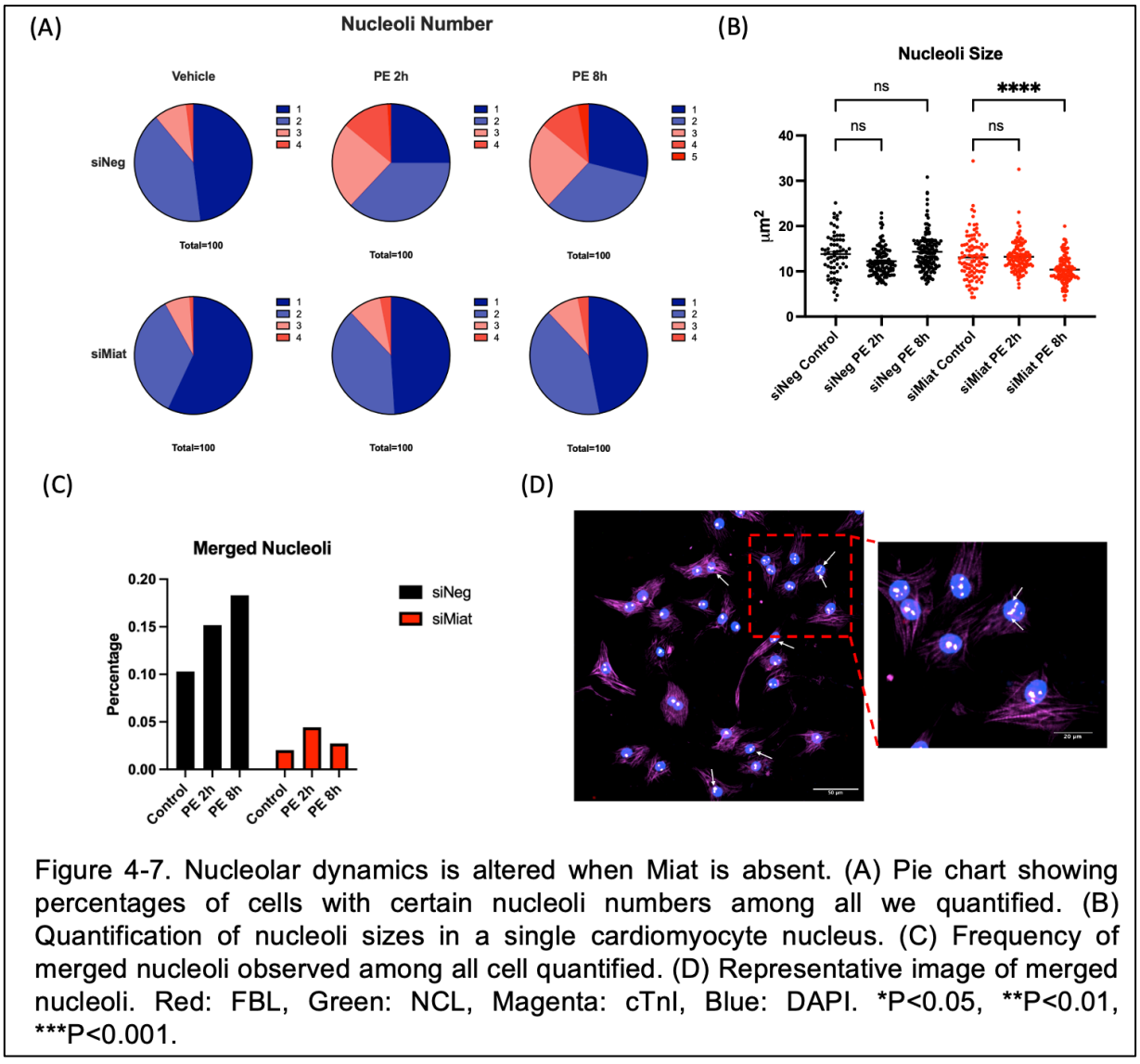

Figure 4-7. Nucleolar dynamics is altered when Miat is absent. (A) Pie chart showing percentages of cells with certain nucleoli numbers among all we quantified. (B) Quantification of nucleoli sizes in a single cardiomyocyte nucleus. (C) Frequency of merged nucleoli observed among all cell quantified. (D) Representative image of merged nucleoli. Red: FBL, Green: NCL, Magenta: cTnI, Blue: DAPI. *P<0.05, **P<0.01, ***P<0.001.

4.3.4 Miat is essential in spatial-temporal regulation of ribosome and target mRNAs

It is well established in the neuroscience field that local protein synthesis is essential to maintain normal cellular function and plasticity, especially at structures like axons and dendrites that are far away from the nucleus. However, not as many efforts have been spent on understanding the dynamics of spatial distribution of ribosome and target mRNAs in heart until recently. A previous study using single molecule RNA in situ hybridization (smFISH) showed that in cardiomyocytes, ribosomes co-localize with sarcomeric mRNAs and translation hotspots at Z-lines for sarcomeric maintenance. Moreover, another study done in NRVMs showed that sarcomeric mRNA accumulated at baseline rapidly moved away from nucleus after PE treatment. Finally, this whole transportation process was found to be mediated by microtubules.

To check if Miat is involved in spatial-temporal regulation, we used RNAscope to monitor subcellar localization of 28S rRNA (marking ribosome) and a representative sarcomeric gene Actc1 in both WT and Miat KO mice injected with PE. Ribosomes localized to Z-lines with or without PE treatment in both genetic backgrounds, which is consistent with what was observed before in other studies. Interestingly, we saw Actc1 mRNA accumulated in WT heart after a very short time after PE injection and dissipated at a later time point. In contract, we do not see changes of localization pattern of Actc1 in Miat KO hearts (**Figure 4-8A**). We then did a line scan analysis to check co-localization of 28S and Actc1 based on fluorescent signals. We saw perfectly overlapping peaks in WT heart throughout PE treatment. However, mis-localized ribosomes and Actc1 mRNA was observed after PE treatment in Miat KO hearts (**Figure 4-8B**). One prevalent theory

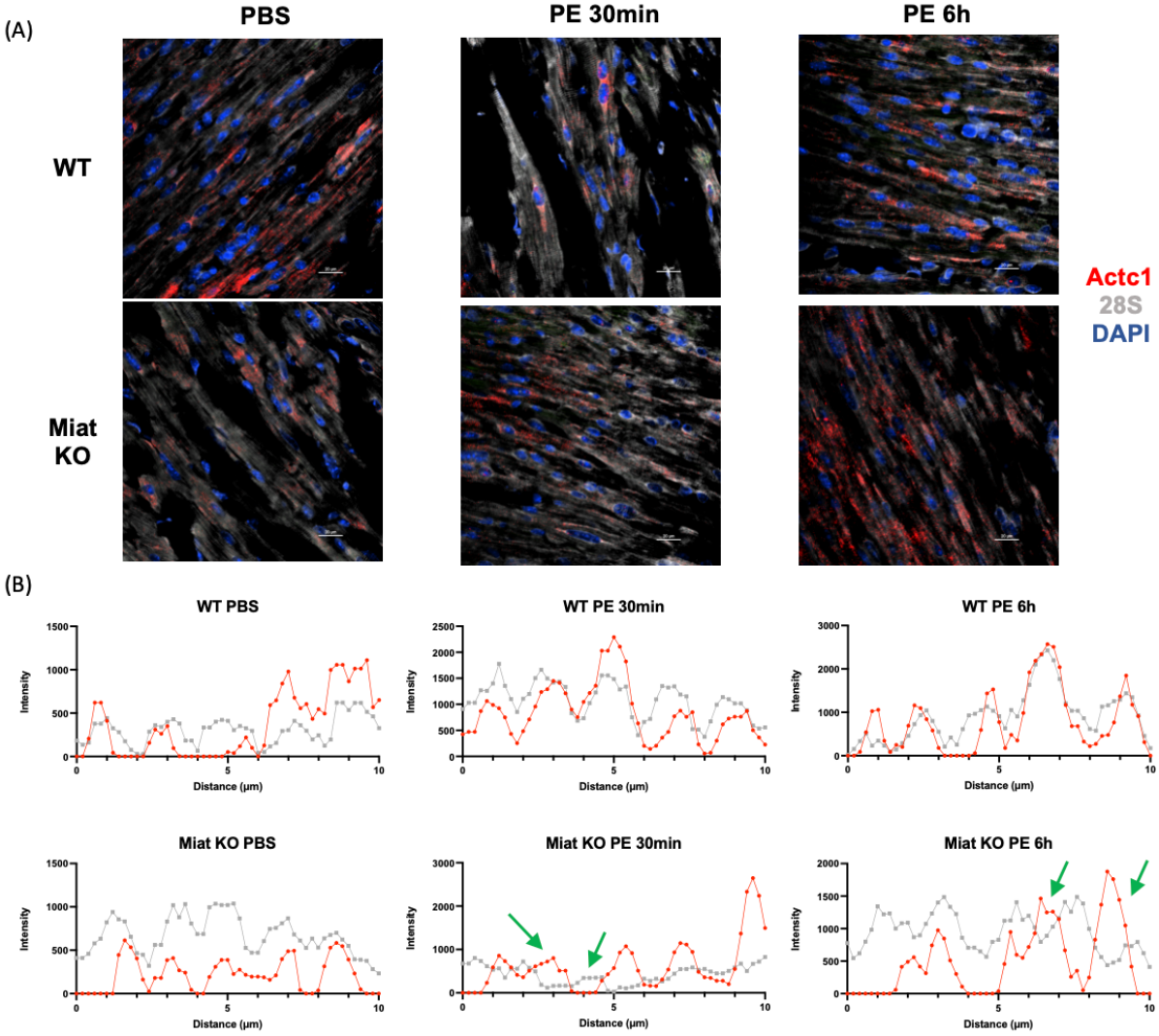

Figure 4-8. Miat is essential in spatial-temporal regulation of translation in cardiomyocytes. RNAscope was performed to examine subcellular localization of 28S (white, marking ribosome) and Actc1 (red, marking sarcomeric mRNA) in **(A)** WT heart and **(B)** Miat KO heart. By quantifying fluorescent intensity, the line scan analysis showed perfect co-localization of 28S and Actc1 peaks in WT heart throughout PE treatment, which is disrupted in Miat KO hearts (Green arrows).

suggested that ribosomes and their target mRNAs were transported together following microtubules in cardiac muscles. However, the discrepancy of their signal observed in Miat KO mice showed decoupled mRNA from ribosomes when Miat is absent. Taken together, these data suggested that Miat is important in mediating spatial-temporal regulation of protein synthesis. The molecular mechanism remains to be explored.

4.4 Discussion

In this chapter, we explored molecular mechanism and identified Miat-NCL binding to be essential in ribosomal biogenesis, hence proteins synthesis. We characterized NCL binding motif on Miat, and we saw a dominant negative effect when overexpressing Miat1. We also found that Miat is critical in regulating nucleoli dynamics in various ways, and Miat KO is disruptive to nucleoli assembly and maintenance. In addition, we explored spatial-temporal regulation of translation and found that Miat may be important in maintaining proper ribosome and mRNA localization in cells, especially during stress. However, further experiments are needed to uncover the mechanism of how Miat-regulated ribosome biogenesis transcends to the spatial-temporal regulation in the cytosol. One mechanism we hypothesized involving ribosome heterogeneity is that Miat may promote the biogenesis of a certain ribosome species that preferentially binds and translates a subset of mRNAs, such as sarcomeric gene mRNAs. Future experiments may test this hypothesis using smFISH and proteomics analysis on ribosome compositions.

Acknowledgements

We would like to thank Iris (He) Wang for preliminary experiments on Miat-NCL interaction. Image analysis and nucleoli quantification was supported by Yea-Lyn Pak. We would like to thank Tomohiro Yokota for his guidance on optimizing the RNAscope protocol. All animal breeding was supported by Haiying Pu. Schematic diagrams were generated with Biorender.com

CHAPTER V. SUMMARY AND FUTURE DIRECTIONS

5.1 Working Model

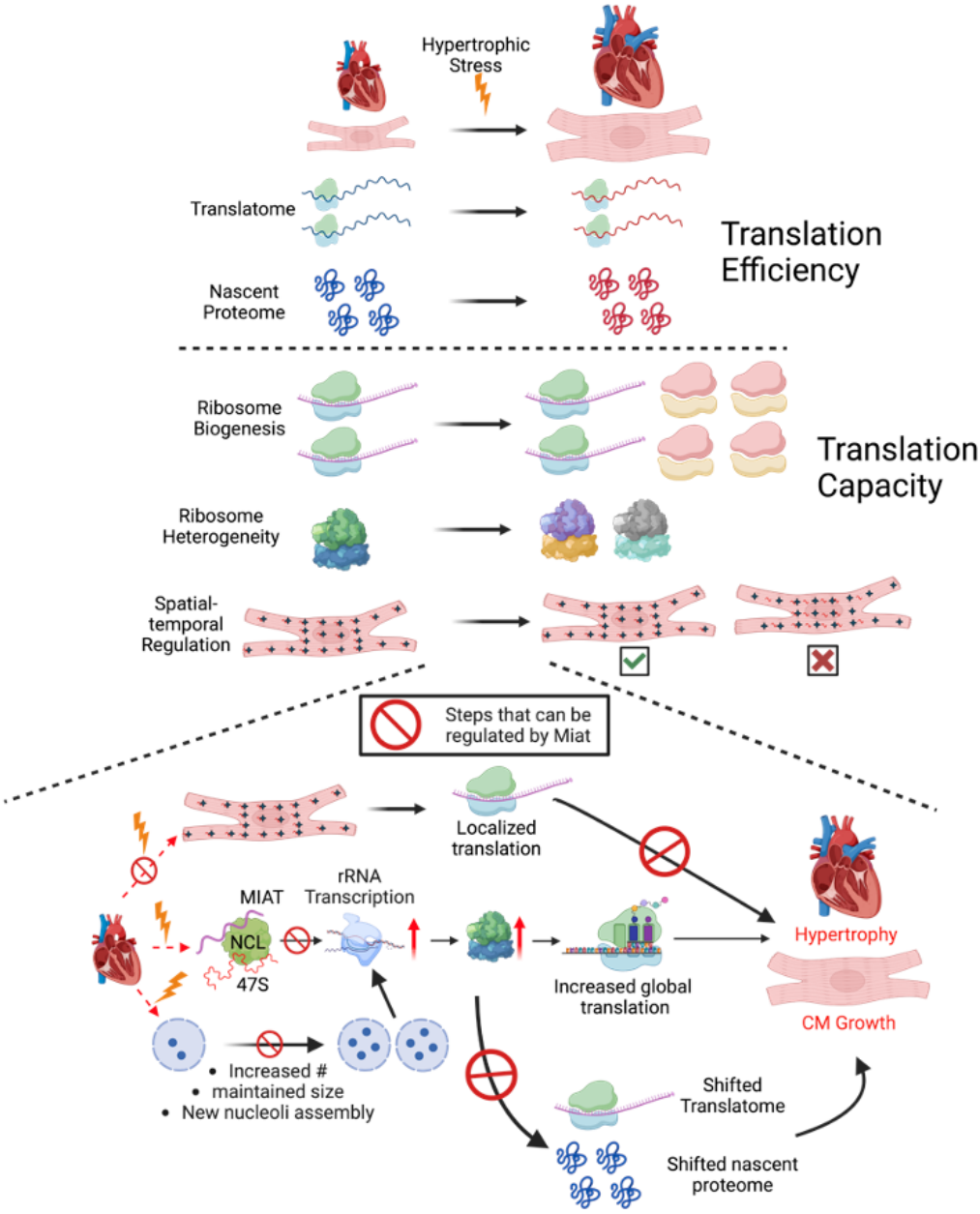

Figure 5-1. Working model. Upper: translation regulation in hypertrophic heart. Lower: Molecular mechanisms of Miat-regulated cardiac hypertrophy.

In this thesis, we established the dynamics of translatome reprogramming during cardiac hypertrophy and remodeling. We demonstrated a robust increase in protein synthesis

during acute hypertrophic response. We discovered cardiomyocyte-specific changes in both translation efficiency and translation capacity with prioritized mRNA pool that cells need to cope with growth stimuli.

Mechanistically, we identified lncRNA Miat as an important molecule mediating protein synthesis both qualitatively and quantitatively. NCL-Miat binding is necessary for NCL-47S interaction to promote rRNA transcription and ribosome biogenesis. Miat can also mediate nucleoli dynamics in their number, size, and morphology and subsequently affect the maintenance of nucleoli and ribosome biogenesis. Moreover, Miat regulates subcellular localization of sarcomeric mRNAs, which are essential for the muscular growth during hypertrophy. Taken together, this lncRNA is a powerful regulator of both qualitative and quantitative change in protein synthesis during hypertrophic stress, leading to the reprogramming of translatome that support various cellular processes to allow cellular growth.

5.2 Limitations and Future Directions

Although this thesis established translatome landscape in cardiac hypertrophy from many different angles and readouts and discovered the regulatory role of lncRNA Miat during early hypertrophic stress, there are some limitations and many questions remaining to be addressed. We will list and discuss each one of them in this section.

5.2.1 Integration of translatome and nascent proteome *in vivo*

In this thesis, we used TRAP mice to profile cardiac translatome *in vivo*. However, our data on nascent proteome was done *in vitro* with cultured NRVMs. Although we are looking at essentially the same cell types, *in vitro* cell culture lacks the physiological environment and crosstalk between cardiomyocytes and cell types in the heart, such as

fibroblasts and endothelial cells. It will be helpful if future studies could examine translatome *in vivo* with the same experimental design to induce acute hypertrophic stress. In this case, data from both omics can be compared to identify newly synthesized proteins with important functional implications. In fact, a mouse model carrying point mutation in methionyl-tRNA synthetase (MetRS) was developed recently and may address this problem[43]. In short, this mutant of MetRS can incorporate azidonorleucine (ANL), a non-canonical amino acid, into the synthesizing proteins instead of methionine. These newly synthesized, ANL-containing proteins can later be biotinylated by Click reaction and enriched using streptavidin. Subsequent proteomic analysis could examine nascent proteome *in vivo* in a cell-type specific manner.

5.2.2 Specialized ribosomes in heart

Both our TRAP-seq and proteomics data implicate the existence of specialized ribosomes in cardiomyocytes. There are a few ribosomal proteins we identified that may serve important roles in translating a specific pool of mRNAs in response to upstream stimuli. Future studies can focus on these specific ribosomal proteins and investigate their roles by both gain and loss-of-function studies. Ribo-seq can also be done on enriched specialized ribosome to explore preferentially translated mRNA pool. Moreover, since we have seen altered translation efficiency and incorporation of selected ribosomal proteins during hypertrophy, it will be interesting to further examine whether Miat regulates the biogenesis and specialized ribosomes.

5.2.3 Miat-mediated protein synthesis in physiological hypertrophy

In this thesis, we characterized Miat as a pivotal regulator of protein translation during the early response to pathological cardiac hypertrophy. This is a process where heart

experienced sustained hemodynamic stress that ended up in irreversible, maladaptive remodeling and dysfunctions. However, we have not tested Miat in the context of physiological hypertrophy, which is an adaptative and reversible process that could be commonly observed in athletes with exercise training. These two different types of hypertrophies are determined based on the integration of many concurrent yet distinct signaling pathways and cellular responses, leading to drastically different outcomes in many aspects such as fetal gene programs, mitochondrial dysfunctions, apoptosis, and maladaptive cardiac remodeling. Although they might be transcriptionally, translationally, and biochemically distinct from each other, both types of hypertrophies share the feature of enlarged heart and increased protein synthesis[179]. In fact, increased ribosomal biogenesis is a feature observed in pathological and physiological cardiac hypertrophy[180, 181], and skeletal muscle hypertrophy[182]. Therefore, we believe that Miat-mediated translation regulation, in both capacity and efficiency discussed above, might also be observed in physiological hypertrophy but possibly with distinct dynamics in translation landscape remodeling compared to that of pathological hypertrophy. Future studies could explore the functional impact of Miat in physiological hypertrophy models.

5.2.4 Upstream regulator of Miat

Both ours and many previous studies mainly focused on the downstream targets and events of lncRNA Miat without much emphasis and exploration of the upstream regulator of Miat during cardiac hypertrophy. It will be very interesting to understand how hypertrophic stimuli and signals can transcend to this lncRNA to trigger all the above-mentioned changes and regulations in protein translation.

REFERENCES

1. Heineke, J. and J.D. Molkentin, *Regulation of cardiac hypertrophy by intracellular signalling pathways.* Nat Rev Mol Cell Biol, 2006. **7**(8): p. 589-600.
2. Han, P., et al., *Chromatin remodeling in cardiovascular development and physiology.* Circ Res, 2011. **108**(3): p. 378-96.
3. Liu, C.F. and W.H.W. Tang, *Epigenetics in Cardiac Hypertrophy and Heart Failure.* JACC Basic Transl Sci, 2019. **4**(8): p. 976-993.
4. Akazawa, H. and I. Komuro, *Roles of cardiac transcription factors in cardiac hypertrophy.* Circ Res, 2003. **92**(10): p. 1079-88.
5. Ritterhoff, J. and R. Tian, *Metabolism in cardiomyopathy: every substrate matters.* Cardiovasc Res, 2017. **113**(4): p. 411-421.
6. Ritterhoff, J., et al., *Metabolic Remodeling Promotes Cardiac Hypertrophy by Directing Glucose to Aspartate Biosynthesis.* Circ Res, 2020. **126**(2): p. 182-196.
7. Martin, T.G., M.A. Juarros, and L.A. Leinwand, *Regression of cardiac hypertrophy in health and disease: mechanisms and therapeutic potential.* Nat Rev Cardiol, 2023.
8. Garlick, P.J., M.A. McNURLAN, and V.R. Preedy, *A rapid and convenient technique for measuring the rate of protein synthesis in tissues by injection of [3H] phenylalanine.* Biochemical Journal, 1980. **192**(2): p. 719-723.
9. Lewis, S.E.M., F.J. Kelly, and D.F. Goldspink, *Pre- and post-natal growth and protein turnover in smooth muscle, heart and slow- and fast-twitch skeletal muscles of the rat.* Biochemical Journal, 1984. **217**(2): p. 517-526.

10. Gudbjarnason, S., M. Telerman, and R.J. Bing, *Protein Metabolism in Cardiac Hypertrophy and Heart Failure.* Am J Physiol, 1964. **206**: p. 294-8.

11. McDermott, P.J., et al., *In vivo measurements of the contributions of protein synthesis and protein degradation in regulating cardiac pressure overload hypertrophy in the mouse.* Mol Cell Biochem, 2012. **367**(1-2): p. 205-13.

12. Sanford, C.F., E.E. Griffin, and K. Wildenthal, *Synthesis and degradation of myocardial protein during the development and regression of thyroxine-induced cardiac hypertrophy in rats.* Circ Res, 1978. **43**(5): p. 688-94.

13. Nagai, R., et al., *Efficiency and capacity of protein synthesis are increased in pressure overload cardiac hypertrophy.* Am J Physiol, 1988. **255**(2 Pt 2): p. H325-8.

14. Tebaldi, T., et al., *Widespread uncoupling between transcriptome and translatome variations after a stimulus in mammalian cells.* BMC Genomics, 2012. **13**: p. 220.

15. Liu, Y., A. Beyer, and R. Aebersold, *On the Dependency of Cellular Protein Levels on mRNA Abundance.* Cell, 2016. **165**(3): p. 535-50.

16. Vogel, C. and E.M. Marcotte, *Insights into the regulation of protein abundance from proteomic and transcriptomic analyses.* Nature Reviews Genetics, 2012. **13**(4): p. 227-232.

17. van Heesch, S., et al., *The Translational Landscape of the Human Heart.* Cell, 2019. **178**(1): p. 242-260 e29.

18. Schmidt, E.K., et al., *SUnSET, a nonradioactive method to monitor protein synthesis.* Nat Methods, 2009. **6**(4): p. 275-7.

19. Liu, J., et al., *Imaging protein synthesis in cells and tissues with an alkyne analog of puromycin.* Proc Natl Acad Sci U S A, 2012. **109**(2): p. 413-8.

20. David, A., et al., *Nuclear translation visualized by ribosome-bound nascent chain puromycylation.* J Cell Biol, 2012. **197**(1): p. 45-57.

21. Bastide, A., J.W. Yewdell, and A. David, *The RiboPuromycylation Method (RPM): an Immunofluorescence Technique to Map Translation Sites at the Sub-cellular Level.* Bio Protoc, 2018. **8**(1).

22. Buhr, F., et al., *Design of photocaged puromycin for nascent polypeptide release and spatiotemporal monitoring of translation.* Angew Chem Int Ed Engl, 2015. **54**(12): p. 3717-21.

23. Enam, S.U., et al., *Puromycin reactivity does not accurately localize translation at the subcellular level.* eLife, 2020. **9**: p. e60303.

24. Dieterich, D.C., et al., *In situ visualization and dynamics of newly synthesized proteins in rat hippocampal neurons.* Nat Neurosci, 2010. **13**(7): p. 897-905.

25. Marciano, R., G. Leprivier, and B. Rotblat, *Puromycin labeling does not allow protein synthesis to be measured in energy-starved cells.* Cell Death & Disease, 2018. **9**(2): p. 39.

26. Soderberg, O., et al., *Direct observation of individual endogenous protein complexes in situ by proximity ligation.* Nat Methods, 2006. **3**(12): p. 995-1000.

27. tom Dieck, S., et al., *Direct visualization of newly synthesized target proteins in situ.* Nat Methods, 2015. **12**(5): p. 411-4.

28. Schwanhäusser, B., et al., *Global analysis of cellular protein translation by pulsed SILAC.* Proteomics, 2009. **9**(1): p. 205-9.

29. Imami, K., M. Selbach, and Y. Ishihama, *Monitoring mitochondrial translation by pulse SILAC.* bioRxiv, 2022: p. 2021.01.31.428997.

30. Dieterich, D.C., et al., *Selective identification of newly synthesized proteins in mammalian cells using bioorthogonal noncanonical amino acid tagging (BONCAT).* Proc Natl Acad Sci U S A, 2006. **103**(25): p. 9482-7.

31. Dieterich, D.C., et al., *Labeling, detection and identification of newly synthesized proteomes with bioorthogonal non-canonical amino-acid tagging.* Nat Protoc, 2007. **2**(3): p. 532-40.

32. Aviner, R., T. Geiger, and O. Elroy-Stein, *Novel proteomic approach (PUNCH-P) reveals cell cycle-specific fluctuations in mRNA translation.* Genes Dev, 2013. **27**(16): p. 1834-44.

33. Ingolia, N.T., et al., *Genome-wide analysis in vivo of translation with nucleotide resolution using ribosome profiling.* Science, 2009. **324**(5924): p. 218-23.

34. Arava, Y., et al., *Genome-wide analysis of mRNA translation profiles in Saccharomyces cerevisiae.* Proc Natl Acad Sci U S A, 2003. **100**(7): p. 3889-94.

35. Clamer, M., et al., *Active Ribosome Profiling with RiboLace.* Cell Rep, 2018. **25**(4): p. 1097-1108 e5.

36. Adil, A., et al., *Single-Cell Transcriptomics: Current Methods and Challenges in Data Acquisition and Analysis.* Front Neurosci, 2021. **15**: p. 591122.

37. Bennett, H.M., et al., *Single-cell proteomics enabled by next-generation sequencing or mass spectrometry.* Nat Methods, 2023. **20**(3): p. 363-374.

38. Heiman, M., et al., *Cell type-specific mRNA purification by translating ribosome affinity purification (TRAP).* Nat Protoc, 2014. **9**(6): p. 1282-91.

39. Sanz, E., et al., *Cell-type-specific isolation of ribosome-associated mRNA from complex tissues.* Proc Natl Acad Sci U S A, 2009. **106**(33): p. 13939-44.

40. Doroudgar, S., et al., *Monitoring Cell-Type-Specific Gene Expression Using Ribosome Profiling In Vivo During Cardiac Hemodynamic Stress.* Circ Res, 2019. **125**(4): p. 431-448.

41. Zhou, P., et al., *Interrogating translational efficiency and lineage-specific transcriptomes using ribosome affinity purification.* Proc Natl Acad Sci U S A, 2013. **110**(38): p. 15395-400.

42. Boileau, E., et al., *A Multi-Network Comparative Analysis of Transcriptome and Translatome Identifies Novel Hub Genes in Cardiac Remodeling.* Front Genet, 2020. **11**: p. 583124.

43. Alvarez-Castelao, B., et al., *Cell-type-specific metabolic labeling of nascent proteomes in vivo.* Nat Biotechnol, 2017. **35**(12): p. 1196-1201.

44. Fukao, A., T. Tomohiro, and T. Fujiwara, *Translation Initiation Regulated by RNA-Binding Protein in Mammals: The Modulation of Translation Initiation Complex by Trans-Acting Factors.* Cells, 2021. **10**(7).

45. Morris, D.R. and A.P. Geballe, *Upstream open reading frames as regulators of mRNA translation.* Mol Cell Biol, 2000. **20**(23): p. 8635-42.

46. Jackson, R.J., C.U. Hellen, and T.V. Pestova, *The mechanism of eukaryotic translation initiation and principles of its regulation.* Nat Rev Mol Cell Biol, 2010. **11**(2): p. 113-27.

47. Wells, S.E., et al., *Circularization of mRNA by eukaryotic translation initiation factors.* Mol Cell, 1998. **2**(1): p. 135-40.

48. Sonenberg, N., et al., *A polypeptide in eukaryotic initiation factors that crosslinks specifically to the 5'-terminal cap in mRNA.* Proc Natl Acad Sci U S A, 1978. **75**(10): p. 4843-7.

49. Marcotrigiano, J., et al., *Cocrystal structure of the messenger RNA 5' cap-binding protein (eIF4E) bound to 7-methyl-GDP.* Cell, 1997. **89**(6): p. 951-61.

50. Matsuo, H., et al., *Structure of translation factor eIF4E bound to m7GDP and interaction with 4E-binding protein.* Nat Struct Biol, 1997. **4**(9): p. 717-24.

51. Makhlouf, A.A. and P.J. McDermott, *Increased expression of eukaryotic initiation factor 4E during growth of neonatal rat cardiocytes in vitro.* Am J Physiol, 1998. **274**(6): p. H2133-42.

52. Ueda, T., et al., *Mnk2 and Mnk1 are essential for constitutive and inducible phosphorylation of eukaryotic initiation factor 4E but not for cell growth or development.* Mol Cell Biol, 2004. **24**(15): p. 6539-49.

53. Waskiewicz, A.J., et al., *Mitogen-activated protein kinases activate the serine/threonine kinases Mnk1 and Mnk2.* EMBO J, 1997. **16**(8): p. 1909-20.

54. Figueiredo, V.C., et al., *Phosphorylation of eukaryotic initiation factor 4E is dispensable for skeletal muscle hypertrophy.* Am J Physiol Cell Physiol, 2019. **317**(6): p. C1247-C1255.

55. McKendrick, L., et al., *Phosphorylation of eukaryotic initiation factor 4E (eIF4E) at Ser209 is not required for protein synthesis in vitro and in vivo.* European journal of biochemistry, 2001. **268**(20): p. 5375-5385.

56. Korneeva, N.L., et al., *Inhibition of Mitogen-activated Protein Kinase (MAPK)-interacting Kinase (MNK) Preferentially Affects Translation of mRNAs Containing Both a 5'-Terminal Cap and Hairpin.* J Biol Chem, 2016. **291**(7): p. 3455-67.

57. Spruill, L.S., et al., *Selective translation of mRNAs in the left ventricular myocardium of the mouse in response to acute pressure overload.* J Mol Cell Cardiol, 2008. **44**(1): p. 69-75.

58. Kahvejian, A., et al., *Mammalian poly(A)-binding protein is a eukaryotic translation initiation factor, which acts via multiple mechanisms.* Genes Dev, 2005. **19**(1): p. 104-13.

59. Ivanov, A., et al., *PABP enhances release factor recruitment and stop codon recognition during translation termination.* Nucleic Acids Res, 2016. **44**(16): p. 7766-76.

60. Kajjo, S., et al., *PABP prevents the untimely decay of select mRNA populations in human cells.* EMBO J, 2022. **41**(6): p. e108650.

61. Yi, H., et al., *PABP Cooperates with the CCR4-NOT Complex to Promote mRNA Deadenylation and Block Precocious Decay.* Mol Cell, 2018. **70**(6): p. 1081-1088 e5.

62. Chorghade, S., et al., *Poly(A) tail length regulates PABPC1 expression to tune translation in the heart.* Elife, 2017. **6**.

63. Nairn, A. and H. Palfrey, *Identification of the major Mr 100,000 substrate for calmodulin-dependent protein kinase III in mammalian cells as elongation factor-2.* Journal of Biological Chemistry, 1987. **262**(36): p. 17299-17303.

64. Wang, X., et al., *Regulation of elongation factor 2 kinase by p90(RSK1) and p70 S6 kinase.* EMBO J, 2001. **20**(16): p. 4370-9.

65. Johanns, M., et al., *Direct and indirect activation of eukaryotic elongation factor 2 kinase by AMP-activated protein kinase.* Cell Signal, 2017. **36**: p. 212-221.

66. Everett, A.D., et al., *Angiotensin II regulates phosphorylation of translation elongation factor-2 in cardiac myocytes.* Am J Physiol Heart Circ Physiol, 2001. **281**(1): p. H161-7.

67. Everett, A.D., et al., *Angiotensin II Regulates Cardiac Myocyte Protein Synthesis by Activation of Elongation Factor 2.* Pediatric Research, 1999. **45**(7): p. 22-22.

68. Kameshima, S., et al., *Coordination of changes in expression and phosphorylation of eukaryotic elongation factor 2 (eEF2) and eEF2 kinase in hypertrophied cardiomyocytes.* Biochem Biophys Rep, 2016. **7**: p. 218-224.

69. Saxton, R.A. and D.M. Sabatini, *mTOR Signaling in Growth, Metabolism, and Disease.* Cell, 2017. **168**(6): p. 960-976.

70. Wullschleger, S., R. Loewith, and M.N. Hall, *TOR signaling in growth and metabolism.* Cell, 2006. **124**(3): p. 471-84.

71. Liu, G.Y. and D.M. Sabatini, *mTOR at the nexus of nutrition, growth, ageing and disease.* Nature Reviews Molecular Cell Biology, 2020. **21**(4): p. 183-203.

72. Sciarretta, S., et al., *New insights into the role of mTOR signaling in the cardiovascular system.* Circulation research, 2018. **122**(3): p. 489-505.

73. Sciarretta, S., et al., *mTORC2 regulates cardiac response to stress by inhibiting MST1.* Cell Rep, 2015. **11**(1): p. 125-36.

74. Volkers, M., et al., *Mechanistic target of rapamycin complex 2 protects the heart from ischemic damage.* Circulation, 2013. **128**(19): p. 2132-44.

75. Shende, P., et al., *Cardiac mTOR complex 2 preserves ventricular function in pressure-overload hypertrophy.* Cardiovasc Res, 2016. **109**(1): p. 103-14.

76. Zhang, D., et al., *MTORC1 regulates cardiac function and myocyte survival through 4E-BP1 inhibition in mice.* J Clin Invest, 2010. **120**(8): p. 2805-16.

77. Shende, P., et al., *Cardiac raptor ablation impairs adaptive hypertrophy, alters metabolic gene expression, and causes heart failure in mice.* Circulation, 2011. **123**(10): p. 1073-82.

78. Shioi, T., et al., *Rapamycin attenuates load-induced cardiac hypertrophy in mice.* Circulation, 2003. **107**(12): p. 1664-70.

79. Ikeda, M., et al., *The Akt-mTOR axis is a pivotal regulator of eccentric hypertrophy during volume overload.* Scientific Reports, 2015. **5**(1): p. 15881.

80. Jain, P.K., et al., *Ribosomal protein S6 kinase beta-1 gene variants cause hypertrophic cardiomyopathy.* J Med Genet, 2022. **59**(10): p. 984-992.

81. Holz, M.K., et al., *mTOR and S6K1 mediate assembly of the translation preinitiation complex through dynamic protein interchange and ordered phosphorylation events.* Cell, 2005. **123**(4): p. 569-80.

82. Dorrello, N.V., et al., *S6K1- and betaTRCP-mediated degradation of PDCD4 promotes protein translation and cell growth.* Science, 2006. **314**(5798): p. 467-71.

83. Chauvin, C., et al., *Ribosomal protein S6 kinase activity controls the ribosome biogenesis transcriptional program.* Oncogene, 2014. **33**(4): p. 474-83.

84. Jefferies, H.B., et al., *Rapamycin suppresses 5'TOP mRNA translation through inhibition of p70s6k.* EMBO J, 1997. **16**(12): p. 3693-704.

85. Tang, H., et al., *Amino acid-induced translation of TOP mRNAs is fully dependent on phosphatidylinositol 3-kinase-mediated signaling, is partially inhibited by rapamycin, and is independent of S6K1 and rpS6 phosphorylation.* Molecular and cellular biology, 2001. **21**(24): p. 8671-8683.

86. Ruvinsky, I., et al., *Ribosomal protein S6 phosphorylation is a determinant of cell size and glucose homeostasis.* Genes & development, 2005. **19**(18): p. 2199-2211.

87. Liao, H., et al., *GPR39 promotes cardiac hypertrophy by regulating the AMPK-mTOR pathway and protein synthesis.* Cell Biol Int, 2021. **45**(6): p. 1211-1219.

88. Brunn, G.J., et al., *Phosphorylation of the translational repressor PHAS-I by the mammalian target of rapamycin.* Science, 1997. **277**(5322): p. 99-101.

89. Gingras, A.C., et al., *Regulation of 4E-BP1 phosphorylation: a novel two-step mechanism.* Genes Dev, 1999. **13**(11): p. 1422-37.

90. Hara, K., et al., *Regulation of eIF-4E BP1 phosphorylation by mTOR.* J Biol Chem, 1997. **272**(42): p. 26457-63.

91. Mazelin, L., et al., *mTOR inactivation in myocardium from infant mice rapidly leads to dilated cardiomyopathy due to translation defects and p53/JNK-mediated apoptosis.* J Mol Cell Cardiol, 2016. **97**: p. 213-25.

92. Fu, Y., et al., *Gene expression regulation mediated through reversible m6A RNA methylation.* Nature Reviews Genetics, 2014. **15**(5): p. 293-306.

93. Ye, F., et al., *The effects of NCBP3 on METTL3-mediated m6A RNA methylation to enhance translation process in hypoxic cardiomyocytes.* J Cell Mol Med, 2021. **25**(18): p. 8920-8928.

94. Song, H., et al., *METTL3 and ALKBH5 oppositely regulate m(6)A modification of TFEB mRNA, which dictates the fate of hypoxia/reoxygenation-treated cardiomyocytes.* Autophagy, 2019. **15**(8): p. 1419-1437.

95. Berulava, T., et al., *Changes in m6A RNA methylation contribute to heart failure progression by modulating translation.* Eur J Heart Fail, 2020. **22**(1): p. 54-66.

96. Zhang, B., et al., *Alteration of m6A RNA Methylation in Heart Failure With Preserved Ejection Fraction.* Front Cardiovasc Med, 2021. **8**: p. 647806.

97. Dorn, L.E., et al., *The N(6)-Methyladenosine mRNA Methylase METTL3 Controls Cardiac Homeostasis and Hypertrophy.* Circulation, 2019. **139**(4): p. 533-545.

98. Mathiyalagan, P., et al., *FTO-Dependent N(6)-Methyladenosine Regulates Cardiac Function During Remodeling and Repair.* Circulation, 2019. **139**(4): p. 518-532.

99. Kmietczyk, V., et al., *m(6)A-mRNA methylation regulates cardiac gene expression and cellular growth.* Life Sci Alliance, 2019. **2**(2).

100. Wang, X., et al., *N6-methyladenosine-dependent regulation of messenger RNA stability.* Nature, 2014. **505**(7481): p. 117-20.

101. Xu, H., et al., *YTHDF2 alleviates cardiac hypertrophy via regulating Myh7 mRNA decoy.* Cell Biosci, 2021. **11**(1): p. 132.

102. Kmietczyk, V., et al., *Ythdf2 regulates cardiac remodeling through its m6A-mRNA target transcripts.* bioRxiv, 2022: p. 2022.12. 16.520765.

103. Meyer, K.D., et al., *5′ UTR m(6)A Promotes Cap-Independent Translation.* Cell, 2015. **163**(4): p. 999-1010.

104. Greber, B.J., *Mechanistic insight into eukaryotic 60S ribosomal subunit biogenesis by cryo-electron microscopy.* Rna, 2016. **22**(11): p. 1643-1662.

105. McDermott, P.J., et al., *Accelerated rates of ribosomal RNA synthesis during growth of contracting heart cells in culture.* J Biol Chem, 1989. **264**(30): p. 18220-7.

106. Brandenburger, Y., et al., *Increased expression of UBF is a critical determinant for rRNA synthesis and hypertrophic growth of cardiac myocytes.* FASEB J, 2001. **15**(11): p. 2051-3.

107. Brandenburger, Y., et al., *Cardiac hypertrophy in vivo is associated with increased expression of the ribosomal gene transcription factor UBF.* FEBS Lett, 2003. **548**(1-3): p. 79-84.

108. Hannan, R.D., J. Luyken, and L.I. Rothblum, *Regulation of rDNA transcription factors during cardiomyocyte hypertrophy induced by adrenergic agents.* J Biol Chem, 1995. **270**(14): p. 8290-7.

109. Hannan, R.D., et al., *Overexpression of the transcription factor UBF1 is sufficient to increase ribosomal DNA transcription in neonatal cardiomyocytes: implications for cardiac hypertrophy.* Proc Natl Acad Sci U S A, 1996. **93**(16): p. 8750-5.

110. Friedrich, J.K., et al., *TBP-TAF complex SL1 directs RNA polymerase I pre-initiation complex formation and stabilizes upstream binding factor at the rDNA promoter.* J Biol Chem, 2005. **280**(33): p. 29551-8.

111. Kihm, A.J., et al., *Phosphorylation of the rRNA transcription factor upstream binding factor promotes its association with TATA binding protein.* Proc Natl Acad Sci U S A, 1998. **95**(25): p. 14816-20.

112. Voit, R. and I. Grummt, *Phosphorylation of UBF at serine 388 is required for interaction with RNA polymerase I and activation of rDNA transcription.* Proc Natl Acad Sci U S A, 2001. **98**(24): p. 13631-6.

113. Russell, J. and J.C. Zomerdijk, *RNA-polymerase-I-directed rDNA transcription, life and works.* Trends Biochem Sci, 2005. **30**(2): p. 87-96.

114. Luyken, J., et al., *Regulation of rDNA transcription during endothelin-1-induced hypertrophy of neonatal cardiomyocytes. Hyperphosphorylation of upstream binding factor, an rDNA transcription factor.* Circ Res, 1996. **78**(3): p. 354-61.

115. Sanij, E., et al., *UBF levels determine the number of active ribosomal RNA genes in mammals.* J Cell Biol, 2008. **183**(7): p. 1259-74.

116. Kang, J., et al., *Amino acid-dependent signaling via S6K1 and MYC is essential for regulation of rDNA transcription.* Oncotarget, 2016. **7**(31): p. 48887-48904.

117. Hannan, K.M., et al., *mTOR-dependent regulation of ribosomal gene transcription requires S6K1 and is mediated by phosphorylation of the carboxy-terminal activation domain of the nucleolar transcription factor UBF.* Mol Cell Biol, 2003. **23**(23): p. 8862-77.

118. Tiku, V. and A. Antebi, *Nucleolar Function in Lifespan Regulation.* Trends Cell Biol, 2018. **28**(8): p. 662-672.

119. Boulon, S., et al., *The nucleolus under stress.* Mol Cell, 2010. **40**(2): p. 216-27.

120. Bloom, S. and D. Egli, *Variation of myocardial nucleolar abundance with heart weight.* Proc Soc Exp Biol Med, 1969. **130**(3): p. 1019-21.

121. Kofuji, S., et al., *IMP dehydrogenase-2 drives aberrant nucleolar activity and promotes tumorigenesis in glioblastoma.* Nat Cell Biol, 2019. **21**(8): p. 1003-1014.

122. Neuburger, M., et al., *Change in size, number and morphology of the nucleoli in human hearts as a result of hyperfunction.* Pathol Res Pract, 1998. **194**(6): p. 385-9.

123. Gudkova, A., et al., *[Elevated expression of argentophilic proteins from the nucleolar organizer regions in myocardium of patients with obstructive hypertrophic*

cardiomyopathy and mutations in p53 tumor suppressor gene]. Tsitologiia, 2003. **45**(11): p. 1124-33.

124. Rosello-Lleti, E., et al., *Influence of heart failure on nucleolar organization and protein expression in human hearts.* Biochem Biophys Res Commun, 2012. **418**(2): p. 222-8.

125. Guo, N., et al., *NAP1L5 Promotes Nucleolar Hypertrophy and Is Required for Translation Activation During Cardiomyocyte Hypertrophy.* Front Cardiovasc Med, 2021. **8**: p. 791501.

126. Crick, F.H., *On protein synthesis.* Symp Soc Exp Biol, 1958. **12**: p. 138-63.

127. Gunderson, J.H., et al., *Structurally distinct, stage-specific ribosomes occur in Plasmodium.* Science, 1987. **238**(4829): p. 933-7.

128. Ramagopal, S., *Induction of cell-specific ribosomal proteins in aggregation-competent nonmorphogenetic Dictyostelium discoideum.* Biochem Cell Biol, 1990. **68**(11): p. 1281-7.

129. Williams, M.E. and I.M. Sussex, *Developmental regulation of ribosomal protein L16 genes in Arabidopsis thaliana.* Plant J, 1995. **8**(1): p. 65-76.

130. Shi, Z., et al., *Heterogeneous Ribosomes Preferentially Translate Distinct Subpools of mRNAs Genome-wide.* Mol Cell, 2017. **67**(1): p. 71-83 e7.

131. Gupta, V. and J.R. Warner, *Ribosome-omics of the human ribosome.* RNA, 2014. **20**(7): p. 1004-13.

132. Van Raay, T.J., et al., *A novel ribosomal protein L3-like gene (RPL3L) maps to the autosomal dominant polycystic kidney disease gene region.* Genomics, 1996. **37**(2): p. 172-6.

133. Chaillou, T., X. Zhang, and J.J. McCarthy, *Expression of Muscle-Specific Ribosomal Protein L3-Like Impairs Myotube Growth.* J Cell Physiol, 2016. **231**(9): p. 1894-902.

134. Kao, B.R., et al., *Knockdown of Muscle-Specific Ribosomal Protein L3-Like Enhances Muscle Function in Healthy and Dystrophic Mice.* Nucleic Acid Ther, 2021. **31**(6): p. 457-464.

135. Ganapathi, M., et al., *Bi-allelic missense disease-causing variants in RPL3L associate neonatal dilated cardiomyopathy with muscle-specific ribosome biogenesis.* Hum Genet, 2020. **139**(11): p. 1443-1454.

136. Das, B.B., et al., *Compound Heterozygous Missense Variants in RPL3L Genes Associated with Severe Forms of Dilated Cardiomyopathy: A Case Report and Literature Review.* Children (Basel), 2022. **9**(10).

137. Nannapaneni, H., et al., *Further Evidence of Autosomal Recessive Inheritance of RPL3L Pathogenic Variants with Rapidly Progressive Neonatal Dilated Cardiomyopathy.* Journal of Cardiovascular Development and Disease, 2022. **9**(3): p. 65.

138. Jaouadi, H., et al., *Identification of two variants in AGRN and RPL3L genes in a patient with catecholaminergic polymorphic ventricular tachycardia suggesting new candidate disease genes and digenic inheritance.* Clin Case Rep, 2022. **10**(2): p. e05339.

139. Thorolfsdottir, R.B., et al., *Coding variants in RPL3L and MYZAP increase risk of atrial fibrillation.* Commun Biol, 2018. **1**: p. 68.

140. Grimes, K.M., et al., *Rpl3l gene deletion in mice reduces heart weight over time.* Front Physiol, 2023. **14**: p. 1054169.

141. Milenkovic, I., et al., *Dynamic interplay between RPL3- and RPL3L-containing ribosomes modulates mitochondrial activity in the mammalian heart.* Nucleic Acids Research, 2023.

142. Mofatteh, M. and S.L. Bullock, *SnapShot: Subcellular mRNA Localization.* Cell, 2017. **169**(1): p. 178-178 e1.

143. Holt, C.E., K.C. Martin, and E.M. Schuman, *Local translation in neurons: visualization and function.* Nat Struct Mol Biol, 2019. **26**(7): p. 557-566.

144. Nikcevic, G., et al., *Translation is regulated via the 3' untranslated region of alpha-myosin heavy chain mRNA by calcium but not by its localization.* J Muscle Res Cell Motil, 2000. **21**(6): p. 599-607.

145. Heidkamp, M.C. and B. Russell, *Calcium not strain regulates localization of alpha-myosin heavy chain mRNA in oriented cardiac myocytes.* Cell Tissue Res, 2001. **305**(1): p. 121-7.

146. Lewis, Y.E., et al., *Localization of transcripts, translation, and degradation for spatiotemporal sarcomere maintenance.* J Mol Cell Cardiol, 2018. **116**: p. 16-28.

147. Tsutsui, H., K. Ishihara, and G.t. Cooper, *Cytoskeletal role in the contractile dysfunction of hypertrophied myocardium.* Science, 1993. **260**(5108): p. 682-7.

148. Tagawa, H., et al., *Cytoskeletal role in the contractile dysfunction of cardiocytes from hypertrophied and failing right ventricular myocardium.* Proc Assoc Am Physicians, 1996. **108**(3): p. 218-29.

149. Ishibashi, Y., et al., *Role of microtubules in myocyte contractile dysfunction during cardiac hypertrophy in the rat.* Am J Physiol, 1996. **271**(5 Pt 2): p. H1978-87.

150. Sato, H., et al., *Microtubule stabilization in pressure overload cardiac hypertrophy.* J Cell Biol, 1997. **139**(4): p. 963-73.

151. Koide, M., et al., *Microtubule depolymerization normalizes in vivo myocardial contractile function in dogs with pressure-overload left ventricular hypertrophy.* Circulation, 2000. **102**(9): p. 1045-52.

152. Scopacasa, B.S., V.P. Teixeira, and K.G. Franchini, *Colchicine attenuates left ventricular hypertrophy but preserves cardiac function of aortic-constricted rats.* J Appl Physiol (1985), 2003. **94**(4): p. 1627-33.

153. Tsutsui, H., et al., *Chronic colchicine administration attenuates cardiac hypertrophy in spontaneously hypertensive rats.* J Mol Cell Cardiol, 1999. **31**(6): p. 1203-13.

154. Fassett, J., et al., *Adenosine kinase attenuates cardiomyocyte microtubule stabilization and protects against pressure overload-induced hypertrophy and LV dysfunction.* J Mol Cell Cardiol, 2019. **130**: p. 49-58.

155. Scarborough, E.A., et al., *Microtubules orchestrate local translation to enable cardiac growth.* Nat Commun, 2021. **12**(1): p. 1547.

156. Bogdanov, V., et al., *Distributed synthesis of sarcolemmal and sarcoplasmic reticulum membrane proteins in cardiac myocytes.* Basic Res Cardiol, 2021. **116**(1): p. 63.

157. Ma, Y., et al., *Quantitative analysis of newly synthesized proteins.* Nat Protoc, 2018. **13**(8): p. 1744-1762.

158. Patro, R., et al., *Salmon provides fast and bias-aware quantification of transcript expression.* Nat Methods, 2017. **14**(4): p. 417-419.

159. Love, M.I., W. Huber, and S. Anders, *Moderated estimation of fold change and dispersion for RNA-seq data with DESeq2.* Genome Biol, 2014. **15**(12): p. 550.

160. Hughes, C.S., et al., *Ultrasensitive proteome analysis using paramagnetic bead technology.* Mol Syst Biol, 2014. **10**(10): p. 757.

161. Da, C.M., et al., *The role of long non-coding RNA MIAT in cancers.* Biomed Pharmacother, 2020. **129**: p. 110359.

162. Fasolo, F., et al., *Long Noncoding RNA MIAT Controls Advanced Atherosclerotic Lesion Formation and Plaque Destabilization.* Circulation, 2021. **144**(19): p. 1567-1583.

163. Aonuma, T., et al., *MiR-150 Attenuates Maladaptive Cardiac Remodeling Mediated by Long Noncoding RNA MIAT and Directly Represses Profibrotic Hoxa4.* Circ Heart Fail, 2022. **15**(4): p. e008686.

164. Bai, X., et al., *LncRNA MIAT impairs cardiac contractile function by acting on mitochondrial translocator protein TSPO in a mouse model of myocardial infarction.* Signal Transduct Target Ther, 2021. **6**(1): p. 172.

165. Qu, X., et al., *MIAT Is a Pro-fibrotic Long Non-coding RNA Governing Cardiac Fibrosis in Post-infarct Myocardium.* Sci Rep, 2017. **7**: p. 42657.

166. Yao, L., et al., *LncRNA MIAT/miR-133a-3p axis regulates atrial fibrillation and atrial fibrillation-induced myocardial fibrosis.* Mol Biol Rep, 2020. **47**(4): p. 2605-2617.

167. Chen, Y., et al., *Serum extracellular vesicles containing MIAT induces atrial fibrosis, inflammation and oxidative stress to promote atrial remodeling and atrial fibrillation via blockade of miR-485-5p-mediated CXCL10 inhibition.* Clin Transl Med, 2021. **11**(8): p. e482.

168. Zhou, X., et al., *lncRNA MIAT functions as a competing endogenous RNA to upregulate DAPK2 by sponging miR-22-3p in diabetic cardiomyopathy.* Cell Death Dis, 2017. **8**(7): p. e2929.

169. Zhu, X.H., et al., *LncRNA MIAT enhances cardiac hypertrophy partly through sponging miR-150.* Eur Rev Med Pharmacol Sci, 2016. **20**(17): p. 3653-60.

170. Li, Y., et al., *LncRNA myocardial infarction-associated transcript (MIAT) contributed to cardiac hypertrophy by regulating TLR4 via miR-93.* Eur J Pharmacol, 2018. **818**: p. 508-517.

171. Ghazalpour, A., et al., *Hybrid mouse diversity panel: a panel of inbred mouse strains suitable for analysis of complex genetic traits.* Mamm Genome, 2012. **23**(9-10): p. 680-92.

172. Rau, C.D., et al., *Mapping genetic contributions to cardiac pathology induced by Beta-adrenergic stimulation in mice.* Circ Cardiovasc Genet, 2015. **8**(1): p. 40-9.

173. Zhang, X. and S. Liu, *RBPPred: predicting RNA-binding proteins from sequence using SVM.* Bioinformatics, 2017. **33**(6): p. 854-862.

174. Muppirala, U.K., V.G. Honavar, and D. Dobbs, *Predicting RNA-protein interactions using only sequence information.* BMC Bioinformatics, 2011. **12**: p. 489.

175. Carvalho, L.S., et al., *Cancer Stem Cells and Nucleolin as Drivers of Carcinogenesis.* Pharmaceuticals (Basel), 2021. **14**(1).

176. Cong, R., et al., *Interaction of nucleolin with ribosomal RNA genes and its role in RNA polymerase I transcription.* Nucleic Acids Res, 2012. **40**(19): p. 9441-54.

177. Mongelard, F. and P. Bouvet, *Nucleolin: a multiFACeTed protein.* Trends Cell Biol, 2007. **17**(2): p. 80-6.

178. Monte, E., et al., *Systems proteomics of cardiac chromatin identifies nucleolin as a regulator of growth and cellular plasticity in cardiomyocytes.* Am J Physiol Heart Circ Physiol, 2013. **305**(11): p. H1624-38.

179. Nakamura, M. and J. Sadoshima, *Mechanisms of physiological and pathological cardiac hypertrophy.* Nat Rev Cardiol, 2018. **15**(7): p. 387-407.

180. Hammarstrom, D., et al., *Ribosome accumulation during early phase resistance training in humans.* Acta Physiol (Oxf), 2022. **235**(1): p. e13806.

181. Jiao, L., et al., *Ribosome biogenesis in disease: new players and therapeutic targets.* Signal Transduct Target Ther, 2023. **8**(1): p. 15.

182. Figueiredo, V.C. and J.J. McCarthy, *Regulation of Ribosome Biogenesis in Skeletal Muscle Hypertrophy.* Physiology (Bethesda), 2019. **34**(1): p. 30-42.